POLSKA AKADEMIA NAUK
INSTYTUT CHEMII FIZYCZNEJ

Robert Kołos

Carbon-Nitrogen Chain Molecules in the Laboratory and in Interstellar Medium

Warszawa 2003

CARBON-NITROGEN CHAIN MOLECULES

IN THE LABORATORY

AND IN INTERSTELLAR MEDIUM

BY

ROBERT KOŁOS

Institute of Physical Chemistry of the Polish Academy of Sciences

Warsaw 2003

ISBN 83-913520-4-8

Przygotowanie do druku
z materiałów *camera ready*:
Sekcja Wydawnicza IChF PAN

to the memory of my Father

Preface

Science sans conscience n'est que ruine de l'âme. –Rabelais (1532)

The simplest and broadest definition of the interstellar matter – "everything but stars" – may be misleading. Is Earth a piece of it? Are humans the interstellar matter, with all material products of the terrestrial civilization? Avoiding the perils of semantics, I will rather use the term in its narrow sense. In what follows, it will primarily be applied to immense clouds of gas and dust, without which the stars would have nothing to be born from, and – when their time comes – nothing to disperse into.

It is only 35 years now, since an important, yet largely unnoticed discovery has been made. The interstellar matter was found to be *more* than just hydrogen, helium, mineral dust, and a small admixture of heavier atoms, their ions, and few simplest diatomics – as was originally believed. In addition to this blend (not very promising for a chemist) the presence of quite complex organic molecules was revealed. By plain chemical standards, some of the compounds given the "interstellar" tag may seem bizzare (or useless), like the largest ones: rod-shaped polyacetylenic nitriles. Still, all these merit our closest attention. If a molecule is abundant enough to show up in the interstellar medium – in spite of present rudimentary detection methods – then it inevitably has to be conceived as one of most important arrangements of atoms in the Galaxy, and possibly also in the entire Universe.

Our means of exploration will always be inadequate or incomplete. This is particularly obvious for any research dealing with vast interstellar spaces. Nevertheless, the short history of organic astrochemistry gives an account of the remarkable progress in observational techniques. Achievements of the microwave spectroscopy, employed by radio astronomers, are hard to overvalue. Importantly, however, the tool especially well suited for the identification of new compounds was refined at the turn of the century: the *infrared spectroscopy*. The dramatic progress in this field was possible due to the new generation of radiation detectors.

Still, strange as it may seem, for the majority of polyatomic interstellar molecules the spectroscopic characterization remains reduced to their microwave, *i.e.* pure rotational spectra. The current need for complementary information, especially from the infrared domain, can hopefully be met, to some degree, with the contents of this monograph. While it took the shape of a *review* on unsaturated carbon-nitrogen molecules of known or possible interstellar significance, I realize that the choice of contents reflects my own background, scientific interests, and occasionally my desire to present some otherwise unpublished results. I do apologize to the reader for all instances of loosing the proper balance, and overexposing certain areas of research.

A very brief introduction to selected problems of physics and chemistry of the interstellar medium is given in the first chapter of this monograph; the second one is devoted mostly to the methodology of the inert gas matrix isolation – one of the most successful techniques of the "experimental astrophysics". Topics concentrated around specific molecules are reviewed in the third part. Finally, an outlook for further studies is presented.

I wish to thank all the friends, with whom I could share my astrochemical interests, who were the source of fruitful ideas, and whose work and advice greatly contributed to the subject, namely Zbigniew R. Grabowski, Jacek Waluk, Andrzej L. Sobolewski, and Jan Cz. Dobrowolski. Special thanks are due to Vladimir E. Bondybey and his matrix-isolation team in Garching – in particular to Alice M. Smith-Gicklhorn – for their fruitful offer to collaborate, rather than compete. I am indebted to Peter Botschwina (Göttingen), who took interest in a spectroscopic result obtained in Warsaw, eventually backing it with advanced calculations. I address my sincere *merci* to Jean-Pierre Aycard and his group, whose experimental work in Marseille supported the validity of a theoretical approach adopted here. Finally, my thoughts go to Jacek Krełowski and Andrzej Strobel, who once introduced me to the astrophysics of the interstellar medium.

Warsaw, May 2003

CONTENTS

I

The Interstellar Medium

I.1. Morphology of the interstellar medium

The gas and dust between stars account for at least 10% of the Galaxy mass. In fact, everybody can see it with a naked eye in form of dark patches or lanes that obscure the starlight and give to the Milky Way its familiar, irregular appearance. Such observations introduce the basic property of the interstellar matter, namely that a large part of it is clumped together in "clouds" rather than uniformly spread.

Several main forms of the interstellar medium (ISM) are traditionally distinguished. The *intercloud region* (number density[1] $n < 1$ cm^{-3}) and *diffuse clouds* (n = 10–100 cm^{-3}) are penetrated by the visible radiation. The *H II regions* (n = 100–1000 cm^{-3}) are dominated by the H^+ ion. *Dense* (also called *dark* or *molecular*[2]) *clouds* ($n = 10^4$–10^6 cm^{-3}), opaque in the visible, can be explored at microwave frequencies. The *translucent clouds* are intermediate between diffuse and dark ones. Typical kinetic temperatures vary from 10–20 K deep within dark clouds to ~100 K in diffuse clouds, to ~10 000 K in the intercloud space or in H II regions. From the laboratory standpoint even the "dense" interstellar clouds seem extremely diluted; their highest densities correspond to pressures of the order of 10^{-11} Torr, equivalent to a perfect ("ultra-high") vacuum.

It should be noted that the intercloud medium, diffuse clouds, and dense clouds are usually *near* the pressure equilibrium with each other: higher densities tend to be compensated by lower temperatures (Cole *et al.* 2002). Ideally, for an equilibrium to be reached, the processes of heating (mostly by cosmic rays), and those of cooling (*e.g.* by the excitation of atoms or molecules, and subsequent photon emission, or by the thermal emission from mineral grains) should be balanced. Lack of this balance leads to the evolution of clouds, which in fact takes place on a relatively short time scale (see the next section).

About 1% of the ISM mass is dust, most of it probably in form of submicron particles, mainly carbonaceous (soot-like) and silicate (sand-like). The remaining

---

[1] number of atoms or molecules per unit volume

[2] The author will follow the common practice of using these terms interchangeably. This seems natural, since the visual opacity of interstellar clouds is accompanied by the presence of polyatomic molecules. Some authors make the distinction between *dark*, *molecular*, and *giant molecular* clouds (Duley & Williams 1984), first of this terms covering optically thick clouds with linear dimensions of ~5 parsecs, the second one being reserved for larger (<30 parsecs) and very dense ($n \approx 10^6$ cm^{-3}) regions associated with some sources of excitation, and the last one for even larger (up to ~100 parsecs), relatively low density ($n \approx 600$ cm^{-3}) clouds. In fact, the morphology of interstellar clouds is a vast subject in itself, and involves additional characteristics, *e.g.* their proper motions (Heithausen 2001).

99% is the interstellar gas composed, to a good approximation, of just hydrogen and helium. The conversion of atomic hydrogen into H_2 molecules is partial in diffuse and almost total in dense clouds. A tiny admixture of other elements and molecules constitutes the base for astrochemistry. Table I.1 gives the topmost positions in the list of cosmic (solar) abundances. It should be noted that chief "life elements": oxygen, carbon, nitrogen, and even sulphur, are there.

Table I.1. Solar Abundances of Elements Relative to Hydrogen (Lang 1980)

Element	lg (n/n_H)
H	0
He	–1.16
O	–3.17
C	–3.43
N	–3.92
Ne	–3.97
Mg	–4.48
Si	–4.50
Fe	–4.58
S	–4.80
Ar	–5.43

I.2. Circulation of matter in the Galaxy

Molecular clouds are relatively quickly evolving, gravitationally unstable objects. Their lifetimes depend on size, and typically vary between 10^6 and 10^8 years. Clumps of matter within the clouds can collapse on a much shorter time scale. This process, with gravity converted to heat, eventually gives birth to stars.

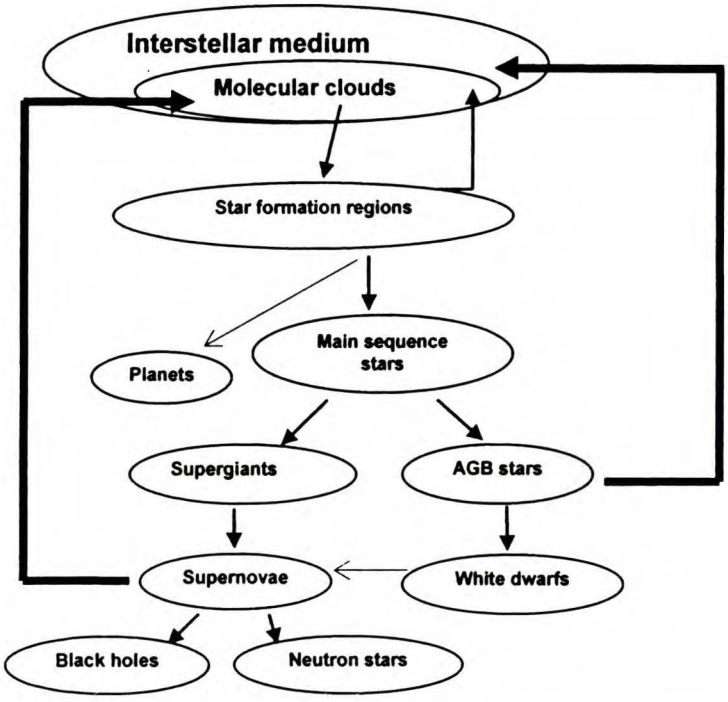

Figure I.1. Schematic representation of main Galactic mass flows. Relative sizes of fields do not correspond to their actual importance.

Stars continuously interact with the interstellar medium. In its early stage the young star (a protostar) expels much of enveloping dust and gas, often in form of concentrated bipolar jets (Shepherd & Churchwell 1996). Even when the hydrostatic equilibrium is reached, and the star calms down as a member of the main sequence on Hertzsprung-Russel diagram, it keeps on supplying some matter to ISM by stellar winds. The influence of short-living, high mass stars is very pronounced; as strong ultraviolet and far-ultraviolet emitters, they ionize the surrounding medium, producing brightly glowing HII regions. Further away, they

constitute a source of radiation for so-called photon-dominated (photodissociation) regions (PDR). The stellar radiation can also release the material accumulated on the surface of interstellar grains.

The star↔ISM interaction becomes dramatic towards the end of the stellar evolution. The most massive stars explode as supernovae, rapidly returning the matter, converted by the nucleosynthesis, to the ISM. Such stars live for too short a time to depart from the natal medium. Shock waves associated with supernovae may trigger local gravitational collapses within the molecular cloud, and thus promote the birth of new stars[1]. More common low-mass stars (< 6 solar masses) experience a gentler decay (Habing 1996). In the asymptotic giant branch (AGB) stage (a star similar to Sun enters it after ~10^{10} yr) they gradually loose outer shells until a small, extremely dense core is exposed. This produces very strong winds of gas and mineral particles. In fact, AGB stars are believed to be the main source of interstellar dust. The ejecta form a circumstellar envelope, which finally gives rise to a planetary nebula – a toroidal cloud of dust and gas. Planetary nebulae emit the radiation excited by UV flux from dead, yet still very hot central stars (white dwarfs). With time, the nebula is dispersed in space.

Processes of stellar decay eventually add matter to the ISM, which in the long run leads to the recreation of a molecular cloud. This is schematically depicted in Fig. I.1. Roughly a half of the stellar mass is expected to return to the ISM (Kaifu 1990). Both main sources of interstellar matter are important. Supernovae supply heavy and superheavy elements, while AGB and post-AGB objects release heavy elements. A substantial number of heavy atoms is bound within dust particles.

[1] Supernovae also inject heavy element coolants into space, which may locally lower the temperature and promote the compression of the surrounding medium (see preceding section).

I.3. Interstellar extinction features

The exploration of intercloud regions and diffuse clouds is traditionally (though not exclusively) accomplished by means of the optical spectroscopy. Grains of interstellar dust can scatter, polarize, and absorb the light on its way from distant stars to our instruments. The term *extinction* is used for the sum of scattering and absorption. Everyday experience proves that tiny particles (like those of smoke, fog or atmospheric dust) are more effective in scattering the blue then the red light, thus leading to the apparent reddening of light sources. The traditional measure of extinction – *color excess* – makes use of stellar magnitudes[1] B (*blue*) and V (*visual*), which correspond to standard photometric bands centered at 4350 and 5550 Å, respectively. The color excess is defined in terms of *color indices* (B – V) and $(B - V)_0$, derived, respectively, from apparent (*i.e.* observed) magnitudes, and the magnitudes of an unobscured standard star of a given spectral type:

$$E(B - V) = (B - V) - (B - V)_0$$

The higher the color index value, the more "red" the starlight is. Thus the color excess E(B – V) can be understood as an additional (*i.e.* higher than standard) reddening. Trumpler (1930) interpreted this addendum as due to interstellar effects.

On average, neglecting the highly inhomogeneous nature of the ISM, every 1000 parsecs[2] adds roughly 0.75 to the visual magnitude of a star (Lyngå 1982).[3] A similar law, 1 mag/kpc, was proposed already by Struve (1847), who rationalized the fact that the number of stars per unit volume apparently declined with the growing distance.

Analogous measures of the interstellar extinction are defined for other photometric systems, and for other spectral ranges, in particular for IR and UV (*e.g.* Gałęcki *et al.* 1983, Wegner 1995, 2002).

As long as there prevails just one type (size, composition) of grains responsible for the extinction, the "reddening curve" – usually defined as the optical density *vs.* λ^{-1} or $E(\lambda - V)/ E(B - V)$ *vs.* λ^{-1} – is expected to be a straight line (Huffman 1977, Whitford 1958). This indeed holds, to the first approximation, in the visible, as illustrated by Fig. I.2.

Ultraviolet measurements, however, revealed the presence of a broad and intense extinction feature (Stecher 1965) commonly known as the 2200 Å hump (or

---

[1] Brightness of astronomical objects is commonly measured in magnitude units. The *increase* of 5 magnitudes corresponds to the 100-fold *decrease* of luminosity in a given spectral range; photometry of standard stars defines the zero point of this logarithmic scale.

[2] Conversion factors for some non-SI units are listed in Appendix C.

[3] The validity of this law is currently being questioned (*e.g.* Galazutdinov & Galazutdinova 2003).

"bump") [1]. In the far-UV region the linear dependence of extinction on λ^{-1} is to some extent restored; deviations from the linearity, however, are often substantial, and may reflect the complex morphology of agents responsible for light scattering or absorption processes.

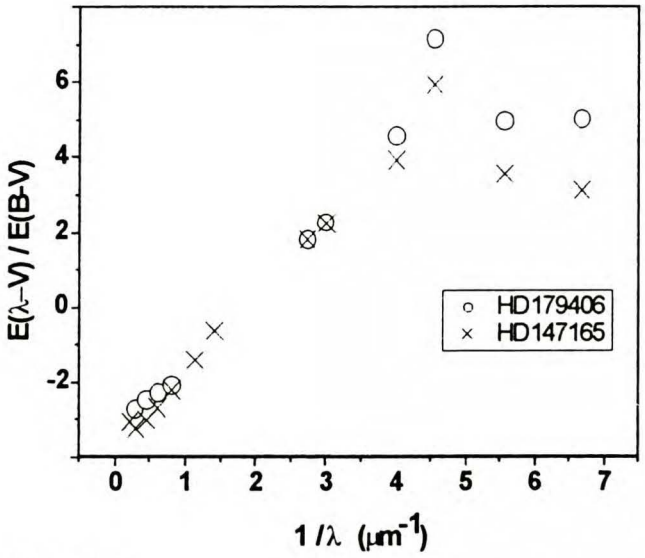

Figure I.2.
Interstellar extinction, as measured towards the stars 20 Aquilae (HD 179 406) and σ Scorpii (HD 147165). Adopted from the Wegner's (2002) atlas.

Generally, interstellar extinction characteristics for different lines of sight and for broad spectral ranges (Fitzpatrick 1999, Gnaciński & Sikorski 1999, Wegner 2002), may reflect the changing proportions of several major grain populations, as proposed by many authors, *e.g.* Kiszkurno *et al.* (1984) or more recently by Mathis (1996), Greenberg & Li (1996), Zubko *et al.* (1996, 1998) or Wegner (1995, 2002)

Apart from the 2200 Å hump (which is widely, though not unanimously[2], believed to be caused by graphite particles, as originally postulated by Stecher & Donn in 1965), the interstellar extinction curve exhibits more subtle features – the diffuse interstellar bands (DIB). These have been known for more than 80 years; first two bands being observed by Heger (1922). Their interstellar origin was established by Merill in 1934. Galazutdinov *et al.* (2000) list over 270 bands in a recent atlas. Some DIBs are partly correlated with the colour excess (Figure I.3.),

[1] Some authors refer to it by giving the more exact central wavelength of 2175 Å. This value is remarkably constant, deviations do not usually exceed 9 Å (Mathis 1990). However, large deviations (~100 Å) were also found.

[2] In fact, the combined absorption by any huge random collection of organic molecules is likely to show a broad maximum in a similar region of UV. This issue, however, has never been systematically studied.

i.e. with dust components of the ISM. The majority of current concepts link the DIB phenomenon to the interstellar gas rather than to dust (Snow 2001, Krełowski 2002); this line of research was pioneered by Douglas (1977), who suggested bare (hydrogen-less) carbon chains as their carriers.[1]

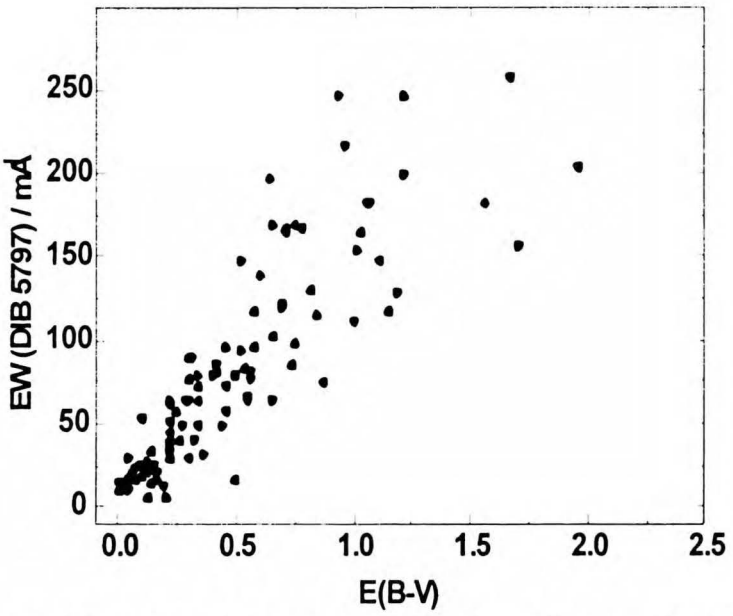

Figure I.3. Equivalent widths of the diffuse interstellar band 5797 Å, plotted against reddening. Points represent lines of sight towards 117 stars. The author is indebted to G. A. Galazutdinov for the access to observational data, prior to the publication.

The progress in the high resolution astronomical spectroscopy has permitted to detect, very recently, the substructure in some DIBs (Sarre *et al.* 1995, Galazutdinov *et al.* 2002a), see Figure I.4. These features often bear some resemblance to rotational envelopes in rovibrational bands of gas-phase molecules. Several research teams proposed particular molecular candidates for DIBs. These included open-chain species, like linear C_n and C_n^- clusters (Szczepanski *et al.* 2001), and specifically C_7^- (Kirkwood 1998) or C_5 (Galazutdinov *et al.* 2002b). Motylewski *et al.* (2000) proposed the dicyanoacetylene cation $C_4N_2^+$. Among the recommended branched species were propadienylidene, C_3H_2, neutral (Hodges *et al.* 2000) and anionic (Güthe 2001). The most appealing candidates for DIBs carriers from among more complex molecules are polycyclic aromatic hydrocarbons (PAH), both neutral (Léger & Puget 1984) and ionized (Léger &

[1] C_n chains are the structural units in *carbyne* (El Goresy & Donnay 1968, Whittaker & Kintner 1969, Kudryavtsev *et al.* 1997), a white allotropic form of elemental carbon, found *e.g.* in carbonaceous chondrites (Whittaker *et al.* 1980).

d'Hendecourt 1985, Crawford *et al.* 1985, Bréchignac *et al.* 2001, Hudgins *et al.* 2001), and fullerenes, in particular C_{60}^+ (Fulara *et al.* 1993). No unambiguous assignments were possible thus far[1], and the origin of DIBs remains one of the major astrophysical mysteries.

Discrete absorption features overlap the extinction curve also in the infrared range, as is briefly reviewed in Section I. 5.

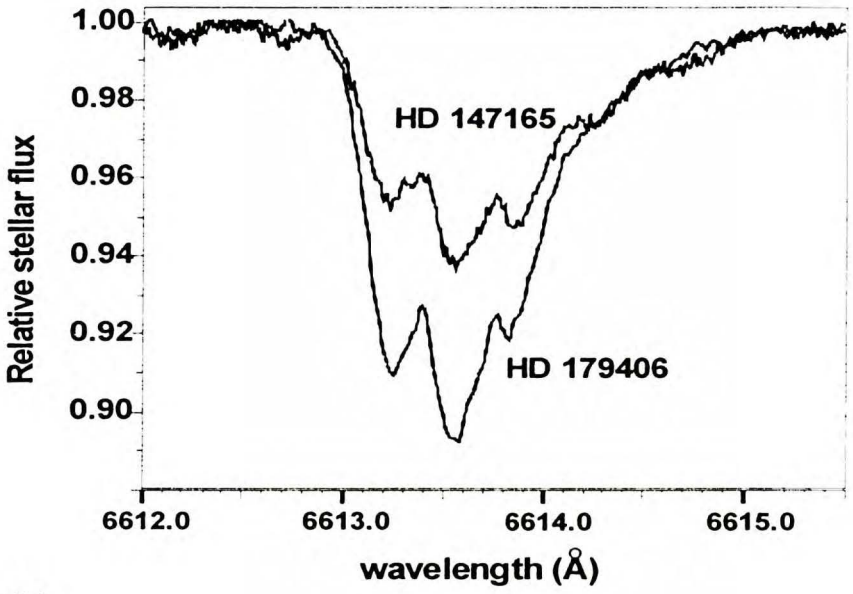

Figure I.4.
High resolution ($\lambda/\Delta\lambda$ = 220 000) profiles of the diffuse interstellar band 6614 Å obtained by Galazutdinov *et al.* (2002a) at the European Southern Observatory (3.6 m telescope) along lines of sight towards the stars 20 Aquilae (HD 179 406) and σ Scorpii (HD 147165). The author is indebted to G. A. Galazutdinov for numerical data.

[1] With the possible exception of C_{60}^+ (Foing & Ehrenfreund, 1994). Here, however, two weak near-IR interstellar absorption bands *supplemented* the known DIB collection, as a result of the search inspired by the experimental work of Fulara *et al.* (1993). The assignment, based on the comparison of neon matrix spectra to gas-phase interstellar bands, cannot currently be considered as absolutely irrevocable.

I.4. Interstellar molecules

In addition to diffuse interstellar bands, distinct optical absorption traces of *identified* atoms and molecules have been known for a long time to embellish the interstellar extinction curve. Interstellar calcium was recognized already by Hartmann (1904), who noticed that Ca lines in the spectrum of a binary system δ Ori were sharp and of constant intensity, in contrast to other (stellar) atomic lines, the latter being diffuse and variable[1]. Another important interstellar atomic species found at optical wavelengths was H^+ (Struve 1939).[2] Today the list of observed interstellar atoms and atomic ions includes H, H^+, Li, Li^+, C, C^+, N, O, Na, Na^+, Mg, Mg^+, Al, Al^+, Si, Si^+, P^+, S, S^+, Cl, Cl^+, Ar, K, K^+, Ca, Ca^+, Ca^{2+}, Ti, Ti^+, Mn, Mn^+, Fe, Fe^+, Ni, Ni^+, Cu, Cu^+, Zn^+ (Duley & Williams 1984)

Spectra of simple *diatomic* constituents of the interstellar gas: CH, CN and CH^+ were detected in space by Swings & Rosenfeld (1937), McKellar (1940), Douglas & Herzberg (1941). For almost three decades following these discoveries astronomers generally considered the interstellar presence of more complicated molecules as highly unlikely, a conviction not altered even by the very advent of radio astronomy – the first molecule detected with microwaves, was another diatomic: OH (Weinreb *et al.* 1963) [3].

The situation changed dramatically when Cheung *et al.* reported on the detection of the microwave transitions of interstellar ammonia (1968) and water (1969). Even more impressive, an interstellar *organic* compound, formaldehyde, was found (Palmer *et al.* 1969). The current list of interstellar molecules (see Appendix *A*) holds more than one hundred entries, roughly half of them organic. The list is usually appended with some three species every year.

Gas phase reactions occur most efficiently when the density of the ISM is high enough to enable a non-negligible rate of collisions, while the temperature remains sufficiently low to guarantee the stability of molecules formed.[4]

It has to be stressed that the interstellar chemistry generally deals with isolated molecules or collision complexes; the surrounding medium – even when formally named "dense" – does not provide a bath to thermalise them. Thus, the removal of the excess energy becomes one of key problems.

Seemingly the simplest of chemical processes in space, that of molecular

---

[1] Further studies of interstellar calcium led Gerasimovič & Struve (1927) to the conclusion that the interstellar matter was diffuse and pervasive, *i.e.* that its occurrence was not a local phenomenon, confined to individual stars or star systems.

[2] The recombination of protons with free electrons is accompanied by the emission of radiation.

[3] At present times, the most important species studied at radio wavelengths are H (21 cm) and CO (2.6 mm), which enable to map the distribution of the interstellar matter in the Galaxy.

[4] Still, the collisions are rare phenomena, by laboratory standards. An atom or molecule collides with another one (usually: with hydrogen, H or H_2) on average every $300/n$ years (Watson 1976), where n stands for ther gas density in cm^{-3}; this is equivalent to a dozen of days for a medium density cloud, $n = 10^4$ cm^{-3}.

hydrogen synthesis $H+H \rightarrow H_2$, supplies the dramatic example of the energy removal problem. First of all, H_2 is *not a polyatomic* product – had it been, the main share of the excess energy could have quickly left the dissociative vibration, being distributed among other internal degrees of freedom. Secondly, this reaction yields *a single product*. Had at least two species appeared, some of the excess energy might have been carried away in form of their kinetic energy. All considered, interstellar molecular hydrogen can not be formed this way. The plausible mechanism involves the surface of grains (Duley & Williams 1984):

$$H + H + \text{grain} \rightarrow H_2 + \text{grain}$$

The third body is necessary to carry out the reaction energy, and thus stabilise the newly formed molecule[1]. On the other hand, the collisions of as many as three atomic or molecular constituents of the interstellar gas are extremely unprobable. Consequently, the molecular hydrogen and interstellar dust have to be closely related.

Graedel *et al.* (1982) estimate that more complicated interstellar chemistry (*e.g.* Winnewisser 1981, Williams 1986, Smith 1992) becomes important when *ca.* 20% of atomic hydrogen is converted into H_2. First key steps consist in the ionization by cosmic rays. The cosmic rays (*C.R.*) flux is rather low (which, in the long run, makes the survival of molecules possible), and as such can directly produce a significant concentration only of those ions, which originate from most abundant species (H, H_2, He).

$$H \xrightarrow{C.R.} H^+ + e$$

$$He \xrightarrow{C.R.} He^+ + e$$

$$H_2 \xrightarrow{C.R.} H_2^+ + e$$

H_2^+ is quickly (on the timescale of hours, in dense clouds) transformed into H_3^+, the simplest polyatomic molecule:

$$H_2^+ + H_2 \rightarrow H_3^+ + H$$

This ion-molecule reaction proceeds with no activation barrier, in contrast to very inefficient ones $H^+ + H$ or $H^+ + H_2$. In diffuse clouds, penetrated by UV photons, the photoionisation of carbon atoms is also important:

$$C + h\nu \rightarrow C^+ + e$$

---

[1] Generally, atomic collisions are ineffective in the absence of the third body, save the habitually negligible radiative association (Gerlich & Horning 1992).

In dense clouds C^+ ions are believed to be mostly formed in the exothermic reaction, which involves CO. Carbon monoxide[1] (perhaps along with C_2) is the main reservoir of interstellar carbon.

$$He^+ + CO \rightarrow He + C^+ + O$$

Hydrogenation processes listed below (Williams 1986) precede the formation of more complex species.

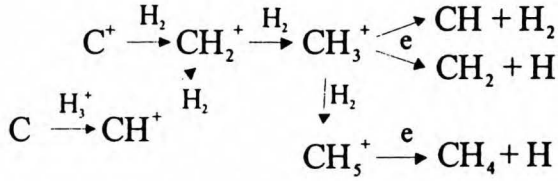

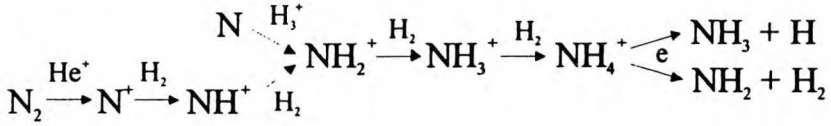

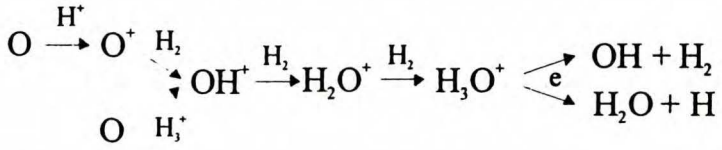

The *dissociative recombination* reactions, which terminate each of the chains above, merit some special attention. Processes of this type proceed with virtually no activation barrier, and cleave the ion into fragments; the latter carry off the dissociation energy by their translational movement.

Growing of the carbon skeleton can be accomplished in reactions starting with

$$C^+ + CH_4 \rightarrow C_2H_2^+ + H_2$$
$$C_2H_2^+ + e \rightarrow C_2H + H$$

$$C^+ + CH_4 \rightarrow C_2H_3^+ + H$$
$$C_2H_3^+ + e \rightarrow C_2H_2 + H\,,$$

[1] Reaction $C^+ + OH \rightarrow CO + H^+$ is commonly proposed as the main source of interstellar CO.

after which the condensation, *e.g.*

$$C_2H_3^+ + C_2H_2 \rightarrow C_4H_3^+ + H_2$$

or carbon insertion reactions of the general form

$$C^+ + C_mH_n \rightarrow C_{m+1}H_{n-1}^+ + H$$

are possible. The neutralization is achieved by the dissociative recombination:

$$C_{m+1}H_n^+ + e \rightarrow C_{m+1}H_{n-1} + H$$

The carbon-nitrogen bond formation is best exemplified by the synthesis of hydrogen cyanide, which starts with the creation of H_2CN^+ (Smith 1992):

$$NH_3 + C^+ \rightarrow H_2CN^+ + H$$

$$CH_3^+ + N \rightarrow H_2CN^+ + H$$

H_2CN^+ was shown by Conrad & Schaefer (1978) to rearrange itself to the more stable linear isomer $HCNH^+$. Qualitatively, $HCNH^+$ is as good a precursor for HCN as it is for hydrogen isocyanide, HNC (Watson 1976, Herbst 1978):

$$HCNH^+ + e \rightarrow HCN + H$$

$$HCNH^+ + e \rightarrow HNC + H$$

All species involved in this mechanism were detected in space. The scheme agrees well with a near-unity relative abundance of HCN *vs.* its higher energy isomer HNC (Table I.2).[1]

Table I.2 Fractional abundances of HCN and HNC isomers in dark interstellar clouds TMC-1 and L134N, with respect to H_2 (Ohishi *et al.* 1992).

	TMC-1	L134N
HCN	2×10^{-8}	4×10^{-9}
HNC	2×10^{-8}	6×10^{-9}

[1] HNC is *ca.* 15 kcal/mol richer in energy than HCN (Pau & Hehre 1982). In hot interstellar sources, like OMC-1 the lower energy isomer clearly prevails, probably due to the H + CNH ↔ HCN + H exchange reaction (Talbi *et al.* 1996).

The possible routes leading to interstellar cyanoacetylene – which is the archetype for a whole family of compounds (related isomers and *poly*cyanoacetylenes) found in space – were thoroughly analyzed. It was found that in addition to the ion-molecule scheme (Morris *et al.* 1976, Freeman *et al.* 1979, Osamura *et al.* 1999) below:

$$C_2H_2^+ + HCN \rightarrow HC_3NH^+ + H$$
$$C_2H_2^+ + HNC \rightarrow HC_3NH^+ + H$$

$$HC_3NH^+ + e \rightarrow HC_3N + H\,,$$

the neutral-neutral reactions should be taken into account (Herbst & Leung 1990, Woon & Herbst 1997, Fukuzawa & Osamura 1997, Balucani *et al.* 2000, Huang *et al.* 2000), in particular

$$C_2H_2 + HCN \rightarrow HC_3N + H$$

The interstellar synthesis of cyanoacetylene and its isomers will be discussed thoroughly in Section III.1*f*.

As first postulated by Herbst & Leung (1990), the termination of a carbon backbone with the nitrile group may be accomplished in reactions like:

$$C_4H_2 + HCN \rightarrow HC_5N + H$$

It is anticipated that the longer $HC_{2n+1}N$ chain is, the more time it takes to synthesize it in space. This inspired Strahler (1984) to formulate the *chemical clock* concept: use abundances of longer cyanoacetylenes as age indicators for a molecular cloud. In fact, only the fastest reactions (those characterised by bimolecular reaction rates $\sim 10^{-10}$-10^{-9} cm^3 s^{-1}) can contribute to the interstellar chemistry of highly diluted (*e.g.* 10^{-4} cm^{-3}) species, slower processes may prove inefficient in, say, 10^6 years of the cloud lifetime.

It has to be pointed out that ion-molecule reactions were originally selected as an obvious choice for the modeling of interstellar chemistry, since these are usually exothermic and require negligible activation energies (Smith 1992). However, numerically simulated processes of this type, though fast, often fail to synthesize polyatomic molecules in their observed concentration ratios. The rôle of neutral-neutral reactions was recognized rather recently (Herbst & Leung 1990, Chernchеff & Glassgold 1993, Clary *et al.* 1994; Kaiser & Suits 1995; Bettens, Lee & Herbst 1995, Kaiser 2002); somewhat lower rate constants are often compensated by higher abundances of neutral precursors when compared to ionic species. For example, the rate constants for reactions with acetylene are $k(C^+) = 2.6\times10^{-9}$ cm^3 s^{-1} (Jonas *et al.* 1992), and $k(C) = 2.0\times10^{-10}$ cm^3 s^{-1} (Clary *et al.* 1994) – but $[C]/[C]^+$

ratios in the range 30-150 are found in molecular clouds and circumstellar envelopes (Le Bourlot *et al.* 1993). Reactions between neutral polyatomic molecules were also proposed to explain the growth of carbon chains (Cherchneff *et al.* 1993).

The occurrence of HC_n and HC_nN homologous series is perhaps the most striking feature of the molecular composition of ISM. Interestingly, subsequent members of these series, differing by the carbon chain length, often appear with quite comparable column densities when observed in the same source (Tables I.3 & I.4).

Table I.3
Column densities (in cm^{-2}) of HC_n molecules (Winnewisser & Walsley 1979).

source	HC_2	HC_3	HC_4
TMC 1	5×10^{13}	5×10^{12}	5×10^{13}
IRC +10°216	5×10^{14}	3×10^{13}	4×10^{14} to 3×10^{15}

Successive members of the cyanopolyyne series (easily detectable because of their high polarities; Kroto *et al.* 1978) usually differ in abundances by a factor of 2 to 5 in TMC1 and in smaller Taurus cloudlets (Bell & Matthews 1985, Cernicharo *et al.* 1986). For higher members of the series, the decrement factor, as measured by Bell *et al.* (1997), is close to 6. Similarly, in the circumstellar shell around IRC +10°216 the amounts of consecutive cyanopolyynes do not differ very much.

Table I.4 Column densities (in cm^{-2}) for cyanopolyynes, $H(C\equiv C)_nCN$; after Winnewisser & Walsley (1979), unless otherwise noted.

source	HCN	H-C≡C-CN	$H(C\equiv C)_2CN$	$H(C\equiv C)_3CN$	$H(C\equiv C)_4CN$
TMC 1	10^{14}	6×10^{13} [d]	3.5×10^{13} [b]	1.4×10^{13} [b,e]	3×10^{12} [f]
L 183	3×10^{12}	10^{12}	2×10^{12} [c]		
Ori A	10^{15}	2×10^{13}	2×10^{12} [d]		
Sgr B2		2×10^{14}	2×10^{14}		
Sgr A		10^{15} [a]			
IRC+10°216	10^{15}	2×10^{14}	4×10^{14}	10^{14}	

[a] 8×10^{14} to 1.4×10^{15} cm^{-2}, dependent on the location (Walmsley *et al.* 1986)
[b] Cernicharo *et al.* (1986)
[c] Benson & Myers (1983)
[d] Irvine *et al.* (1987); other results are higher: 1.3×10^{14} (Avery 1980) to 1.7×10^{14} cm^{-2} (Suzuki *et al.* 1992)
[e] 1.1×10^{13} cm^{-2} according to Bell *et al.* (1997)
[f] 1.9×10^{12} cm^{-2} according to Bell *et al.* (1997)

Taking into account the large margins of error, the abundances of free radicals HC_2 and HC_4 can be regarded as roughly equal (these of HC_3 are by one order of magnitude lower), irrespective whether in the cold and dark Taurus Molecular Cloud, or in a rather warm expanding envelope of the carbon star IRC +10°216.

What is the cause for the strikingly high abundance of relatively large, unsaturated molecules in a generally harsh and reductive (hydrogen-rich) medium? The preference for unsaturated compounds most probably results from an important selection factor: the stability of multiple bonds against the photodissociation. To understand the profusion of large species, one should invoke some chemical kinetics.

The concentration $[M]$ of a given species M depends on the difference between formation and decay rates. In the stationary state approximation:

$$\frac{d[M]}{dt} = 0 = \sum_i k_{f,i}[P_i] - [M]\sum_j k_{d,j}$$

where $k_{f,i}$ represent rate constants for the formation of M from precursors P_i, while $k_{d,j}$ are the rates of the decay of M in different processes, j. Mechanisms in favour of relatively large species can be expected in the formation, as well as in decay processes.

In pure bimolecular reactions, the efficiency of encounters is strongly dependent on the complexity of reactants. As discussed above, collisions between two hydrogen atoms cannot be expected to yield a molecule in interstellar conditions. The reaction of two diatomic species may still need a third body to remove the excess energy from the collisional complex. Radiative deactivation rates are by many orders of magnitude slower than the dissociation. With growing molecular complexity (increasing number of vibrational modes, increasing density of rotational levels) the lifetime of the collisional complex and the probability of effective reactions increase. Indeed, a stimulating finding related to chain growth reactions, was that neutral C atoms react with neutral hydrocarbons with rates *increasing* (yet slowly) with the hydrocarbon chain length: $k \sim \sqrt[3]{n_C}$, n_C being the number of carbon atoms in the molecule (Clary *et al.* 1994).

Aside from exceptionally rare collision-induced processes, the decay of any interstellar molecular species, M, can result from the absorption of a visible or UV photon. A molecule in its electronic excited state M^* undergoes several competitive processes:

$M^* \rightarrow$ products	photodissociation, k_{dis}
$M^* \rightarrow M^+ + e^-$	photoionisation, k_{ion}
$M^* \rightarrow M + h\nu$	luminescence emission (radiative transition), k_{rad}
$M^* \rightarrow M$	nonradiative transition, k_{nrad}

The first two processes contribute to the decay rate, the last two preserve the identity of M. The radiative lifetime, $\tau_{rad}=1/k_{rad}$, represents the average lifetime of

M^* in the absence of all other competitive deactivation channels. The photodissociation efficiency of the excited molecule can be expressed as $k_{dis}/(k_{dis}+k_{ion}+k_{rad}+k_{nrad})$. From among these rates, k_{dis} decreases with the growing molecular complexity (Stevens 1957), provided the excitation is delocalized (Bersohn 1987).

For isolated molecules, the *nonradiative transitions* denote internal processes of equienergetic electronic to rovibrational energy transfer; the electronic excitation energy being redistributed to a multitude of vibrational and rotational levels. These levels act as an inner thermal bath, effectively diminishing the average energy in any vibrational mode of the molecule, including the dissociative modes. Vibrational or rotational emission (IR or microwave, respectively), may eventually occur and stabilise the ground, usually bound, electronic state. The nonradiative rate k_{nr} dramatically increases (given the same energy gap between upper and lower electronic states), from virtually zero in diatomic molecules to very high values with a growing density of rovibrational states, equienergetic with the excited electronic state M^* (Jortner & Bixon 1968, Jortner *et al.* 1968). The photo-stability of larger molecules has already been indicated as an evolutionary preference for the growth of carbon chains in the discussion on the diffuse interstellar bands (Douglas 1977). Similar arguments apply to the expected abundance of polycyclic aromatic hydrocarbons.

Prior to a brief outline of the possible rôle of interstellar dust particles in the synthesis of complex compounds, it should be stressed that the importance of gas phase processes is backed with ample evidence. Many specific relations between observed abundances of chemical constituents of the ISM are modelled by ingenious sets of known or suggested gas phase reactions and their rates (e.g. Bettens, Lee & Herbst 1995, Terzieva & Herbst 1998). The predicted ratio of [HNC]/[HCN] (discussed above) serves as a very good illustration. Another example is the agreement with observations achieved for the C_3H_3 cyclic-to-linear ratio (Kaiser *et al.* 1996). Also, such specific features as the isotopic enrichment in deuterated molecules observed for dark clouds (Duley & Williams 1984) were explained, basing mostly on laboratory gas-phase data.

Mineral dust is formed at relatively high gas densities, in outer atmospheres of cool stars (see Section I.2). The possible function of these particles in the interstellar chemical synthesis is an old concept. A well known *core-mantle* idea (van de Hulst 1949, Greenberg and Hong 1974, Greenberg 1976, Allamandola 1990, Sandford *et al.* 1991) assumes covering a cold, submicron mineral grain (in molecular clouds, away from the site of the *core* nucleation) with a layer (*mantle*) of easily condensable atoms (mainly O, C and N) or simple molecules.[1] These would react with hydrogen to yield the *dirty ice*, a mixture of species like H_2O, NH_3, CH_4 or CO. Such a solid is likely to undergo important transformations within the radiation field; intermediately created radicals would initiate the production of complex compounds. It sholud be remarked that the neighbourhood of any molecule in the mantle, and hence the choice of feasible reaction products, is purely accidental.

[1] The issue of interstellar H_2 solids will be invoked in Section II.4.

Along with some "dark" reactions (often proceeding *via* a tunneling mechanism), one can expect radiative or high energy particle excitations within the mantles, leading either to dissociation or ionisation, and subsequently to reactions with neighbouring molecules. On grain surfaces, and within the bulk mantle, the concentration of potential reactants is very high – unlike in the gas phase. The reaction (or a whole chain of reactions) between adjacent molecules can be triggered with the absorption of a single UV photon. The reaction heat, temporarily softening the matrix in the vicinity of the reaction site, should dissipate in the surrounding solid, provided the grain is large enough. This mechanism may efficiently produce quite complex compounds. All that should result in the molecular growth, „knitting together" small chemical species and ending, possibly, with the formation of irregular macromolecules, as those found in carbonaceous chondrites, similar to synthetic *tholines* (Sagan & Khare 1979). Far-reaching hypotheses exist (Goldanskii 1977), which assign to "dirty ices" some prebiotic importance, and treat the interstellar grains as plausible „cold seeds of life".

Releasing the molecules to gas may occur either in the collisional sputtering, thermal heating, or due to the photodesorption. Another process, in which many reactive species (predominantly free radicals) are likely to be formed, consists in an explosive disruption of the mantle. Indeed, it seems likely that the thermal softening of ices may start the diffusion of reactants; a chain of highly exothermic processes would eventually end up with the sudden desorption (Schutte & Greenberg 1991). The properties of interstellar dust (largely deduced, partially known from experiments) are successfully used to model the physics of comets (Greenberg & Hagen 1990). Remarkably, complex organic species including cyanoacetylene, found in recent studies on comet Hale-Bopp, may point to a close relation between cometary and interstellar material (Bockelée-Morvan *et al.* 2000).

Chemical models of dense interstellar clouds exist (Hasegawa & Herbst 1993a,b; Shalabiea & Greenberg 1994) which include both gas-phase and dust surface reactions.

I.5. Infrared spectroscopy of the ISM

The very existence of ISM became evident due to the interpretation of observational data gathered in the visible spectral region. Yet the majority of contemporary knowledge on the chemistry of ISM comes from radio-astronomical observations or, more specifically, from the microwave emission spectroscopy. In particular, it is *via* microwave rotational spectra that cyanoacetylene, its isomers, and polycyanoacetylenes were detected. Microwave spectroscopy supplies ground state rotational constants – the basic molecular parameters, directly related to interatomic distances and angles. The interplay of observational output, laboratory spectra and theoretical predictions more often than not led to unambiguous assignments. While radio telescopes will certainly continue to extend the list of interstellar molecules[1], the limitations of this technique are evident. Microwave rotational spectra can only be detected for species bearing a non-zero permanent electric dipole moment. Thus, current listings of interstellar molecules (*cf.* Appendix *A*) inevitably suffer from an unwanted selection effect: non-polar (highly symmetric) species are eliminated, just as those, which bear only small dipole moments.

It is an obvious choice to employ the infrared spectroscopy as an alternative or complementary spectroscopic tool. Indeed, in spite of problems posed by the atmospheric absorption and by low sensitivity of detectors, astrophysicists were interested in the IR region for a relatively long time. The infrared photometry supplied additional data on the interstellar extinction curve, and on the morphology of interstellar dust grains in different lines of sight (Wegner 1995, 2002). Main IR absorption features were assigned to solid particles, the most important of these being perhaps the solid water band at 3.08 μm (Gillet & Forest 1973). Meticulous studies of this feature revealed that it could not be explained by pure H_2O ice; model calculations predicted the admixture of molecules like H_2CO, N_2, O_2, CO_2, H_2O_2, or NH_3 (Tielens & Hagen 1982).

Silicate bands were found at 9.7 μm (Si—O stretching vibration) and 18 μm (Si—O—Si bending mode). Also, the C—H stretch, an obligatory feature of hydrocarbons, shows up at 3.4 μm. In addition to these, the so called unidentified infrared bands (UIB) were observed *in emission*. Their wavelengths, 3.3, 6.2, 7.7, 8.6, and 11.3 μm quite closely correspond to C—H and C—C vibrations in aromatic molecules, and as such are often attributed to mixtures of UV-excited polycyclic aromatic hydrocarbons, either neutral or partly ionized (Léger & Puget 1984, Léger *et al.* 1989, Allamandola *et al.* 1985, 1989, 1999). An alternative explanation of the UIB phenomenon involves carbon chain anions C_{2n}^- (Szczepanski *et al.* 2001).

[1] In fact a number of detected interstellar microwave lines still awaits the identification.

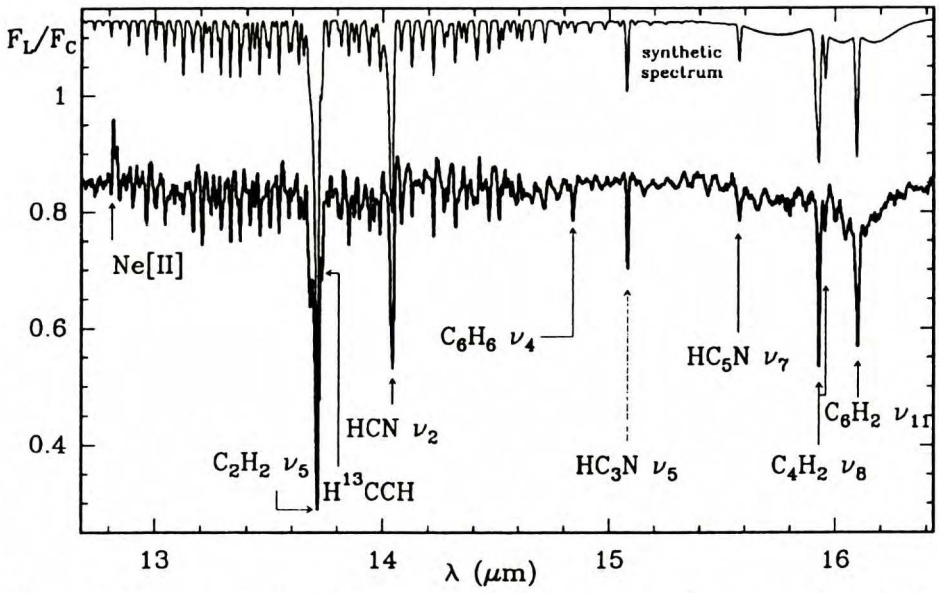

Figure I.5. IR absorption features observed in a protoplanetary nebula CRL 618 by the Short Wavelength Spectrometer aboard ISO satellite (Cernicharo *et al.* 2001). F_L/F_C is the relative stellar flux (line-to-continuum ratio). The author is greatly indebted to José Cernicharo for the original artwork, which is reprinted here by permission of the American Astronomical Society.

The two very important discoveries, accomplished at IR wavelengths, should be emphasized. First of these is the direct prove for the existence of bare carbon chains in space (*cf.* Section I.3) – the finding of rovibrational bands of C_3 (Hinkle *et al.* 1988) and C_5 (Bernath *et al.* 1989) around the carbon star IRC +10°216. The second one consisted in the detection of interstellar H_3^+ (Geballe & Oka 1996), a long sought-after molecule, often regarded as the corner stone of interstellar cloud chemistry (*cf.* Section I.4). Indeed, the vibrational spectroscopy was the technique of choice, since none of these species could be detected by pure rotational transitions[1]. Moreover, the electronic spectrum is missing for H_3^+ (no bound excited electronic state[2]).[3] Oka and co-workers managed to detect H_3^+ not only in the dense interstellar medium; the species was also found, as the first polyatomic molecule, in diffuse clouds (McCall *et al.* 1998). Very important in these observations was that they introduced IR spectroscopy as the tool for unambiguous identifications of crucial circum- and interstellar molecules, and opened up the way to similar future

[1] C_3 and C_5 are centrosymmetric, while H_3^+ has but a very small dipole moment (Oka 1983).
[2] Except for a high-lying triplet state (the ground electronic state is of singlet multiplicity).
[3] The interstellar electronic spectrum of C_3 *was* detected (Maier *et al.* 2001, Galazutdinow *et al.* 2002c, Oka *et al.* 2003), while for the interstellar C_5 only an upper abundance limit could be derived from optical observations (Galazutdinov *et al.* 2002b).

achievements.

United Kingdom Infrared Telescope (UKIRT), with which H_3^+ was detected, is probably the best ground based IR instrument for astronomy. Next great discoveries, however, came from the Infrared Space Observatory (ISO), active within the period 1995-1997. An ISO satellite, operated by the European Space Agency, not only offered the possibility to perform observations outside the Earth's strongly absorbing atmosphere – it also gave the unparalleled sensitivity.

Four important new molecules (all of them around the protoplanetary nebula CRL 618) were so far disclosed in rich ISO archive: acetylene, di- and triacetylene, and benzene (Cernicharo *et al.* 1999, 2001). The discovery of these highly symmetrical molecules, beyond the grasp of microwave rotational spectroscopy, nicely demonstrates the main advantage of IR observations. Another potential benefit stems from the fact, that IR spectral continuum sources are more common than continuum radio sources. Thus, the astronomical molecular microwave spectra are only rarely observed in absorption. Rather, the rotational emission is detected, which requires certain excitation, mostly of thermal (collisional) origin. Infrared spectra, on the other hand, are easily seen in absorption, giving the possibility to spot the chemical species, which reside in extremely cool regions.

Along with new species, ISO detected some of those already known (from other spectral ranges), among them cyanoacetylene and hydrogen cyanide. The telltale IR spectrum of CRL 618, obtained by Cernicharo *et al.* (2001), is shown in Figure I.5.

II

A Laboratory Approach to Exotic Chemical Species

II.1. Principles of rare gas matrix isolation

This classic technique, which makes use of rare gas (RG) solids for the isolation and spectral characterization of chemical species, stems from two, initially separate, fields. First, it was noticed towards the end of 19th century that the phosphorescence of many substances, organic and inorganic, increased – in intensity as well as in duration – with decreasing temperature. The effect was perfectly clear in experiments performed by Dewar (1894), who cooled luminescent solutions down to the liquid air temperature. In the beginning, this cryogenic spectroscopy was carried out exclusively in emission; the samples scattered light heavily, and as such were useless for optical absorption measurements. With time, highly transparent glassy solutions were mastered, like the famous "EPA" mixture[1] found by Lewis & Kasha (1945). Frozen hydrocarbons (Shpol'skii & Personov 1960), or organic glasses like EPA, are still important media for many photophysical studies.

The second foundation of contemporary matrix isolation technique consists in pioneering studies performed by Vegard (1924), and by McLennan & Shrum (1924), who irradiated RG solids with X-rays and electrons to excite the luminescence from intentionally added atmospheric gases. The goal was to explain the origin of auroral light. Experiments with frozen rare gases were extremely difficult at the time, and required the ability to liquefy helium; Vegard collaborated with famous Dutch physicist Heike van Kamerlingh Onnes, Mc Lennan was able to produce large quantities of liquid He himself.

It took further three decades until the cryogenic technique sufficiently matured, and until the true value of solidified inert gases for spectroscopic work was recognized by George C. Pimentel. The resulting article (Whittle *et al.* 1954) opened up a vast research field (Andrews & Moskovits 1989). The new medium turned out to possess at least three crucial advantages:

- chemical inertness;
- no absorption throughout an extremely broad spectral range, from far-IR to vacuum-UV;
- ability to form clear (*i.e.* non-scattering) polycrystalline samples.

With such characteristics inert gas solids offer the perfect environment for an *in-situ* generation, trapping and conventional spectroscopy of reactive chemical compounds, such as free radicals, ions or highly strained molecules. Alternatively, such species can be studied by complicated time-resolved methods, often applicable only to well-chosen systems. The technique of matrix isolation is sometimes employed also for stable compounds. Corresponding spectra are usually well resolved – weak guest-host interactions result in but a small inhomogenous

[1] Ether, isopentane and alcohol (ethanol) in a 5:5:2 ratio.

broadening (Bajdor *et al.* 1999).

Small hydrogenated and deuterated species, *e.g.* OH, NH, hydrogen halides, water, ammonia, and H_2 itself, can rotate in matrices almost freely. The rotation of heavier species is hindered. Diatomics like CO, NO, CN, N_2 perform only the librations (torsional vibrations around equilibrium positions); for other molecules the rotational movement is completely suppressed.

Table II.1

Selected parameters of inert gas solids, after Jodl (1989) and Meyer (1971)

		Ne	Ar	Kr	Xe	N_2
Atomic (molecular) diameter (Å)		3.0	3.8	4.4	4.6	4.3/3.4
Lattice constant (Å)		4.47	5.31	5.65	6.13	5.66
Substitutional hole (Å)		3.16	3.75	3.99	4.34	3.99
Polarizability (Å^3)		0.39	1.63	2.46	4.02	1.76
Lennard-Jones ε (cm^{-1})		24.3	84.0	118.2	155.0	66.3
Lennard-Jones σ (Å)		2.76	3.41	3.62	4.03	3.75
Compressibility (10^{-11} cm^2/dyne) at 4.2 K		10.1	3.9	3.9	2.8	4.6
Triple point	(K)	24.6	83.8	115.8	161.4	63.15
	(bar)	0.43	0.69	0.73	0.81	0.13
Sublimation temp. (K) at 10^{-6} Torr		9	31	42	58	

Table II.1 lists selected properties of most important inert gas matrices. Neon is the most inert of these, as indicated by its lowest polarizability and, consequently, the lowest gas-to-matrix spectral shifts. Ne matrices are also known to be of particularly good optical quality. It should be noticed, however, that solid Ne is remarkably soft (highly compressible). This may be a drawback in some applications, for example when the matrix rôle is to hold highly strained molecules. Krypton and xenon are less inert but much easier to condense (in fact, this was the reason why the first RG matrix isolation study, by Pimentel, made use of xenon). Moreover, Xe and Kr introduce an external heavy atom effect (Birks, 1975), which was found to be of crucial importance for some applications, like the single molecule fluorescence spectroscopy in matrices (Sepioł *et al.* 1999). Some less common materials, often regarded as inert, include H_2, D_2, SF_6, CH_4, or even water. Yet, argon matrices are the most popular and versatile, due to their high inertness, relative ease of preparation, agreeable optical characteristics, and low cost.

IR frequency shifts of matrix-isolated species, with respect to the gas phase, are generally small. As analysed by Jacox (1984, 1985), for most diatomics these are within ±1%, and only seldom fall out of ±2%. The shifts usually increase in the order of the increasing host polarizability *i.e.* Ne<Ar<Kr<Xe; red shifts (*i.e.* towards lower frequencies) are more common then blue shifts.

The very simple principles of inert gas matrix preparation did not change for half a century. The host gas is mixed with a chemical substance of interest, admitted through a nozzle to the vacuum chamber of the cryostat, and solidified onto a cold surface therein (Dunkin 1998).

For guest substances characterized by a sizeable vapour pressure, the host-guest mixture can be prepared at room temperature. This is achieved by routine gas handling operations within the vacuum line; finally the gas is expanded to the vacuum through a nozzle, towards the cold target surface. The flow rate, or the *deposition rate*, is usually within the range of 1 to 60 milimols of total gas per hour. Less volatile compounds have to be evaporated, typically inside the heated nozzle. The standard value of the *matrix ratio*, *i.e.* the host-to-guest proportion is of the order of 1000. The target (a window or a reflective metal surface) is attached to the "cold finger" of the cryostat. The selection of window materials (*e.g.* fused silica, fluorite, alkali metal halides) depends on the spectral range of interest. Conventional liquid helium cryostats are expensive to run, but remain the best choice for special spectroscopic tasks, where lowest temperatures and/or extremely low mechanical vibration levels are necessary. For the majority of applications, however, the advantages of closed cycle helium refrigerators are unquestionable. These devices rely on compression and subsequent adiabatic expansion of He, usually in two stages; temperatures well below 6 K (low enough to solidify Ne) are possible with high-end models. The routinely achieved low temperature limit of 10-12 K permits to obtain standard argon matrices.

The rigidity of matrices deserves an additional comment. As stated above, this characteristic is an obvious asset, which makes possible to isolate the molecules from each other. However, one can intentionally warm up the sample to increase the diffusion coefficient, and to let the molecules reorient or even migrate through the matrix. This is usually done in three steps known as the "annealing": the temperature is first appropriately raised, than kept high for a certain amount of time, and finally lowered again to the original value. Various bands often behave differently upon annealing, which may facilitate their assignment. Furthermore, the annealing may promote the chemical reactions within matrices.

II.2. Formation and identification of transient species in rare gas solids

The main advantage of the inert gas matrix technique consists in its capacity to isolate otherwise unstable molecules. Therefore, the *production* of "unusual" chemical compounds is a closely related issue. Although a multitude of methods exist[1], just two principally dissimilar approaches can be discerned. The species of interest may either *i*) arise within the matrix ("*in situ*"), after the isolation of a suitable precursor compound, or *ii*) be generated at some distance from the cold surface (usually in its close vicinity), mix with the host while in the gas phase, and eventually get embedded within the matrix.

Either way, the challenges encountered by an experimentalist, who isolates exotic molecules in matrices, quite often consist not in the scarcity of species obtained – but rather in their overabundance and/or in difficulties with making proper spectral assignments. The first problem can be solved by the suitable choice of precursor molecules and dissociation methods (photolysis *vs.* discharges, appropriate irradiation wavelengths/intensities, *etc.*). The assignment of IR spectra is usually possible with the aid of quantum chemical calculations or, even better, with the combination of theoretical predictions on one hand and the results of isotopic substitution experiments on the other. The best approach (rarely used, owing to technical difficulties; see Section II.3) consists in the matrix isolation of *mass-selected* species.

The description of various theoretical chemistry methods specified throughout the text would fall beyond the scope of this book. The reader can find necessary information in original papers or references therein. Generally, the density functional theory (Hohenberg & Kohn 1964, Kohn & Sham 1965), abbreviated *DFT*, proved highly effective in the prediction of ground state equilibrium geometries and vibrational frequencies (Koch & Holthausen 2001). The most popular is the B3LYP hybrid functional (Becke 1993, Lee, Yang & Parr 1988). DFT inherently takes account of the electron correlation energy, at reasonable computational costs. Various functionals, including B3LYP, are implemented to commercial software packages like Gaussian 98 (Frish 1995) or Spartan 5.0 (Wavefunction Inc.). When the best quality of predictions on energetics or electron population is needed, much more costly post-SCF *ab initio* computational schemes have to be employed. These include the Møller-Plesset (1934) perturbation theory, configuration interaction (Pople *et al.* 1977), coupled electron pair approximation (Meyer 1973) or coupled clusters[2] (Ragavachari et al.

---

[1] The photolysis and electrical discharges are presented here to some detail; other matrix research employed means like laser vaporisation (Bondybey *et al.* 1996), X-rays, electron or proton bombardment, pyrolysis, sonication, or chemical reactions.

[2] Results derived with the CCSD(T) method – single, double and perturbative triple excitations coupled-clusters (Pople *et al.* 1987) – are often cited throughout this monograph.

1989) methods. Molecules presented in this monograph are relatively small (by current computational standards), which grants them the admittance to the realm of reliable quantum chemical calculations.

The reproduction of vibrational frequencies with the density functional theory deserves an additional comment. To achieve the agreement with experimental results, calculated data have to be scaled, *i.e.* multiplied by a constant factor. This procedure takes account for the neglect of anharmonicity, incomplete inclusion of electron correlation or for effects stemming from the deficiency in basis set. Published values of B3LYP scaling factor for stretching modes are all close to 0.96 (see for example the studies by Scott and Radom (1996), Palafox (2000) or the recent extensive work by Halls *et al.* (2001), who compared the calculated and experimental results for over 100 molecules). Kołos and Sobolewski (2001, **paper VI**) and Kołos (2002, **paper IX**) confirmed the adequacy of the factor 0.96 for calculations on cyanoacetylene-like molecules performed with the B3LYP functional, and basis sets of the triple-zeta quality.

II.2.a. Photolysis

Perfect light transmission properties of RG matrices make them appropriate media for photophysical and photochemical experiments in a very broad spectral range. This gives access to a multitude of research projects, like IR pumping followed by intermolecular vibrational energy transfer (Kołos *et al.* 1996), proton transfer in complex organic compounds provoked by the visible light (*e.g.* Radziszewski *et al.* 1989), or the dissociation induced by UV photons – to name just three qualitatively different possibilities.

The last example, well illustrated by Milligan & Jacox (1967) studies on the dissociation of cyanides (HCN, FCN, ClCN, BrCN, C_2N_2) in Ar matrices, may serve to explain the basic concept of the *in situ* matrix photolysis, namely the "cage effect". Milligan & Jacox photolysed their samples with a UV light, energetic enough to detach the CN radical. They were equipped to detect the IR vibrational band as well as violet electronic transitions of CN, but the radical production was substantial only when HCN served as the precursor. Some CN was still produced from FCN, but for heavier precursors the yield notably decreased, approaching zero for cyanogen.

Only a part of absorbed energy was consumed for the bond breaking in these experiments, the excess amount should be transformed into the kinetic energy of separating fragments. Indeed, results indicated, that it was possible for the tiny H atom to reach a permanent trap somewhere out of the "cage", in which HCN molecule originally dwelled, thus leaving the isolated radical behind. Such a scenario was dramatically hampered, however, when bulkier elements, hard to eject outside the cage, replaced hydrogen.

It has to be emphasized, however, that the X—CN bond rupture *did* efficiently took place in every case studied by Milligan & Jacox, as was evidenced by the formation of respective isocyanides, XNC. This work nicely demonstrated the main difference between photochemical processes occurring *in situ*, within rigid matrices, and those possible in the gas phase. It is often practical to take advantage

of the fact that the matrix limits the number of possible reactions and/or directs the molecular system towards an unusual arrangement.

II.2.b Electric discharges

In Chapter III the reader will find quite a few examples (of importance to the laboratory astrophysics) speaking for the validity of the remark, which closed the preceding paragraph.

Quite often, however, experimentalists want to overcome the limitations posed by the matrix cage effect. In such cases it is advisable to dissociate precursor substances prior to the matrix formation. This can be conveniently accomplished by electrical discharges.

An often cited idea of Prochaska & Andrews (1977) featured the co-deposition of two gas streams, coming from independent nozzles. One of these delivered the guest species (either diluted with the rare gas or not). The other nozzle supplied the rare gas, previously (*i.e.* several centimeters downstream) subjected to microwave discharges. The streams had some space to interact before reaching the cold surface. Argon cations and excited atoms produced in the discharge collided with precursor molecules, which could yield a variety of products. In such set-ups one can also expect some action of the vacuum-UV emitted from the discharge zone. This radiation may illuminate the target, unobstructed by any absorbing windows.

A conceptually simple and easy to operate discharge nozzle was build by Bondybey and coworkers (Thoma *et al.* 1992), who assembled two electrodes, one high voltage, the other grounded, in vacuum, behind a pulsed valve (of the type used in automotive fuel injectors), which admitted the gas mixture. Even though the voltage was continuously applied, the discharge spontaneously glowed only during brief periods when the nozzle was opened and some pressure built up between the electrodes. This arrangement, which permitted to make samples of reproducible thickness and processing degree, was employed in some experiments described in Sections III.2*a* and III.4.

Szczepanski *et al.* (1991*a*)[1] built a more complicated apparatus, with a pulsed glow discharge in the terminal section of the gas delivery tube, and a positively charged metal grid outside the tube. The rôle of the grid was to repel ions in the direction of the cold window, thus increasing the matrix ion-to-neutrals ratio.

Another type of discharge arrangement, acronymed CWRD – *cold window radial discharge* – proved very efficient in experiments with unsaturated carbon-nitrogen chain molecules (Kołos 1995, **paper I**)[2].

Figure II.1 is the schematic cross-section through the vacuum shroud of the cryostat with the CWRD assembly. A circular substrate window (made of caesium iodide, a crystal material transparent from far-IR to UV), with a small conical channel drilled through its centre, is mounted in a circular frame, and attached to

---

[1] In the research group of Martin Vala at the University of Florida, Gainesville, USA.

[2] References to selected articles authored or coauthored by R. Kołos are discernible by Roman numerals.

the "cold finger" of a closed cycle helium refrigerator. The tip of the needle-shaped stainless steel electrode is introduced into the channel without touching the window or passing to the other side of it. The vacuum-tight connection between the shroud and the electrode is accomplished by means of a greaseless cylindrical joint. This mount permits to shift and tilt the electrode at will, until the exact position of the tip is reached. The gas mixture supply tube, equipped with a Teflon needle valve, is attached to the opposite port across the vacuum shroud.

Two main types of CWRD experiments produced interesting results (see Sections III.1 and III.3.).

Discharges during the matrix deposition. The high voltage (ca. 5 to 15 kV, from a regulated AC power supply) is applied to the needle electrode. The discharge starts immediately upon opening of the gas mixture supply valve. One can use any reasonable gas flow rate, which conforms to the cryostat cooling capacity. The plasma glow arises on one side of the window, facing the deposition tube. It extends from the central orifice to the grounded frame of the window, thus uniformly covering the growing matrix. The advantage of this set-up, when compared to other constructions, is that the distance between the trapping surface and the discharge is practically zero; the glowing zone "slides" on the cold window. This offers the chance to catch primary species created in the discharge, before secondary reactions occur.

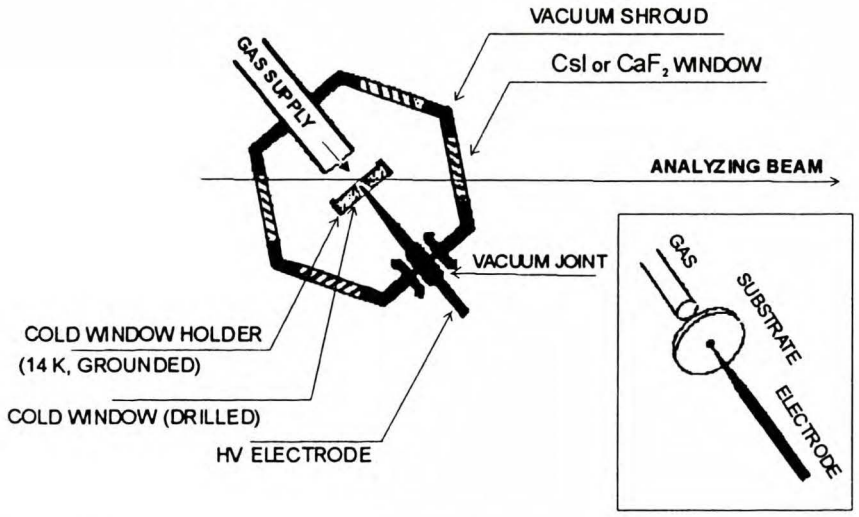

Figure II.1. Cryostat cross-section showing the "cold window radial discharge" arrangement and a schematic view of its principal elements (insert). Not to scale. Reprinted with the permission from Elsevier Ltd. (Kolos 1995)

High voltage treatment of matrices. Interestingly, the oscillating high voltage can be applied to the needle electrode *after* the matrix (doped with a suitable precursor) is prepared by routine methods. When this is the case, the sample begins to glow brightly. Occasionally, narrow discharge channels, propagating radially on the matrix surface, are observed. This method, like the former one, may lead to the formation of transient species, but its efficiency is at least an order of magnitude lower. Also, the range of obtained products is more limited – but it seems that the cage effect is not rigorously valid. The discharge is ignited due to the remnant RG vapor pressure over the matrix surface. Then, when it glows, some recycling of the matrix material between solid and gas phases is possible. A slight rise of the cold finger temperature (1-2 K) takes place during discharges, but the physical properties of the sample are not noticeably altered, as evidenced by no spectral traces of the parent molecules aggregation. The great advantage of this type of CWRD is the possibility to compare (usually by subtraction) the spectra obtained before and after the high voltage treatment – which bear a resemblance to photolysis experiments. In fact, during this processing, just like in the formerly described gas-phase variant of CWRD, the transformations of parent species are most likely due to the resonance radiation from excited argon atoms, namely 105 and 107 nm.[1]. This can be regarded as a vacuum-UV argon lamp – a low power one, but expediently placed. Series of tests demonstrated that the CWRD device is effective enough to ionize matrix-isolated *p*-dichlorobenzene. Both IR and optical transitions of *p*-dichlorobenzene cation were detected in respective difference spectra. The efficiency of this method was similar as in the previous experiment carried out by Szczepanski *et al.* (1991*b*), who used the same compound, employed the microwave discharge through the gaseous Ar / *p*-dichlorobenzene mixture, and had means to preferentially deposit the cations.

[1] Additionally, in the gas phase, collisions with metastable atoms, and with accelerated ionic species may be of importance.

II.3. Matrix isolation of mass-selected species

The principal idea behind the title method is apparently simple, and consists in the preparation of a rare gas matrix seeded with species of known mass – the latter selected by a mass spectrometric technique. The practical implementation of this concept proves complicated, the main difficulty lying in the preparation of a low energy ion beam, which, when colliding with a cold target, would not lead to a molecular fragmentation and/or matrix melting.

Several laboratories have nevertheless managed to construct operational apparata, two of which should be mentioned here – since both served in experiments with unsaturated chain molecules of astrophysical significance (see Sections III.4-5.). These are located in Basel, Switzerland and in Garching, Germany, in the laboratories of John P. Maier (Maier 1992) and Vladimir E. Bondybey (Lorenz & Bondybey 2000), respectively. Figure II.2 presents a schematic view of the latter set-up.

Ions are first generated within the electron impact source **A**, which consists of an outer cylinder with three heated tungsten filaments located near its periphery. Electrons emitted from the filaments are repelled by the casing kept at a potential 20 V lower than the filaments, and are then accelerated by a potential difference of *ca.* 80 V towards an inner cage formed by a wire mesh cylinder. The cylinder potential, +30 V with respect to ground, determines the kinetic energy of ions produced from parent molecules by the electron impact. The ions are then removed from the cage by the electric field provided by the extraction electrode held at -500 V.

The ion beam enters the detection chamber via a skimmer **B**. There it is collimated by the first einzel-lens **L1** and then deflected 90° by an electric quadrupole field within the deflection unit, **D**. Lens **L2** serves to focus the ions upon the entrance aperture of a quadrupole filter **Q**. Finally, the mass-selected ion beam is focused by means of the lens **L3** onto the target window (**C**) surface, held at 7 K. The ion beam is deposited simultaneously with the matrix gas. Overall sample neutrality is achieved by continuous irradiation of the matrix with electrons from a tungsten filament, **W**. Faraday cups, **F1** and **F2**, serve to measure two ion currents; the total, produced by source A, and the mass-resolved one, respectively.

A typical experiment is preceded by the measurement of the mass spectrum. The mass value of interest is then selected by an appropriate quadrupole field, the matrix is produced, and finally the spectra are taken. While this method is best suited for ions, one can also count on a substantial recombination of cations with electrons (as these are continously sprayed onto the growing matrix surface), and on the resulting isolation of mass-selected neutrals (see Section III.4).

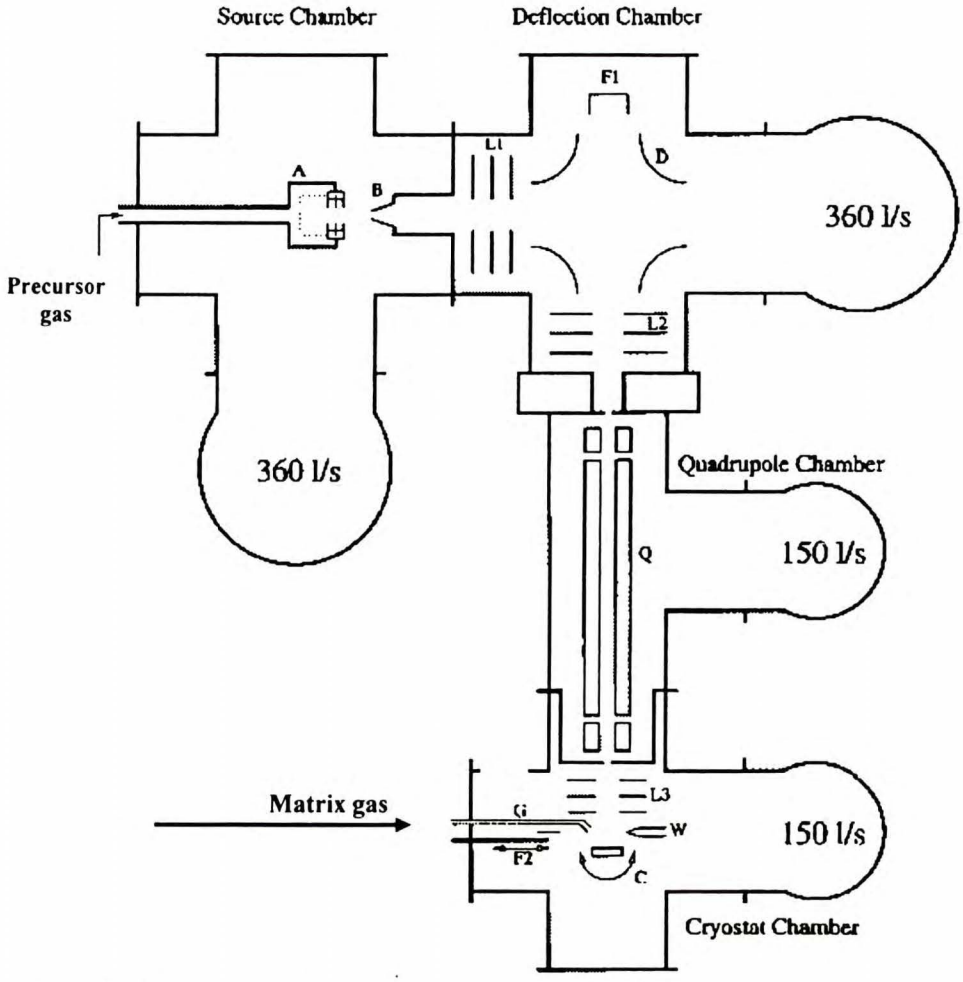

Figure II.2. Scheme of the set-up for matrix isolation of mass-selected species after Lorenz & Bondybey (2000). See text for the explanation of symbols. The apparatus was designed and built in Garching, Germany.
Reprinted with the permission of the American Institute of Physics.

II.4. Interstellar matrices?

Let us conclude this down-to-earth chapter with related astrophysical reflections.

The main objective of inert gas matrix experiments in laboratory astrophysics is usually not to *simulate* the interstellar processes. Rather, matrices are taken for granted as a useful, though highly artificial medium for the creation of otherwise elusive species, and for their spectroscopic characterization.

However, as mentioned in Section I.4., the interstellar dust grains may exist in a core-mantle form – consistently with IR observational data (see Section I.5.), which point to the presence of water ice (Gillet & Forest 1973, Merrill *et al.* 1976), probably doped with other molecules. This "dirty ice" can be regarded as a matrix, and as the playground for various radiation-induced processes (Greenberg 1976, d'Hendecourt & Dartois 2001).

Apart from such considerations, an interesting question arises – whether inert gas matrices, of the kind familiar to experimentalists, may exist in space. Given the cosmic abundance (see Table I.1), the most promising choice could be neon, which belongs to the "great six" of most widespread elements. Can neon solidify in space? Figure II.3 does not provide an unambiguous answer. The number density of interstellar Ne in very dense clouds (where the number density of hydrogen, n_H+2n_{H2} may approach 10^7 cm^{-3}) could be of the order of 10^3 cm^{-3}. The lack of experimental gas pressure data makes impossible to find the temperature corresponding to the onset of Ne crystallisation at this density; one could estimate it to be around 5 K.

In reality, such low kinetic gas temperatures are not necessary for the condensation *onto grains* to occur. Dust and gas are not in the thermal equilibrium, the former being efficiently cooled by the IR emission. Extremely low dust temperatures, perhaps even approaching 3 K, seem possible within dense clouds. This was discussed by Solomon & Wickramasinghe (1969), who first recognised the potential importance of molecular hydrogen mantles around mineral grains.

The solid hydrogen concept was more recently revitalised by White (1996), in connection to the missing mass of the universe. According to White, hydrogen objects could form in cold and dense clouds. Hydrogen "balls" of 10 km and 100 km radii, subjected to the heating by cosmic rays, could retain their masses for 0.7 and 7 billion years, respectively. Taking the advantage of this idea, one should notice that all molecules condense more readily than H_2, so it is reasonable to expect their presence in H_2 "ices", and their conversions by photo- or radiochemical phenomena therein. Processed substances, possibly quite complex, would finally be returned to the gas phase.

These loose remarks point to hydrogen matrices, rarely used in laboratories, as promising media for photochemical experiments with astrophysically significant molecules.

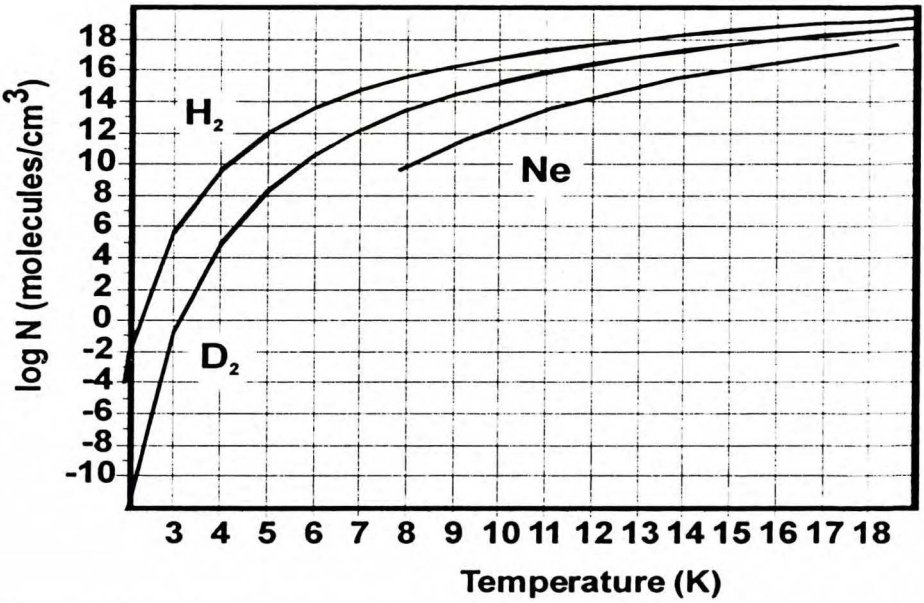

Figure II.3. Number density of gas molecules in equilibrium with their condensed phases. Note that in the interstellar space the equilibrium is *not* attained, solid grains being much cooler than the gas.

Moreover, it is of interest to include the search for vibrational bands of solid molecular hydrogen in upcoming astronomical IR spectroscopic projects. Obviously, H_2 has no permanent electric dipole moment, which results in the lack of allowed vibrational transitions. In the solid, however, it is possible to observe such transitions due to dipole moments (asymmetric distortions) induced by intermolecular forces (Welsh *et al.* 1949, Allin *et al.* 1955, Gush *et al.* 1960).[1] Foreign molecules (impurities) can contribute to the effect by deforming the centrosymmetric field around hydrogen molecules (Carr *et al.* 1980). This is illustrated by Figure II.4., which gives the vibrational-rotational spectrum of H_2 in argon, in the presence of CO (Kołos *et al.* 1996).

[1] This is a solid-phase analogue of pressure-induced rovibrational spectra of homonuclear diatomic molecules.

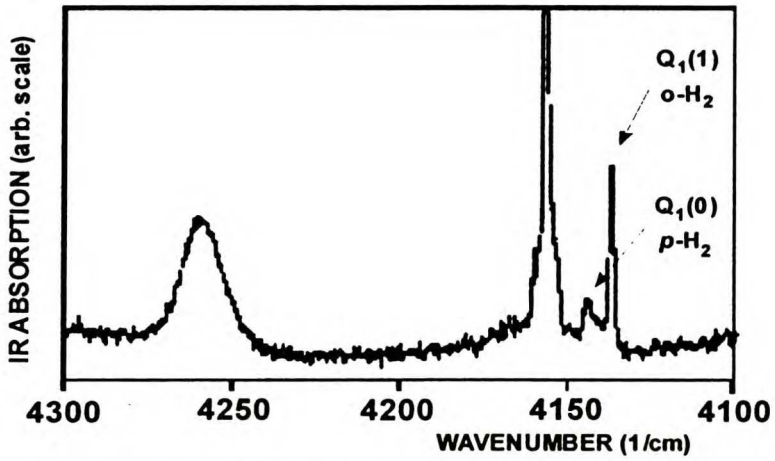

Figure II.4. Induced absorption $Q_1(0)$ and $Q_1(1)$ lines of H_2 in an $Ar/H_2/CO$ (100:10:1) matrix (Kolos *et al.* 1996). The band at 4157 cm^{-1} originates from $^{13}C^{16}O$; the leftmost broad feature is a phonon sideband due to localized translations of H_2 within the lattice cage (Kriegler & Welsh 1968). Reprinted with the permission from Elsevier Ltd.

III

Occurrence and Characteristics of Cyanoacetylene-Related Molecules

III.1. Isomers of cyanoacetylene, HC_3N

Cyanoacetylene (*1,2*-propynenitrile) was first synthesized by Moureu & Bongrand (1920b)[1]. Despite interesting chemical characteristics, there was not much concern about this compound until late 1950s, when, along with other cyanoacetylenes, it was considered as a potential rocket fuel. Only then were electronic and vibrational spectra measured. The next wave of interest, which remains high, came with the recognition of cyanoacetylene as an interstellar compound (Turner 1971). It has also been found in cometary spectra (Bockelée-Morvan *et al.* 2000), and is the constituent of the atmosphere of Titan, Saturn's largest satellite (Coustenis 1991)[2]. Potential technological applications include using the molecule as a monomer for semiconducting polymers (Manassen & Wallach 1965).

Two decades after the radio astronomical discovery of interstellar cyanoacetylene, other isomers of this molecule were found in space, namely isocyanoacetylene HCCNC (Kawaguchi 1992a), and an imine HNCCC (Kawaguchi 1992b). Corresponding microwave spectra matched the laboratory measurements done by Krüger (1991) and Hirahara (1993). The IR-spectroscopic work on these species, isolated in rare gas matrices, is reviewed in Sections III.1*b-c*. Then, in Sections III.1*d-e*, the reader's attention will be brought to theoretical studies on other possible isomers of cyanoacetylene, to the ensuing experimental outcome, and to related astrochemical issues.

III.1a Cyanoacetylene

The interatomic distances within HC_3N were derived by a highly accurate approach, which combined both experimental and theoretical results (Botschwina *et al.*, 1993b). A set of ground-state rotational constants for 6 different isotopomers of cyanoacetylene was supplied by the microwave spectroscopy study (Mallinson & De Zafra, 1978), while the high level calculations (coupled-electron-pair method) gave vibration-rotation coupling constants α_i for all vibrational modes. The rotational constants for ground vibrational states (B_0) are linked to the equilibrium rotational constants (B_e) by the relation:

$$B_e \approx B_0 + \frac{1}{2}\sum_{i=1}^{N} d_i \alpha_i \quad ,$$

where d_i are degeneracy factors, and N is the number of vibrational modes. Given the set of six B_e values, Botschwina *et al.* could obtain the equilibrium bond lengths (Figure III.1). Formally, the molecule forms a chain with alternating single and

---

[1] Moureu & Bongrand used ammonia to transform a propiolic acid ester into the respective amide, then dehydrated the amide to yield cyanoacetylene. This procedure proves to be the most effective until present days.

[2] Even before the onset of astrochemical research, Sanchez *et al.* (1966) reported that HC_3N is a major nitrogen-containing product of the action of electrical discharges on methane-nitrogen mixtures. Moreover, they found substantial amounts of asparagine, aspartic acid and cytosine among the products of HC_3N hydrolysis, which may suggest its rôle in the prebiotic synthesis.

triple bonds. However, the linear arrangement of π orbitals leads to some electron delocalization. When compared to interatomic distances in hydrogen cyanide, HCN, lengths of C—H and C≡N bonds are by 0.003 Å reduced, and by 0.007 Å elongated, respectively (Botschwina *et al.* 1997a).

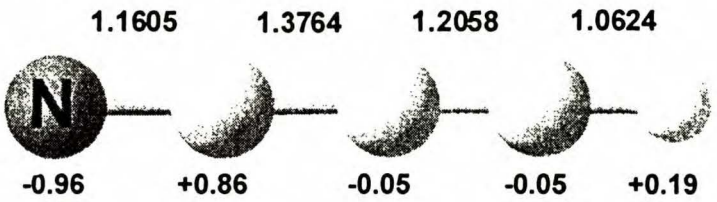

Figure III.1. The best available equilibrium geometry of cyanoacetylene (interatomic distances in Å; after Botschwina *et al.* 1993b). Partial atomic charges (MP2, atoms-in-molecules analysis) were calculated by Platts *et al.* (1998). MP2 leads to the electric dipole moment of 3.75 D, the experimental value is 3.73172 D (DeLeon & Muenter 1985).

Cyanoacetylene is an acid; it reacts with OH^- almost 5 orders of magnitude more readily than does acetylene (Powell *et al.* 1983). Consequently, a number of cyanoacetylene salts were prepared (Rappaport 1970).

Table III.1. Fundamental modes of cyanoacetylene, as measured by IR absorption spectroscopy

	Gas [a]		Crystalline [b]		Ar matrix [c], frequencies for three isotopomers (cm^{-1})			Assignment [d]
	Freq. (cm^{-1})	Intens. km/mol	Freq. (cm^{-1})	Intens. km/mol	natural ^1H, ^{14}N	^2H	^{15}N	
ν_1	3328.5	60	3203	356	3314.6	2601	3314.6	C–H stretch
ν_2	2271.0	10	2270	109	2268.6	2246	2252.3	C≡N stretch
ν_3	2078	2	2066 2057 2047 2030	32	2076.5	1964	2065.8	C≡C stretch
ν_4	863	~0.06	883	4				C–C stretch
ν_5	663.7	68.4	759	57	667.3, 665.8	524.2, 528.8		C-C-H bend
ν_6	499.2	8.0	505	14	503.5, 502.1			C-C-N bend
ν_7	223.5	0.18	227	1				C-C-C bend

[a] Uyemura & Maeda (1974) and Uyemura *et al.* (1982). The gas-phase spectrum was also measured by Khlifi *et al.* (1990).
[b] Based on the data of Dello Russo & Khanna (1996).
[c] Kołos, unpublished data.
[d] Stretches ν_2 and ν_3 are highly delocalised.

In the crystalline state cyanoacetylene molecules adopt a linear head-to-tail arrangement (Uyemura & Maeda 1974), which results in the substantial gas→crystal intensity increase for the bands corresponding to stretching

fundamentals (Table III.1). The formation of crystalline phase and/or molecular aggregates is commonly observed in matrices characterised by high guest/host ratios. Borget (2000) reported on cyanoacetylene dimer and trimer bands in argon.

The first electronic transition of cyanoacetylene, $^1A''$—$^1\Sigma^+$ (Job & King 1966a), corresponds to weak bands known as the "2600 Å system". The second transition, $^1\Delta$ ($^1\Sigma^-$)—$^1\Sigma^+$ ("2300 system" of Job & King (1966b); see Fig. III.2) is an order of magnitude stronger, with molar absorption coefficients approaching 300 $dm^3mol^{-1}cm^{-1}$ (Halpern *et al.* 1988), while the most intense UV bands, observed in the vacuum region, represent the fully allowed $^1\Sigma^+$—$^1\Sigma^+$ transition. The latter bands are characterised by absorption coefficients as high as 60 000 $dm^3mol^{-1}cm^{-1}$ (Connors *et al.* 1974).

The gas-phase photochemistry of cyanoacetylene was studied by several research groups (Okabe & Dibeler 1973; Halpern *et al.* 1988; Clarke & Ferris 1995, 1996; Seki *et al.* 1996; Titarchuk & Halpern 2000). Halpern *at al.*, who monitored the UV photolysis by the laser-induced violet fluorescence from CN fragments, concluded that the quantum yield of the reaction:

$$HC_3N + h\nu \rightarrow C_2H + CN \qquad (i)$$

was about 5%. This pointed to:

$$HC_3N + h\nu \rightarrow H + C_3N \qquad (ii)$$

as the chief photolytic process, which was later confirmed by Seki *et al.* (1996). Halpern *et al.* managed also (*via* an indirect method, involving the parallel dicyanoacetylene study) to derive a wavelength threshold for reaction (*ii*), which was 244 ± 8 nm.

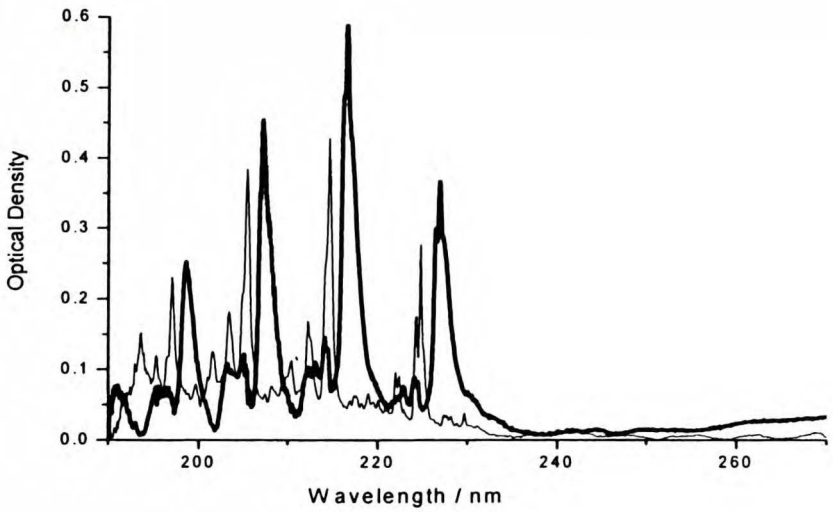

Figure III.2. Electronic absorption of cyanoacetylene in the gas phase (thin line), and in solid argon (bold line).

Efforts of Kołos *et al.* (1991, 1992) to detect the electronic transitions of C_3N

radical (following the gas-phase *di*cyanoacetylene photolysis) were not successful. Sadlej & Roos (1991), based on CAS SCF calculations, predicted following vertical excitation energies to the first three states of C_3N: 0.50, 3.93, and 5.71 eV. These transitions are expected to be weak, with oscillator strengths of the order of 10^{-4}. More recently, Titarchuk & Halpern (2000) suggested the luminescence from C_3N as one of possible explanations for an unidentified emission they detected following the multiphoton excitation of HC_3N. This point merits further studies.[1]

III.1b Formation of H-CC-NC

Experiments, which employ the *in situ* photodissociation of cyanoacetylene in rare gas matrices, stem directly from gas phase studies described above. With energetic enough photons from the quartz-UV range, one can expect to cleave any single bond. This is likely to trigger either the permanent splitting of the molecule or – due to the matrix cage effect (see Section II.2*a*) – the rearrangement of its atoms (isomerisation).

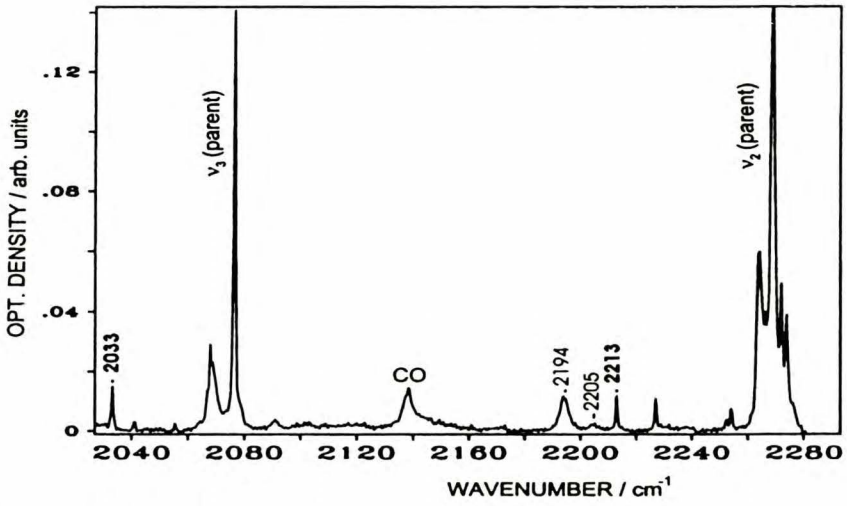

Figure III.3. IR absorption spectrum resultant from the 193 nm irradiation of HC_3N/Ar matrices.

Table III.2 lists the experimental output obtained by Kołos & Waluk (1997, **paper II**), who used an ArF* excimer laser radiation (193 nm) to photolyse cyanoacetylene in solid argon below 20 K. The resultant IR spectrum is presented in Fig. III.3. To facilitate the assignment of bands developed during the irradiation, three isotopomers of cyanoacetylene were studied: $^1HCCC^{14}N$, $^2HCCC^{14}N$, and

[1] C_3N is an important interstellar species detected via the microwave emission in the cicumstellar envelope of IRC+10°216 (Guélin & Thaddeus 1977), and in the Taurus molecular clouds (Friberg *et al.* 1980).

$^{1}HCCC^{15}N$.[1] Upon the *annealing* (see Section II.1) product bands faded in parallel to the aggregation of parent molecules, and disappeared completely at 35-40 K.

One should expect to find isocyanoacetylene, HCCNC, among the photolysis products, in analogy to the classical isomerisations of matrix-isolated halogen cyanides (Milligan & Jacox 1967) or to the isomerisations of dicyanoacetylene discovered by Smith *et al.* (1993, 1994a). Indeed, the sharp features from Table III.2 fit to the gas phase spectrum of isocyanoacetylene (Bürger *et al.* 1992). An equally good fit is obtained for a deuterated precursor. Table III.3 summarises the details of this assignment, together with previously unobserved frequencies for ^{15}N-substituted cyanoacetylene.

Table III.2 IR features developed upon the 193 nm photolysis of cyanoacetylene in Ar matrices. (Kołos & Waluk 1997)

cm^{-1}	$^{14}N \rightarrow {}^{15}N$ shift (cm^{-1})	$^{1}H \rightarrow {}^{2}H$ shift (cm^{-1})	Width	Remarks
2033	-24	-71	narrow	see Table III.3
2090	-0.5	0	broad	usually weak, poorly reproducible
2194	-24	0	broad	not correlated to 2090 cm^{-1} band
2213	-16	-62	narrow	see Table III.3
3328	0	-717	narrow	see Table III.3

Table III.3. IR bands of isocyanoacetylene in Ar (Kołos & Waluk 1997)

Wavenumber (cm^{-1})	Gas-to-Matrix Shift* (cm^{-1})
$^{1}HCC^{14}NC$	
2033	-4
2213	-6
3328	-11
$^{1}HCC^{15}NC$	
2009	
2197	
3328	
$^{2}HCC^{14}NC$	
1962	-3
2151	-7
2611	-7

*) based on Bürger's *et al.* (1992) gas-phase data

[1] The precursor molecule is highly acidic, thus its hydrogen is readily substituted with deuterium (from heavy water). To obtain ^{15}N-cyanoacetylene, appropriately enriched ammonia was used during the otherwise regular synthesis.

III.1c Formation of H-NCCC

Radicals C_2H and CN were missing from the products of the 193 nm photolysis, which is well understood in terms of the matrix cage effect. The most likely possibility after a C—C bond cleavage, neglecting the direct recombination (parent molecule restoration), is the isomerisation *via* the rotation of a cyano moiety. As described above, the 193 nm gas-phase photolysis studies indicated a rather low quantum yield for C—C dissociation, and a much higher one for the breaking of another single bond, C—H.

It was tempting to find some direct evidence for the latter process. While Kołos & Waluk (1997) could not recognize the molecules responsible for spectral features at 2194 and 2090 cm^{-1} (Table III.2), they pointed to the first of these – identified as due to a nitrogen-bearing non-hydride – as the plausible candidate for the fundamental vibration of CCCN radical. As discussed in Section II.2*a*, the hydrogen atom is small enough to get out of the original matrix cage – and leave the remaining radical fragment behind. However, the agreement with state-of-the-art *ab initio* calculations was poor. The coupled-electron-pair predictions obtained for CCCN by Botschwina *et al.* (1993a) were (intensities, in km/mol, given in brackets): 2280±15 cm^{-1} (2.6), 2090±15 cm^{-1} (0.1) and 883±15 cm^{-1} (0.8). Even with a matrix shift taken into account, the 2194 cm^{-1} band would definitely fall out of the recommended error range for the strongest CCCN fundamental. It is conceivable that CCCN escapes the detection because of its low IR absorption intensities[1]. Incidentally, the CASSCF MRCI study by Sadlej & Roos (1991) led to very low probabilities of *electronic* transitions, also. The oscillator strengths for first three transitions, with excitation energies 0.50, 3.93, and 5.71 eV were predicted as, respectively, 4.3×10^{-4}, 2.3×10^{-4}, and 5.7×10^{-4}. These characteristics make CCCN an object very hard to detect (Kołos *et al.* 1991, 1992).

Nonetheless, the cleavage of C—H may give access to another reaction channel, apart from the production of the CCCN radical. The migration of hydrogen to the opposite end of the CCCN fragment should lead to the imine HNCCC (3-imino-1,2-propadienylidene). First calculations on this molecule are due to Green & Herbst (1979); then, after its interstellar discovery, the structure (*zigzag*, with a small barrier to linearity) was theoretically established by Botschwina *et al.* (1992, 1993a).

One can expect the isomerisation of HCCCN → HNCCC to compete with the production of CCCN (in matrices) if the excess energy released during the C—H dissociation is low. The thermochemical threshold derived by Halpern *et al.* (1988) implies that the 193 nm photolysis sets free as much as 10800±1300 cm^{-1} of excess energy.

When the less energetic radiation, 222 nm from a KrCl* excimer laser, was used by Kołos & Waluk (1997), an intense absorption band at 2205 cm^{-1} appeared, which was hardly detectable after the 193 nm photolysis. Since the excess energy decreased to 4000±1300 cm^{-1}, it seemed realistic to expect the imine formation. Additional argument came from the observation that the 2205 cm^{-1} feature was at

[1] The problem of 2194 and 2090 cm^{-1} absorption bands will be revoked in Section III.5*b*.

least 2 times broader than the bands of isocyanoacetylene. It qualitatively agreed with a scenario involving the creation of a zigzag molecule out of the linear parent. The imine isomer does not comfortably fit to the matrix cage tailored for its cyano precursor – which may broaden the corresponding energy distributions.

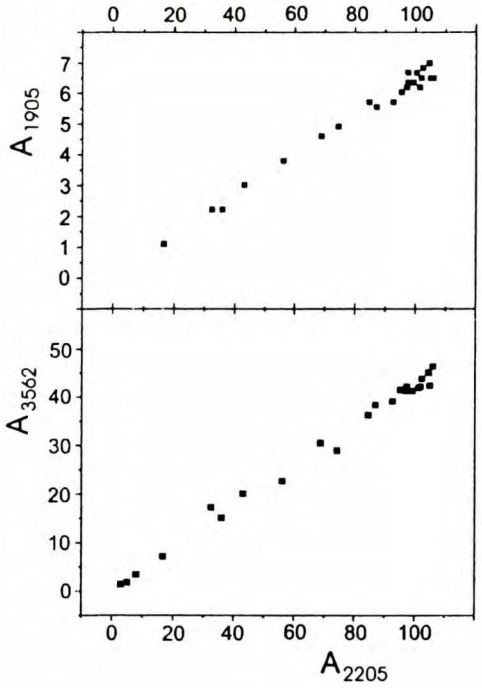

Figure III.4. Cross-correlations of the integrated optical density (A, arbitrary units) for three IR absorption bands (1905, 2205 and 3562 cm^{-1}) assigned to HNCCC. Bands were generated with the CWRD source in a HCCCN / Ar matrix. Points correspond to different extent of CWRD processing (Kołos & Sobolewski 2001). Reprinted with the permission from Elsevier Ltd.

The isotopic substitution studies, the use of CWRD electrical discharge method for the efficient generation of the imine, and DFT calculations enabled Kołos & Sobolewski (2001, **paper VI**) to make an unambiguous spectral assignment. Two additional vibrational fundamental bands, well correlated with the 2205 cm^{-1} feature (see Figure III.4), and of the similar width, were found. Table III.4 gives the wavenumbers measured in argon matrix spectra; these agree very well with the scaled harmonic frequencies predicted by the density functional theory for three isotopomers of HNCCC.

Table III.4. Stretching frequencies and IR intensities for three HNCCC isotopomers. Experiment vs. theory (Kołos & Sobolewski 2001).

SPECIES	mode	DFT B3LYP/6-311++G** (scaled) [a]		Experimental (Ar matrix)	
		cm^{-1}	km/mol	cm^{-1}	relative int. [b]
$^1H^{14}NCCC$	ν_1	3567	448	3562	0.4
	ν_2	2202	1590	2205	1
	ν_3	1880	27	1905	0.06
$^2H^{14}NCCC$	ν_1	2658	560	2611	0.5
	ν_2	2171	1408	2162	1
	ν_3	1855	12	1890 [c]	
$^1H^{15}NCCC$	ν_1	3557	435	3552	0.4
	ν_2	2193	1591	2195	1
	ν_3	1869	17	1895 [c]	

[a] scaling factor 0.96
[b] the intensity of ν_2 band taken as 1 for each species, accuracy *ca.* 15%
[c] tentative assignment, intensity too low for reliable measurements

All stretching fundamentals of HNCCC, which were expected to show up, were indeed detected. It should be noticed that some bands are predicted as much more intense than those of the parent compound (the absolute intensities of cyanoacetylene stretches do not exceed 60 km/mol, as measured by Uyemura and Maeda, 1974). This probably explains the promptness, with which the bands of this highly energetic species (*ca.* 50 kcal/mol less stable than cyanoacetylene[1]) develop during the photolysis.

Table III.5. Fundamental frequencies of HNCCC as derived with B3LYP/6-311++G (Kołos & Sobolewski 2001).**

	Wavenumber (cm^{-1})	IR intensity (km/mol)
ν_1	3715	448
ν_2	2293	1590
ν_3	1958	27
ν_4	965	0.7
ν_5	596	62
ν_6	593	2.3
ν_7	461	409
ν_8	191	1.6
ν_9	180	3.5

[1] The energetics of cyanoacetylene isomers is fully discussed in the next section.

The whole set of calculated vibrational frequencies is listed in Table III.5. The bending bands ν_5 and ν_7 (predicted to give an important contribution to the spectrum) were not detected by Kołos & Sobolewski, possibly due to lower than expected intensities and/or due to the poor performance of the IR detector (HgCdTe), at the edge of its sensitivity range.

Experiments with matrices containing two isotopic modifications of the precursor (at a known ratio, usually close to 1:1), permitted to compare the intensities of product bands coming from different isotopomers. The ^{14}N- and ^{15}N-related bands developed with the same efficiency, as illustrated by Fig. III.5.

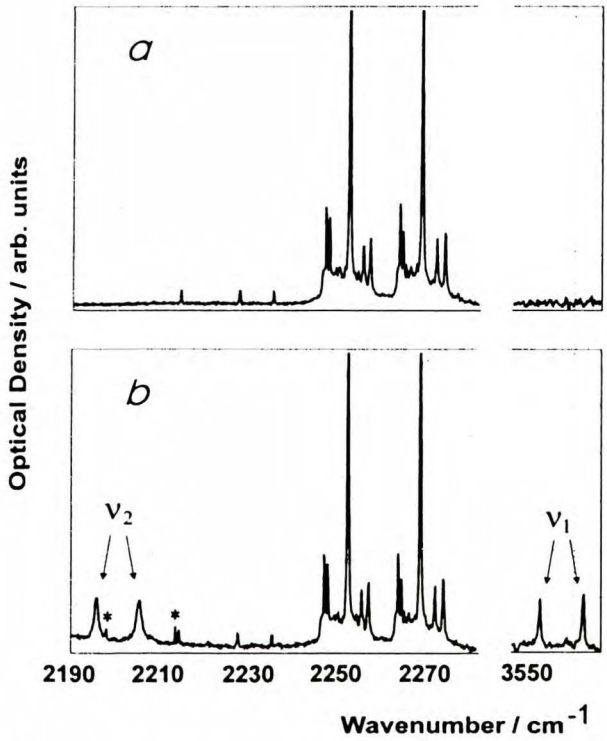

Figure III.5. IR absorption spectra for a HCCC^{14}N / HCCC^{15}N / Ar (1:1:3000) matrix; before (*a*) and after (*b*) the 222 nm irradiation. All bands in (*a*) arise from isotopomers of cyanoacetylene. The structure in a pair of prominent central bands comes from numerous matrix sites; the intensity of the contribution from the main site surpasses the vertical scale span (approx. three times). Doubling of bands assigned to HNCCC modes ν_1 and ν_2 is indicated. Weak asterisked bands come from the isotopically doubled ν_2 transition of another photoproduct, HCCNC (*cf.* Fig.III.3). Reprinted with the permission from Elsevier Ltd. (Kołos & Sobolewski 2001)

However, the bands assigned to DNCCC were 2 – 2.5 times weaker than those due to HNCCC, even though the DFT-computed absolute intensities (*cf.* Table III.4) were quite similar for both isotopomers (this applied to ν_1 and ν_2, the intensities of ν_3 were too low for a reliable analysis). Therefore, DNCCC is being formed less efficiently than HNCCC. This can be understood in terms of the dynamic isotope effect: in order to form the imine isomer, the detached H atom has to reach the opposite side of the NCCC chain. Such a diffusion must slow down when a heavier isotope of hydrogen is involved. As expected, no similar effect was noticed for isocyanoacetylene bands.

The calculated geometry of HNCCC is similar to those previously obtained (Botschwina *et al.* 1992, 1993a), with an almost linear NCCC skeleton, and H—N bond tilted significantly off-axis (Table III.6). The interatomic distances within the heavy atom chain substantially differ from those in other HC_3N isomers. Cyanoacetylene, H—C≡C—C≡N, shows a shortening of the single C—C bond (*cf.* Figure III.1) due to the conjugation of triple bonds. The isocyanoacetylene linear structure can be approximated by a carbene formula H—C≡C—N=C: with the lengths (Botschwina *et al.* 1992) of C≡C, C—N and N=C bonds equal to 1.2032, 1.3139 and 1.1794 Å, respectively. HNCCC is also a carbene; its bond lengths are consistent with the cumulene-like electron arrangement H—N=C=C=C: .

The DFT geometry derived by Kołos & Sobolewski (2001) leads to very satisfactory values of rotational constants. Their estimate of B_0, 4668.5 MHz, taken as the mean value of constants B_e and C_e (4675.8 and 4661.2 MHz, respectively), matched the experimental (Hirahara *et al.* 1993) value of 4668.3 MHz. This agreement, even though somehow accidental, suggests that the corresponding geometry is realistic, and advocates for a decent predictive power of the density functional theory.

Table III.6. Geometry of H—N=C=C=C:

Distances (Å) and angles	B3LYP/6-311++G** (Kołos & Sobolewski 2001)	CEPA-1 (Botschwina *et al.* 1992)
r(H—N)	1.005	1.0038
r(N=C)	1.188	1.1928
r(C=C)	1.302	1.3076
r(C=C:)	1.268	1.2745
α(H—N=C)	140°	136.1°
α(N=C=C)	175°	173.8°
α(C=C=C:)	178°	175.0°

III.1d HCNCC and cyanovinylidene– the missing isomers

Formally, cyanoacetylene has *four* open chain isomers. Thus, as first recognised by Osamura *et al.* (1999), the HCNCC molecule should also be taken into account. Osamura *et al.* were interested in the gas phase chemistry following the reaction $HCCCNH^+ + e^-$, likely to occur in interstellar molecular clouds. One of their findings was that HCNCC can indeed emerge from rearrangements triggered by this dissociative recombination, in addition to more stable species HCCCN, HCCNC and HNCCC. The energy difference between HCNCC and cyanoacetylene, calculated by Osamura *et al.*, was 67.9 kcal/mol (B3LYP/DZP) or 79.8 kcal/mol (CCSD(T)/cc-pVTZ//B3LYP/DZP[1]). In experiments, despite being highly energetic a species, HCNCC is the conceivable product of electrical discharges through cyanoacetylene. It seems particularly likely to be found among discharge products trapped and isolated in rare gas matrices.

Cyanovinylidene, CC(H)CN (see Fig. III.7), is the most probable structure among four imaginable *branched* isomers of cyanoacetylene. The extensive quantum chemical calculations on this species by Hu and Schaefer (1993) demonstrated that cyanoacetylene and cyanovinylidene are separated by an energy barrier (2.2 kcal/mol), which makes the latter species a true minimum on the C_3HN potential energy hypersurface, and a potentially observable molecule. Indeed, Goldberg and Schwarz (1994) soon reported on the mass-spectrometric detection of cyanovinylidene. Goldberg & Schwarz based their reasoning on the knowledge that the reaction of a *1,1*-substituted ethylene with atomic oxygen radical anions is likely to result in a H_2^+ elimination, and the generation of an anionic carbene:

$$H_2C{=}C(R_1)R_2 + O^- \rightarrow :C{=}C(R_1)R_2^- + H_2O$$

Mass-spectrometric evidence for the creation of $:C{=}C(R_1)R_2$ can then be obtained, with the neutralization-reionization technique directed toward $:C{=}C(R_1)R_2^-$. This hydrogen elimination procedure, applied to ethylene (R_1 and R_2 equal H), enabled Sülzle & Schwarz (1989) to spot the elusive vinylidene molecule, $:C{=}CH_2$; an analogous experiment with acrylonitrile, $H_2C{=}C(H)CN$, indicated the formation of cyanovinylidene, :C=C(H)CN (Goldberg and Schwarz 1994).

Thus, the very *existence* of cyanovinylidene was confirmed in just one experimental paper. However, no spectroscopic measurements on this molecule were ever done, even though the sound theoretical study by Hu & Schaefer predicted, apart from the energy, also the dipole moment, rotational constants, vibrational frequencies, and energies of two lowest triplet states.

Kołos & Dobrowolski (2003a, **paper X**) aimed at producing a uniform set of energy predictions for all five cyanoacetylene isomers – to enable the trustworthy determination of relative thermochemical stabilities. Table III.7 lists most important results of their study, which was accomplished at the CCSD(T) level of theory, with

---

[1] The notation *Method 1/basis set 1//Method 2/basis set 2,* used throughout the text, stands for "single point" calculations (frozen molecular geometry), carried out with the quantum chemical *Method 1* and *basis set 1*, the geometry being previously obtained with the *Method 2* and *basis set 2.*

frozen core electrons and a large, correlation consistent aug-cc-pVTZ basis set (Dunning 1989).

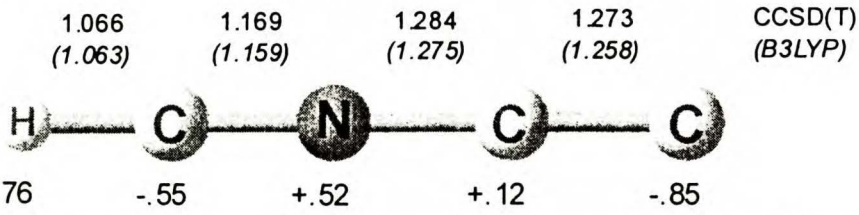

Figure III.6. Bond lengths (Å) and the partition of charges for the $X^1\Sigma$ state of HCNCC. See text for the final geometry prediction based on the appropriate scaling of calculated distances. Atomic charges produced by the Mulliken population analysis (CCD/aug-cc-pVTZ). Kołos & Dobrowolski (2003a); reprinted with the permission from Elsevier Ltd.

Table III.7. Total energies for five C_3HN isomers and relative energies against cyanoacetylene*).

C_3HN species	Total energy (hartree)	Zero-point vibrational energy (kcal/mol)	Relative energy kcal/mol	Reference
HCCCN	-169.223358 [a)]		—	Hu & Schaefer 1993
	-169.265277 [c)]		—	Botschwina *et al.* 1993b
	-169.289101	**16.42**	***0***	**Kołos & Dobrowolski 2003a**
HCCNC	-169.193112 [c)]		26.2	Botschwina *et al.* 1992
			27.2 [d)]	Osamura *et al.* 1999
	-169.245868	**15.85**	***26.6***	**Kołos & Dobrowolski 2003a**
CCCNH			53.8 [c)]	Botschwina *et al.* 1992
			52.5 [d)]	Osamura *et al.* 1999
	-169.206662	**15.56**	***50.9***	**Kołos & Dobrowolski 2003a**
HCNCC			79.8 [d)]	Osamura *et al.* 1999
	-169.162940	**14.87**	***77.6***	**Kołos & Dobrowolski 2003a**
CC(H)CN	-169.145887 [a)]	14.74 [b)]	*47.2*	Hu & Schaefer 1993
	-169.209774	**15.23**	***48.6***	**Kołos & Dobrowolski 2003a**

*)Kołos and Dobrowolski optimized the geometries with CCSD(T)/aug-cc-pVTZ, and derived zero-point vibrational energies with B3LYP/aug-cc-pVTZ. Other methods: **a)** CCSD(T)/TZ2P; **b)** CCSD(T)/DZP; **c)** coupled-electron-pair approximation (CEPA-1) with 118 contracted gaussian-type orbitals (GTOs); **d)** CCSD(T)/cc-pVTZ//B3LYP/DZP. *Entries in italics* corrected for zero-point vibrational energies.

The calculated difference between local minima of HCNCC and cyanoacetylene, 79.2 kcal/mol, is just 0.6 kcal/mol below the value predicted by Osamura *et al.* (1999) at the inferior level of theory. The inclusion of zero-point vibrational energies (as given by B3LYP/aug-cc-pVTZ) diminished this value to 77.6 kcal/mol. Nonetheless, HCNCC is rich in energy. Conversely, hitherto unobserved cyanovinylidene is predicted to be 2.3 kcal/mol *more* stable than the well-characterized *3*-imino-*1,2*-propadienylidene, HNCCC (zero-point energy included).

Figure III.6 presents two geometries of the HCNCC ground state, as given by the coupled-clusters and density functional theory approaches. The molecule is linear[1], similarly to other chain isomers of cyanoacetylene, aside from the quasi-linear (*zigzag*) imine. The substantial separation of charges along this rod-like species results in a very high equilibrium dipole moment, μ_e= 8.10 D; such high a value was also predicted by Osamura *et al.* (1999).

Table III.8. Most populated valence shell Natural Bond Orbitals (NBO) for HCNCC (Kołos & Dobrowolski 2003a)

Orbitals *)	Occupancy (electrons)		Energy (hartree)	
	HF/ aug-cc-pVTZ	B3LYP/ aug-cc-pVTZ	HF/ aug-cc-pVTZ	B3LYP/ aug-cc-pVTZ
σ (H—C1)	2.00	1.99	-0.86	-0.69
σ (C1—N)	2.00	1.99	-1.38	-1.13
π (C1—N)	1.98	1.97	-0.58	-0.46
π (C1—N)	1.98	1.97	-0.58	-0.46
σ (N—C2)	2.00	1.99	-1.12	-1.01
σ (C2—C3)	2.00	1.99	-0.87	-0.81
π (C2—C3)	1.82	1.74	-0.25	-0.27
π (C2—C3)	1.82	1.74	-0.25	-0.27
lone pair C3	1.99	1.97	-0.46	-0.40
π* (C1—N)	0.18	0.26	0.21	-0.03
π* (C1—N)	0.18	0.26	0.21	-0.03

*) atom numbering: H—C1—N—C2—C3

HCNCC is a peculiar molecule, with an unusual electronic organization. To shine some light on it, Kołos & Dobrowolski (2003a) accomplished the natural bond orbitals (NBO) analysis (Brunck & Weinhold 1979, Foster & Weinhold 1980) at SCF and DFT levels. The result (Table III.8) points to the Lewis formula with eight bonding electron pairs, and a lone pair on the terminal carbon atom:

$$H-C\equiv N^{+}-C\equiv \ddot{C}^{-}$$

This picture, while giving some rationale to the predicted charge distribution, is

[1] Excitation to the lowest triplet state (30 kcal/mol above the singlet at the UB3LYP/aug-cc-pVTZ theory level) would distort the linearity. Four other cyanoacetylene isomers were also found to have singlet ground states.

certainly oversimplified; calculated r_{C2-C3} is too long for a true triple bond; in fact it is only slightly shorter than r_{N-C2} (numbering scheme: H—C1—N—C2—C3). This elongation of r_{C2-C3} stems from the sizeable electronic delocalization, most clearly seen in the decreased occupancy of relevant π-type NBOs, and in the corresponding population of antibonding π^*_{C1-N} orbitals. Within the framework of an idealized Lewis structure, π_{C2-C3} and π^*_{C1-N} would be highest occupied (HOMO) and lowest unoccupied (LUMO) orbitals, respectively.

As described in Section II.1*a*, a mixed experimental-theoretical study permitted Botschwina *et al.* (1992b) to obtain highly precise bond lengths for cyanoacetylene. The same approach was possible also for isocyanoacetylene (Botschwina *et al.* 1992). Kołos and Dobrowolski (2003a) used these data to scale their DFT and coupled-clusters predictions for HCNCC. Following the general rule, interatomic distances calculated with B3LYP and CCSD(T) are under- and overestimated, respectively. A simple scaling recipe was adopted, based on the data collected in Table III.9: B3LYP-derived value of C—H distance was taken as exact, while for all remaining bonds the CCSD(T) results were multiplied by 0.995. Applying this procedure to HCNCC, Kołos & Dobrowolski obtained the following corrected values (in Å):

r_{H-C1}=1.063, r_{C1-N} =1.163, r_{N-C2}=1.278, r_{C2-C3}=1.266.

The ensuing value of the equilibrium rotational constant was B_e= 4992 MHz.[1]

Table III.9. CCSD(T)/aug-cc-pVTZ and B3LYP/aug-cc-pVTZ bond lengths (Å) for HCCCN and HCCNC, together with their percent deviations from best known experimental/theoretical values.

method	H—C—C—C—N				H—C—C—N—C			
	R(H-C)	R(C-C)	R(C-C)	R(C-N)	R(H-C)	R(C-C)	R(C-N)	R(N-C)
CCSD(T) *)	1.065	1.212	1.383	1.167	1.064	1.210	1.320	1.186
	0.28%	*0.49%*	*0.51%*	*0.52%*	*0.28%*	*0.58%*	*0.46%*	*0.59%*
B3LYP *)	1.062	1.201	1.368	1.155	1.061	1.199	1.306	1.177
	0%	*-0.41%*	*-0.58%*	*-0.52%*	*0%*	*-0.33%*	*-0.61%*	*-0.17%*
Exp./theor. (Botschwina *et al.* 1992, 1993b)	1.062	1.206	1.376	1.161	1.061	1.203	1.314	1.179

*) Kołos & Dobrowolski 2003a

Table III.10. presents the vibrational transitions of HCNCC calculated with B3LYP. The predicted infrared spectrum is dominated by the C—H stretch band and two highly delocalised modes in the triple bond stretching region.

[1] Very recent predictions based on corrected CCSD(T)/cc-pVQZ calculations (Botschwina 2003b) led to interatomic distances identical within 0.001 Å, and to the B_e value of 5003.6±10 MHz.

Table III.10. Harmonic frequencies (downscaled by 0.96) and absolute intensities for three isotopomers of HCNCC, as derived with B3LYP/ aug-cc-pVTZ (Kołos & Dobrowolski 2003a).

Mode / symmetry	$^1H^{12}C^{14}N^{12}C^{12}C$		$^1H^{12}C^{15}N^{12}C^{12}C$		$^2H^{12}C^{14}N^{12}C^{12}C$	
	cm^{-1}	km/mol	cm^{-1}	km/mol	cm^{-1}	km/mol
ν_1 / σ	3325	415	3324	407	2599	517
ν_2 / σ	2159	772	2121	797	2071	727
ν_3 / σ	1934	272	1931	227	1872	100
ν_4 / σ	948	6.6	943	7.1	933	7.2
ν_5 / π	501	0.7	492	1.0	493	0.6
ν_7 / π	377	42	374	42	342	19
ν_8 / π	183	0.06	183	0.06	184	0.6

In parallel with the article of Kołos & Dobrowolski (2003a), the paper by Guennoun *et al.* (2003) appeared, in which the authors reported on the discovery of HCNCC in cyanoacetylene-doped argon matrices photolysed with far-UV radiation ($\lambda > 120$ nm). Guennoun *et al.* based their assignment on three mutually correlated bands, and backed it with the deuterium substitution experiment. The comparison of these experimental results (Table III.11) with theoretical predictions (Table III.10) is promising but advocates for some additional evidence. In particular, an experiment with the ^{15}N-substituted precursor should be conclusive.

Table III.11. Bands arising from the far-UV photolysis of cyanoacetylene in Ar, assigned to HCNCC (Guennoun *et al.* 2003)

Mode/symmetry	From $^1H^{12}C^{12}C^{12}C^{14}N$ precursor		From $^2H^{12}C^{12}C^{12}C^{14}N$ precursor	
	cm^{-1}	Intens. (%)	cm^{-1}	Intens. (%)
ν_1 / σ	3277	49	2568	58
ν_2 / σ	2102	100	2029	100
ν_3 / σ	1920	8		

It has to be noted that the chances for the detection of HCNCC, either in microwave or infrared ranges – albeit reduced by the molecule high energy – seem substantial due to the prominent dipole moment, and to strong infrared transitions of this molecule.

The vibrational frequencies were calculated also for cyanovinylidene (Table III.12) The CCSD(T) method used by Hu & Schaefer (1993) is expected to give better predictions on intensities, while scaled DFT (Kołos and Dobrowolski 1993b) should produce more reliable frequencies – judging from the performance of both methods applied to cyanoacetylene. Vibrational transitions of cyanovinylidene are of a medium strength, resembling those of cyanoacetylene (Hu & Schaefer 1993),

and are much weaker than for the imine isomer (Kołos & Sobolewski 2001), where maximal intensities approach 1600 km/mol. These predictions on cyanovinylidene did not thus far led to any experimental findings.

Table III.12. Harmonic vibrational frequencies (cm^{-1}) and infrared intensities (km/mol) for cyanovinylidene

mode	CCSD(T)/TZ2P (Hu & Schaefer 1993)		B3LYP/aug-cc-pVTZ (Kołos & Dobrowolski 2003b)	
	frequency	intensity	frequency*)	intensity
ν_1	3162	24	2914	53
ν_2	2257	7	2257	22
ν_3	1648	55	1662	80
ν_4	1021	1	975	2
ν_5	924	3	882	2
ν_6	495	5	627	20
ν_7	396	3	404	2
ν_8	247	3	363	0
ν_9	162	16	147	23

*) scaled with the factor 0.96

Figure III.7 presents the calculated structure of cyanovinylidene. A*b initio* CCSD(T)/aug-cc-pVTZ bond lengths and angles are very close to those obtained by Hu and Schaefer, who used the same method and a slightly smaller basis set. Resulting equilibrium rotational constants are: A_e = 72.053 GHz, B_e = 5.3774 GHz, C_e = 5.0040 GHz. The DFT geometry leads to following values: A_e = 81.501 GHz, B_e = 5.3586 GHz, C_e = 5.0281 GHz.

While the CCSD(T) calculations carried out by Kołos & Dobrowolski (2003a) yielded the best currently available energy of cyanovinylidyne, the question remains (just like in the HCNCC case discussed above) whether CCSD(T) or DFT better predicts its geometry. Kołos & Dobrowolski (2003b) compared calculated B_e constants for cyano- and isocyanoacetylene (and $\frac{1}{2}[B_e+C_e]$ for a quasi-linear imine HNCCC) with available experimental B_0 values (Creswell *et al.* 1977, Krüger *et al.* 1991, Hirahara *et al.* 1993). At this level of accuracy, the differences between equilibrium and ground-state constants are negligible (less than 1 MHz; Botschwina 1992, 1993b). DFT yielded generally lower errors (+1.01%, +0.83%, and +0.44%, for HCCCN, HCCNC, and HNCCC, respectively) than CCSD(T). With the latter method, however, the errors were remarkably stable (-1.01%, -1.01%, -1.10%). Kołos & Dobrowolski (2003b) decided to base their prediction for cyanovinylidene rotational constants on CCSD(T)-derived values increased by 1%, which led to following recommendations: A_e = 72.774 GHz, B_e = 5.431 GHz, C_e = 5.054 GHz.

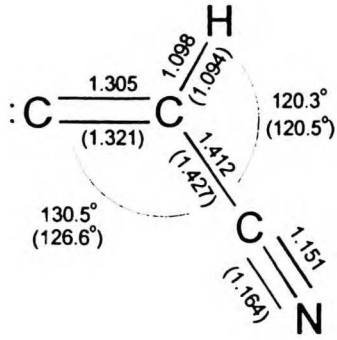

Figure III.7. Structure of cyanovinylidene as predicted at B3LYP/aug-cc-pVTZ and (in parentheses) CCSD(T)/aug-cc-pVTZ levels of theory. Bond lengths in angstroms (Kołos & Dobrowolski 2003b).

III.1e Interstellar synthesis of C_3HN species

The abundances of isomeric molecules HCCNC and CCCNH are low when compared to cyanoacetylene. Respective ratios of *ca.* 1:130 and 1:1000 were found in the molecular cloud TMC-1 (Ohishi & Kaifu 1998). The same isocyano-/cyanoacetylene ratio of 1:130 was reported by Gensheimer (1997) for the expanding envelope of the carbon star IRC +10216. The neutral-neutral reaction C_2H_2 + CN (Woon & Herbst 1997, Fukuzawa & Osamura 1997, Huang *et al.* 2000, Balucani *et al.* 2000), already introduced in Section I.2, is commonly recognised as the main source of interstellar cyanoacetylene, while the dissociative recombination of the known interstellar species HC_3NH^+ (Kawaguchi *et al.* 1994) with electrons is expected to produce, in addition to cyanoacetylene, the desired quantities of other isomers.

Following the capture of a slow ("cold") electron in the interstellar environment, the ground-state $HCCCNH^+$ changes into a diffuse Rydberg state (rather, into a continuum of Rydberg states near the ionization limit) of the HCCCNH radical. The newly formed species is thus rich in energy, which it cannot easily dispose of – the radiative relaxation is slow, and collision-induced energy exchange processes can be neglected at interstellar cloud densities.

In a simplified approach it is assumed that the fate of the system is determined by unimolecular transformations of the highly energetic radical within the ground state potential energy surface of the C_3H_2N system. Indeed, at least some of the molecules may reach the ground electronic state, driven by equienergetic internal conversion processes and by a fast "internal thermalisation", *i.e.* by the redistribution of the excess energy among many internal degrees of freedom. Simple calculation shows that the latter process makes the average vibrational energy *per mode* of HCCCNH (as expressed by the *vibrational temperature*), an order of magnitude lower than the total excess energy. This could permit the excitation energy to dwell (for a certain interval, on the time scale of molecular vibrations) at the bottom of the ground state potential energy surface, distributed

among many modes. Within given vibrations, energy inflows and outflows would promote the rearrangements of atoms or dissociation phenomena.[1]

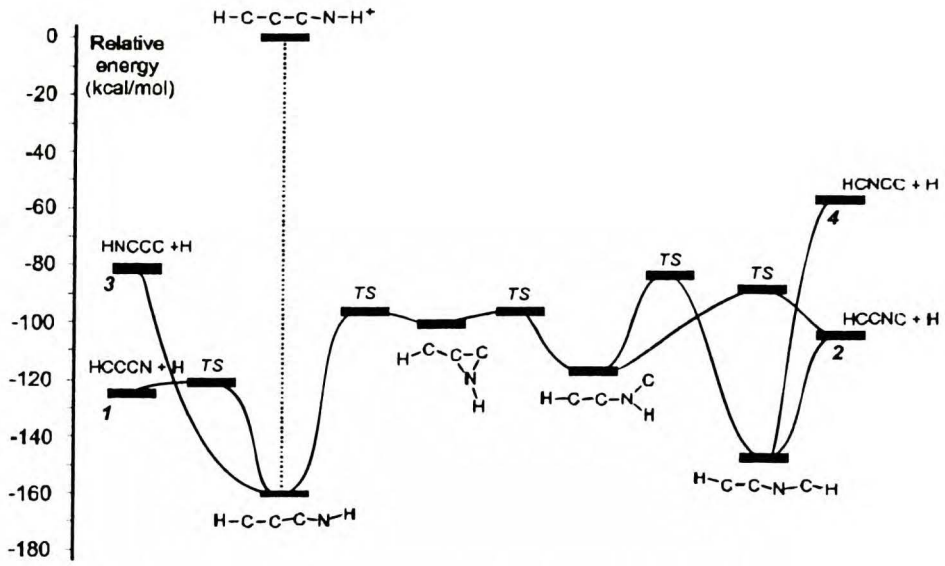

Figure III.8. Schematic representation of a part of the C_3H_2N potential energy surface. The symbolic lines, which connect stationary points found by Osamura *et al.* (1999), lead to four exit channels, and four chain isomers of cyanoacetylene. Transition states (saddle points) marked as *TS*.

Osamura *et al.* (1999) performed a thorough study of the dissociative recombination $HCCCNH^+ + e$. Based mostly on DFT calculations, they analysed the fate of an energy-rich HCCCNH radical within the ground (doublet) C_3H_2N potential energy hypersurface. Figure III.8 depicts the main results of that work.

The most straightforward exit channels, marked as *1* and *3* in the Figure, consist in the removal of hydrogen atoms, from either end of the chain. These processes (analogous to the formation of HCN and HNC from $HCNH^+$, *cf.* Section I.2), resulted in the synthesis of cyanoacetylene, HCCCN, and its imine isomer, HNCCC. In search for a possible reaction path towards isocyanoacetylene, HCCNC, Osamura *et al.* analysed the rearrangements accessible behind certain saddle points (transition states). The route led through three isomers of the original HCCCNH radical, and terminated with two possible exit channels (*2* and *4*), to

[1] The complete picture would have to take into account the excited valence electronic states, and all possible rearrangements of the molecule therein (including the bond breaking, possibly via the predissociation) on respective energy surfaces. This approach, which was already applied to the dissociative recombination of $HCNH^+$ (Shiba *et al.* 1998), becomes exceedingly difficult with the increasing number of vibrational modes.

HCCNC and to HCNCC. (Consequently, the first remark on HCNCC appeared in the literature.)

Kołos & Dobrowolski (2003b) extended this approach by looking for the possibility of cyanovinylidene synthesis, which could follow the $HCCCNH^+ + e$ recombination. The results of their study, as yet unpublished, are presented here in detail. Dashed lines in Figure III.9 represent the pathways formerly derived by Osamura *et al.* (1999). The most likely route towards cyanovinylidene (bold arrows), as calculated with the density functional theory, leads through two consecutive rearrangements of the radical HCCCNH (hereafter: **R1**), followed by the hydrogen atom detachment. First, the hydrogen atom is shifted from nitrogen to the neighbouring carbon, which yields HCCC(H)N radical (**R2**) of the energy very similar to that of **R1**. The same hydrogen is further transferred to the middle carbon atom, which results in the formation of a deeply bound species HCC(H)CN (**R3**). This cyanovinyl radical, described by Fukuzawa & Osamura (1997), Woon & Herbst (1997), Huang *et al.* (2000) and Balucani *et al.* (2000) as an intermediate product in the C_2H_2 + CN reaction (and the direct precursor for cyanoacetylene through **TS3**; thin arrows), should exist in *cis* and *trans* conformations, practically equienergetic and separated by a low barrier, of the order of 10 kcal/mol. Processes **R2** → **R3** → CC(H)CN + H do not markedly depend on the conformation of **R3**, hence, for clarity, only *cis* form is shown in Fig.III.9.

Both transition states, **TS1** and **TS2,** engaged in successive hydrogen shifts, are easily accessible. (The relative energy values for all relevant species are collected in Table III.13). However, the most probable exit channel associated with **R3** leads through the elimination of another hydrogen atom (creation of cyanoacetylene). Thus, the exits from **R3** and **R1** are to some extent similar: in both cases cyanoacetylene is formed via a transition state, and, additionally, a high energy isomer (imine or cyanovinylidene, for **R1** and **R3**, respectively) can arise without a barrier. The small energy difference between the imine and cyanovinylidene is not the decisive parameter determining their actual yields ratio, since – looking from the original minimum (**R1**) – the path on the potential energy surface is much more complicated in the direction of cyanovinylidene than it is in direction of the imine. Thus, prior to the expected re-examination of chemical models for molecular clouds – supplemented with the cyanovinylidene creation and decay – one can anticipate for this isomer an abundance lower than that of the imine. On the other hand, Fig.III.9 indicates that cyanovinylidene should be formed with higher a yield than the species HCNCC. All considered, cyanovinylidene seems to be a non-negligible interstellar species. Its fractional abundance in TMC-1 is probably confined within the range extending from 2×10^{-11} (theoretical predictions for HCNCC by Osamura *et al.* (1999)) to 6×10^{-11} (HNCCC observations by Ohishi & Kaifu (1998)).

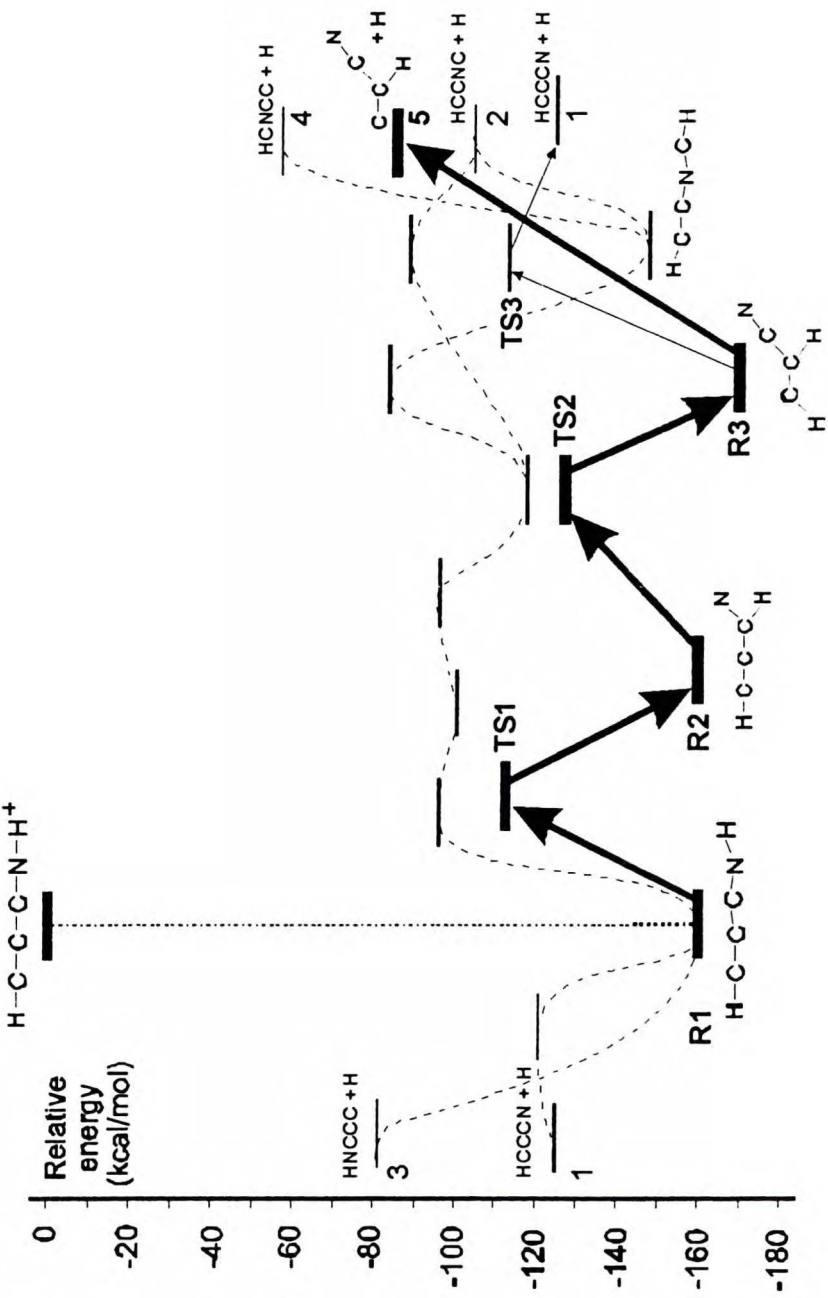

Figure III.9. The proposed pathway towards cyanovinylidene, as calculated with UB3LYP/aug-cc-pVTZ, is marked by bold arrows (Kolos & Dobrowolski 2003b). Position of TS2 is less certain then for TS1 and TS3, its relative energy being calculated at UBP86/DN level of theory. Dashed lines, linking the stationary points derived by Osamura *et al.* (*cf.* Fig. III.8), are given as a reference.**

Table III.13 Relative energies of molecules relevant to the interstellar synthesis of cyanovinylidene, as measured against $HCCCNH^+$ cation. (Kołos & Dobrowolski 2003b)

	UB3LYP/aug-cc-pVTZ (kcal/mol)
R1	-159.4
R2	-157.2
R3	-168.5
TS1	-114.1
TS2	-128*)
5 + H	-75.6

*) Based on calculations with UBP86 functional, and DN** basis set.

However, when taking the imine isomer as a reference in estimating the chances for a microwave detection of cyanovinylidene, it has to be recalled that the electric dipole moment of the latter molecule is only 2.76 debye (Hu & Schaefer 1993), roughly half the value predicted for the imine (5.67 debye; Botschwina *et al.* 1992). Consequently, the detection of cyanovinylidene in interstellar molecular clouds via microwave emission may prove at least as difficult as the detection of highly energetic HCNCC; the lower abundance of HCNCC may be compensated with a fairly large dipole moment, 8.1 debye (Osamura *et al.* 1999, Kołos & Dobrowolski 2003a).

As discussed earlier, the IR detection of cyanovinylidene will also be difficult. The availability of laboratory frequencies, IR and microwave, seems crucial for the interstellar identification of this species, which may serve to verify current concepts on the astrochemistry of cyano- molecules.

III.2 Isomers of dicyanoacetylene, NC_4N

Dicyanoacetylene (2-butynedinitrile) is the first member of the homologous series N≡C—(C≡C)$_n$—C≡N. It was first synthesized by Moureu & Bongrand (1909, 1920a)[1], who at the time baptized it with the name *sous-azote de carbon* (carbon subnitride). Its physical properties are similar to those of cyanoacetylene; at room temperature it is a clear, colourless, and irritant liquid with a high vapour pressure.

Because of no permanent electric dipole moment (lack of pure rotational spectrum), the molecule could not so far be detected in the interstellar medium. During the Voyager mission, it has tentatively been identified as the source of the 478 cm^{-1} absorption in the atmosphere of Titan, the Saturn's moon (Khanna *et al.* 1987, Samuelsson *et al* 1997).

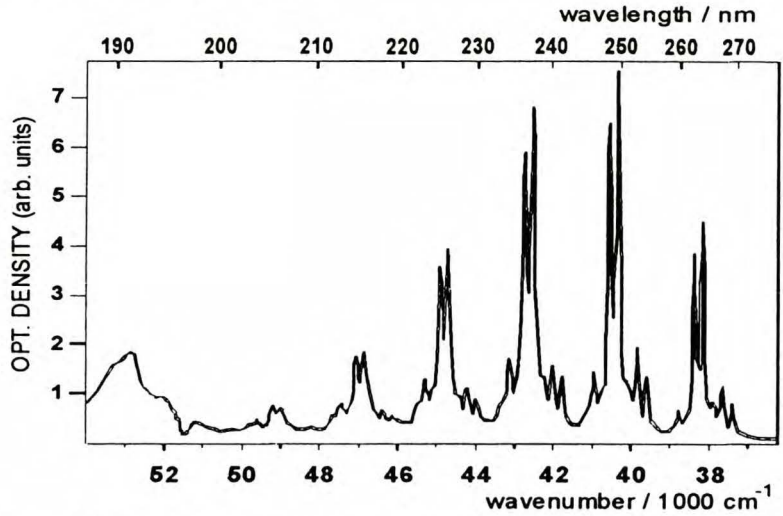

Figure III.10. Electronic absorption of gaseous dicyanoacetylene, C_4N_2, Kolos *et al.* 1991; reprinted with the permission from Elsevier Ltd.

The first electronic transition of NC_4N is the symmetry-forbidden $^1\Sigma_u^-$—$^1\Sigma_g^+$ with the origin at 280 nm (oscillator strength $f \approx 2 \times 10^{-5}$); the second one ($^1\Delta_u$—$^1\Sigma_g^+$), two orders of magnitude more intense ($f \approx 4 \times 10^{-3}$), begins at 268 nm. These two systems were first measured by Miller & Hannan (1958). An extremely strong ($f \approx 1.5$), fully allowed $^1\Sigma_u^+$—$^1\Sigma_g^+$ transition has the peak absorption band around 160 nm (Connors *et al.* 1974). Figure III.10 shows the quartz-UV spectrum of gaseous dicyanoacetylene, as reported by Kołos *et al.* (1991). Smith *et al.* (1993)

[1] The preparation, which starts with the symmetric ester, is analogous to the synthesis of cyanoacetylene (Section III.1)

detected the visible phosphorescence $^3\Sigma_u^+ — ^1\Sigma_g^+$ (with an origin at 391 nm) in their argon matrix isolation study.

The vibrational spectrum of dicyanoacetylene was measured and analysed by Miller & Hannan (1953, 1955), Khanna *et al.* (1987), and Smith *et al.* (1993). Table III.14 lists the vibrational frequencies obtained in solid argon by Smith *et al.*, who, apart from the infrared absorption, have also measured vibrational spacings in a well-resolved $^3\Sigma_u^+ — ^1\Sigma_g^+$ phosphorescence.

Table III.14. Vibrational spectroscopy of dicyanoacetylene (N≡C-C≡C-C≡N)

	Freq. / cm^{-1}	Reference
σ_g	2267, 2333 [a]	Smith *et al.* (1993) (Ar matrix)
	2118 [b]	
	618 [c]	
σ_u	2239.5	
	1154.0	
π_g	504	Khanna *et al.* (1987) (gas)
	263	
π_u	471	
	107	

[a] Fermi resonance pair; measured as the vibrational spacing in $^3\Sigma_u^+ — ^1\Sigma_g^+$ phosphorescence.
[b] Based on a combination band frequency.
[c] Based on the normal coordinate analysis.

Several groups studied the gas-phase photochemistry of dicyanoacetylene, including Sabety-Dzvonik *et al.* 1976, Halpern *et al.* (1988, 1990), Kołos *et al.* (1991, 1992). The basic reaction consists in the breaking of a single bond:

$$NC_4N + h\nu \rightarrow C_3N + CN \qquad (i)$$

Two main products were observed: CN and C_2, the latter most likely being formed in a secondary photodissociation of the free radical C_3N:

$$C_3N + h\nu \rightarrow C_2 + CN \qquad (ii)$$

Despite certain efforts, C_3N itself could not be detected in these studies (see Section III.1*a*).

III.2a Formation of NC-CC-NC and CN-CC-NC

The matrix-isolation work on cyanoacetylenes was pioneered a decade ago by Smith *et al.* (1993) [1] with their study of the dicyanoacetylene dissociation in solid argon. Smith *at al.* noticed that the monochromatic irradiation with 235 nm resulted in the development of very strong bands[2]. Knowledge of the cage effect led

[1] In the group of Vladimir E. Bondybey, Techn. Univ. München, Garching, Germany.
[2] The bands were strong enough to allow for measurements of isotopomeric "satellite" features coming from the natural content of ^{13}C, which supplied data for a normal coordinate analysis.

the group to propose the product of a single CN group reversal, namely NC_3NC (cyanoisocyanodiacetylene), as the carrier of these bands, a supposition confirmed by subsequent *ab initio* calculations (Botschwina *et al.* 1993c, Horn *et al.* 1994, Bartel *et al.* 1998)[1]. Table III.15 presents the details of this assignment. Further measurements enabled Smith *et al.* (1994a) to append the list of bands with 10 weaker features due to combination and overtone modes.

Table III.15. IR vibrational transitions of cyanoisocyanocetylene (N≡C-C≡C-N=C:) in solid Ar (Smith *et al.* 1993)

	Frequency (cm^{-1})	Intensity [b] (km/mol)
ν_1 [a]	2287.1	100.0
ν_2	2203.6	97.0
ν_3	2044.8	186.0
ν_4	1202.3	1.0
ν_5	610.1	1.3
$2\nu_4$ [a]	2408.9	25.0

[a] These frequencies are in a Fermi resonance.
[b] Normalised to the highest absolute intensity given by *ab initio* calculations *i.e.* 186 km/mol (Botschwina *et al.* 1993c).

Two additional, mutually correlated product bands – not related to those of NC-CC-NC, and much weaker – were tentatively assigned by Smith *et al.* (1993) to a molecule resulting from the rotation of *both* cyano groups, that is CN-CC-NC (diisocyanoacetylene). These bands appeared also when, instead of the *in situ* photolysis, the electrical discharges through Ar/dicyanoacetylene mixture were exerted[2]. After discharges, however, the intensities of NC-CC-NC and CN-CC-NC bands were similar. Table III.16 contains the wavenumbers of two bands attributed to ν_4 and ν_5 asymmetric stretching modes of diisocyanoacetylene. Very high absolute intensity of these bands, theoretically predicted by Botschwina *et al.* (1993c), should be noticed.

The photochemical threshold for single bond dissociation in dicyanoacetylene, as measured in the gas phase by Halpern (1988) is 232 ± 1 nm. The effectiveness, with which the 235 nm radiation transforms the molecule, was explained by Smith *et al.* (1993) with a two-photon absorption, involving the triplet state as an intermediary level [3].

---

[1] All these calculations were accomplished in the research group of Peter Botschwina at the Göttingen University, Germany. More recently, a DFT study on acetylenic isonitriles was carried out by Lee (1998).
[2] See Section II.2*b* for the description of the pulsed discharge device (Thoma *et al.* 1992).
[3] Kołos *et al.* (1991, 1992) have also discussed the rôle of two-photon processes in the laser photolysis of dicyanoacetylene.

Table III.16. IR vibrational transitions of diisocyanocetylene (:C=N-C≡C-N=C:) in solid Ar (Smith *et al.* 1993)

	Experimental		CEPA-1 calculations [a]	
	Frequency (cm^{-1})	Intensity [b] (km/mol)	Frequency (cm^{-1})	Intensity (km/mol)
ν_4	2114.9	553	2122	553
ν_5	1287.5	74	1213	9

[a] Unpublished Botschwina's *et al.* results, as cited by Smith *et al.* (1993).
[b] Normalised to the highest absolute intensity given by *ab initio* calculations.

III.2b The search for additional C_4N_2 species. Identification of CCCN-CN.

Formally, dicyanodiacetylene has as many as 9 non-branched chain isomers, hereafter named **1-9** (Figure III.11*a*). Kołos (2002, **paper IX**) carried out a theoretical study, which took account of all these molecules, mostly hypothetical, together with dicyanovinylidene:

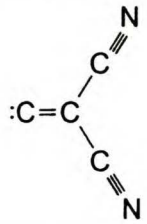

(**10**), presumably the most stable species among branched C_4N_2 structural variants. Additionally, the hexagonal C_4N_2 arrangements with nitrogen atoms in *para* (**11**), *meta* (**12**) and *ortho* positions were considered (Figure III.11*b*).[1] The aim of this work was to find previously overlooked, yet potentially detectable molecules.

The first stage consisted in calculations of preliminary structures (in particular, in finding out what *symmetries* of chain species **1-9** can be expected). Then, the *geometries* and IR spectra were obtained at the reliable DFT level. Finally, the geometry optimizations were repeated for selected species, to improve the predictions on *energies* and dipole moments.

The rudimentary search for equilibrium geometries of chain molecules **1-9** was accomplished at a simple self-consistent-field level (HF/6-31G*). Planar starting geometries, with uniform bond lengths and all combinations of $+133^\circ$ and -133° angles between consecutive bonds were systematically tried. The nature of obtained stationary points on the potential energy surface was disclosed by the normal modes of molecular vibrations, saddle points being indicated by the appearance of imaginary frequencies. For the branched and hexagonal species, the preliminary calculations consisted in geometry optimizations at the B3LYP/6-31G* level. The

[1] The *ortho, meta, para* prefixes, though intuitively comprehensible, have no *formal* applicability to these unsubstituted heterocycles.

hexagon with adjacent nitrogen atoms (*ortho* structure) converged to dicyanoacetylene (**1**) and was rejected from further analysis.

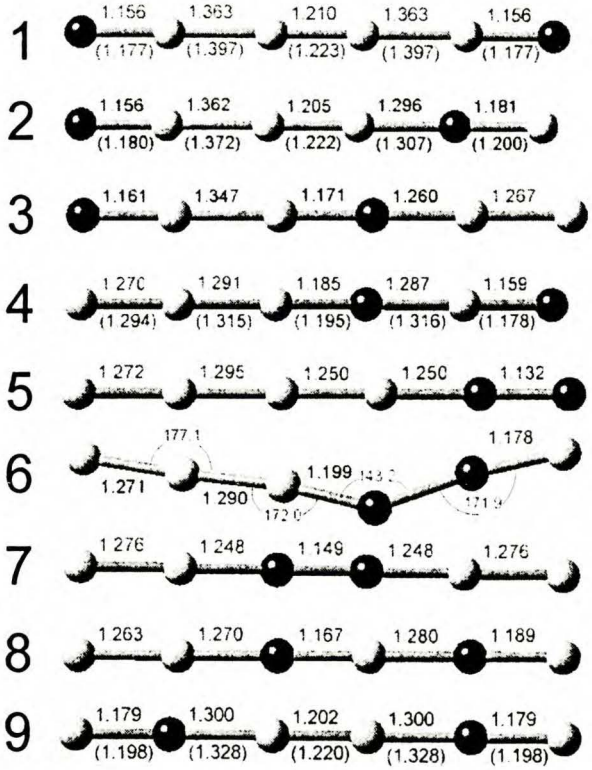

Figure III.11*a*. Equilibrium geometries for open chain C_4N_2 isomers, as predicted with B3LYP/aug-cc-pVTZ (Kołos 2002). Black balls represent nitrogen atoms. Bond lengths given in angstroms. Values in parentheses result from MP4(SDTQ)/cc-pVTZ geometry optimizations. Reprinted with the permission from the American Institute of Physics.

It was checked that the ground electronic states of all molecules under study were of singlet multiplicity. The UB3LYP/6-31G* scheme was used to find the geometries of triplet species for branched and cyclic isomers, while the combination of UHF/6-31G* and UB3LYP/6-31G* served to optimize diverse starting geometries of chain molecules. The potential energy minima of triplets (E_T) were compared to those of singlets (E_S) at the uniform DFT level. The E_T-E_S differences were at least 19 kcal/mol, with the exception of isomer **11**, for which the triplet equilibrium structure was just 1.5 kcal/mol above the singlet.

In the second phase of the study, the B3LYP/aug-cc-pVTZ calculations were performed for singlet isomers **1-12**. This was aimed at producing the realistic predictions for geometries and corresponding harmonic vibrational frequencies, and at selecting the energetically favorable species. For molecules **1-5** and **7-9** arbitrarily chosen zigzag starting geometries converged to linearity. Some bent

structures (yielded by HF calculations) were also subjected to B3LYP/aug-cc-pVTZ geometry optimizations; this usually corrected their structures to linear ones. The only exception was molecule **6**, for which, similarly as in the HF study, the linear conformation was in fact a saddle point, and the energy minimum corresponded to a bent arrangement.

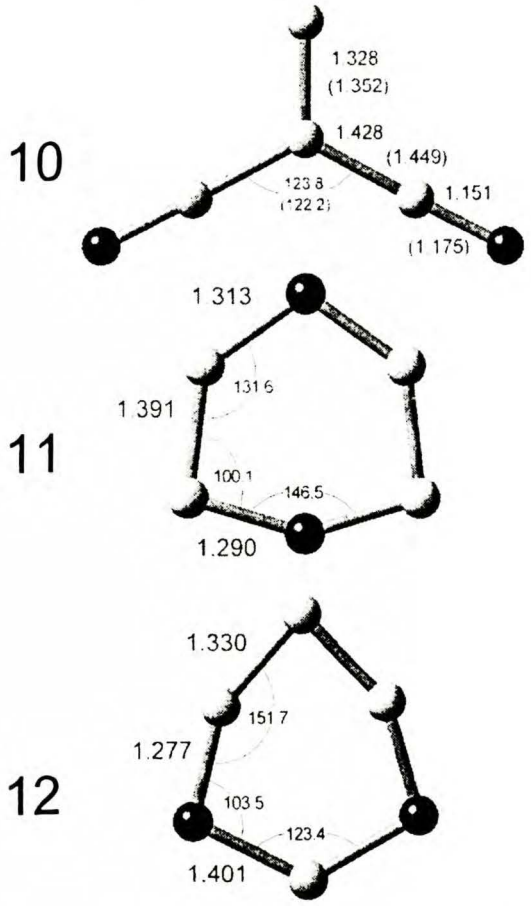

Figure III.11*b*. Dicyanovinylidene and two hexagonal isomers of C_4N_2, predicted with B3LYP/aug-cc-pVTZ (Kołos 2002). Labels as in Fig. III.11*a*. Reprinted with the permission from the American Institute of Physics.

The correctness of DFT-produced equilibrium structures could be checked making use of experimental ground-state rotational constants (B_0), available for isomers **1** (Winther *et al.* 1992) and **2** (Bartel *et al.* 1998). The B_0 values are related to equilibrium rotational constants: $B_e=B_0+\Delta B$, where ΔB is half the sum of vibration-rotation coupling coefficients multiplied by degeneracy factors (*cf.* Section III.1*a*). The ΔB predictions obtained with CEPA-1 for species **1** (Oswald 1995), and with CCSD(T) for **2** (Bartel *et al.* 1998) supplied, together with corresponding measurements of B_0, highly accurate equilibrium rotational constants

(see Table III.20 and references therein). The DFT study accomplished by Kołos led to B_e higher by 1.2% (**1**) and 0.8% (**2**), which suggested that – also for other rod-shaped C_4N_2 isomers – the B3LYP/aug-cc-pVTZ-derived B_e constants should be scaled with the factor 0.99.

Table III.17. Energies, dipole moments and main IR vibrational transitions for C_4N_2 molecules, as predicted by the density functional theory B3LYP/aug-cc-pVTZ (Kołos 2002).

Molecule & symmetry			Total energy [a] (hartree)	**Relative energy [a] kcal/mol**	Rotat. const. [b] (GHz)	μ_e (D)	Main IR vibr. transitions (frequencies scaled by 0.96)	
							Harmonic frequency [d] (cm^{-1})	Intensity (1000 km/mol)
1	NCCCCN	$D_{\infty h}$	-261.883991	**0**	1.3494	0	109, 492, 1142, 2249	0.011, 0.008, 0.00008, 0.012
2	CNCCCN	$C_{\infty v}$	-261.846202	**23.7**	1.4213	1.33	2029, 2205, 2285	0.23, 0.05, 0.11
3	CCNCCN	$C_{\infty v}$	-261.765228	**74.5**	1.467	2.53	1939, 2173, 2262	0.71, 0.33, 0.62
4	CCCNCN	$C_{\infty v}$	-261.791218	**58.2**	1.477	0.94	1918, 2216, 2278	0.25, 0.90, 1.68
5	CCCCNN	$C_{\infty v}$	-261.743732	**88.0**	1.439	4.49	1876, 2134, 2207	0.47, 0.42, 3.04
6	CCCNNC	C_s	-261.712545	**107.6**	103.8 1.619 1.594	1.60	2083, 2194	0.84, 1.47
7	CCNNCC	$D_{\infty h}$	-261.615693	**168.4**	1.582	0	1963	2.46
8	CCNCNC	$C_{\infty v}$	-261.723001	**101.0**	1.546	4.33	1914, 2017, 2296	0.13, 1.30, 0.35
9	CNCCNC	$D_{\infty h}$	-261.805347	**49.3**	1.497	0	1230, 2092	0.004, 0.560
10	CC(CN)CN	C_{2v}	-261.785274	**61.9**	8.860 2.742 2.094	1.28	215, 1554	0.02, 0.05
11	*para*-cyclic	C_{2v}	-261.659069	**141.1**	8.105 7.236 3.823	0.59	347, 873, 897, 1413, 1533	0.12, 0.19, 0.16, 0.21, 0.19
12	*meta*-cyclic	C_{2v}	-261.714886	**106.1**	7.848 7.485 3.831	1.31	614, 1554, 1695	0.11, 0.16, 0.23

[a] zero-point correction included

[b] B_e constants for linear species (B_e multiplied by 0.99 can serve as the prediction for B_o; see text); A_e, B_e and C_e for nonlinear species

[c] the most intense bands for each isomer are listed; transitions predicted as relatively weak are included for **1** and **9** to ease the comparison with available experimental and theoretical data (*cf.* Tables III.14-16, III.20); complete listings of vibrational transitions for species 4 and 10 are given in Table III.18

Mixed experimental-theoretical B_e values obtained for different isotopomers of **2** enabled Bartel *et al.* (1998) to report the following equilibrium geometry (in Å, for N1–C1–C2–C3–N2–C4): R_{N1-C1}=1.1611, R_{C1-C2}=1.3712, R_{C2-C3}=1.2074, R_{C3-N2}=1.3050, R_{N2-C4}=1.1819, with errors presumably smaller than 0.001 Å. DFT calculations yield the bonds shortened by 0.4%, 0.7%, 0.2%, 0.7%, and 0.1%, respectively.

Table III.17 lists the energies and equilibrium electric dipole moments, together with harmonic frequencies and absolute intensities of IR vibrational transitions (the strongest bands are given for each molecule). Values derived for species **1**, **2** and **9** generally agree well with former experimental and theoretical data (*cf.* Table III.20). As expected, however, when compared with advanced *ab initio* treatment of anharmonic vibrations, DFT is much worse in reproducing IR intensities.

Table III.18 Harmonic vibrational wavenumbers and IR intensities of CCCNCN and CC(CN)CN (dicyanovinylidene), as predicted with B3LYP/aug-cc-pVTZ (Kołos 2002).

mode	symmetry	wavenumber [a] (cm^{-1})	intensity (km/mol)
C C C N C N			
ν_1	σ	2279	1679
ν_2	σ	2216	898
ν_3	σ	1918	249
ν_4	σ	1210	8.6
ν_5	σ	660	0.7
ν_6	π	497	4.9
ν_7	π	439	14
ν_8	π	161	3.4
ν_9	π	52	8.9
C C (C N) C N			
ν_1	a_1	2252	2.1
ν_2	b_2	2247	0.4
ν_3	a_1	1554	53
ν_4	b_2	1107	2.5
ν_5	a_1	707	1.9
ν_6	b_1	578	0.8
ν_7	a_1	540	0.0
ν_8	a_2	384	0.0
ν_9	b_2	368	0.2
ν_{10}	b_1	215	20
ν_{11}	b_2	130	4.9
ν_{12}	a_1	127	9.6

[a] scaled with the factor 0.96

The most important predictions of the DFT study concern species **10**, CC(CN)CN, and **4**, CCCNCN. It appears that the energy of **4**, corrected for the zero-point energy (ZPE), is just several kcal/mol above that of the known centrosymmetric isomer **9**. Isomer **4** is remarkable due to the gigantic strength of its infrared bands, approaching 1700 and 900 km/mol – which should facilitate its detection in forthcoming astronomical searches. Isomer **10**, of the similar energy, is expected to have medium intensity IR bands. The full listing of predicted fundamental modes for species **4** and **10** is given in Table III.18.

In the final stage of Kołos's theoretical study, calculations for most important isomers were repeated at the higher level of theory – to refine the energetics. The *ab initio* geometry optimizations, on molecules with fixed symmetries (either $D_{\infty h}$, $C_{\infty v}$ or C_{2v}, as predicted with DFT), were carried out using MP4(SDTQ)/cc-pVTZ[1] with frozen core electrons. CCSD(T)/cc-pVTZ computational scheme was then employed to obtain the energies for MP4-derived geometries.

Ab initio bond lengths and angles for **1**, **2**, **4**, **9** and **10** are given in Fig.III.11. Calculated lengths are expected to be too large by not more than 2%, as exemplified by molecule **2**, for which the experimental data are available (Bartel 1998); the main share of this elongation presumably stems from the neglect of the core electrons correlation. B3LYP/aug-cc-pVTZ geometries seem more accurate.

Table III.19 ***Ab initio*** **potential energy minima, relative energies and equilibrium electric dipole moments for selected C_4N_2 isomers (Kołos 2002)**

Species		CCSD(T)/ cc-pVTZ energy (hartree) [a]	Zero-point energy [b] (kcal/mol)	Energy [c] relative to species **1** (kcal/mol)	Electric dipole moment [d] (D)
1	NCCCCN	-261.364808	16.7		0
2	CNCCCN	-261.323774	16.3	**25.3**	1.10
4	CCCNCN	-261.257982	15.8	**66.1**	1.58
9	CNCCNC	-261.279672	15.9	**52.6**	0
10	CC(CN)CN	-261.270927	15.2	**57.4**	1.88

[a] single point calculation for fixed MP4(SDTQ)/cc-pVTZ geometry
[b] B3LYP/aug-cc-pVTZ
[c] including the zero-point vibrational energy
[d] MP4(SDQ)/cc-pVTZ//MP4(SDQ)/cc-pVTZ

Conversely, the *energies* yielded by CCSD(T)//MP4(SDTQ) (Table III.19) are more reliable than corresponding DFT values. The relative numbers for species **2** and **9** practically match those found by Botschwina *et al.* (*cf.* Table III.20); the latter have to be regarded as highly precise. Importantly, the energies obtained by Kołos for **4** and **10** gave the first indication that these two molecules are potentially detectable C_4N_2 isomers. The reverse – when compared to DFT – energy order for

[1] MP4(SDTQ) stands for the 4th order of the Møller & Plesset (1934) perturbation theory, involving single, double, triple, and quadruple excitations.

compounds **4** and **10** was obtained. Namely, the ZPE-corrected dicyanovinylidene (**10**) potential energy is 5 kcal/mol above that of known species **9**, while the energy of **4** is higher by additional 9 kcal/mol (ZPEs calculated with B3LYP/aug-cc-pVTZ).

The equilibrium electric dipole moment of **2** (derived by MP4(SDQ), Table III.19) is close to the more refined CCSD(T) value reported by Horn *et al.* (1994) (*cf.* Table III.20) – which permits to draw reliable conclusions from two other μ_e values delivered by Kołos's *ab initio* calculations. Specifically, rather low (though higher than predicted by DFT) dipole moments of **4** and **10** indicate that the detection of corresponding interstellar rotational microwave spectra would be difficult, if possible.

The barrier height for dicyanoacetylene←dicyanovinylidene (**1**←**10**) isomerization, calculated at the CCSD(T)//MP4(SDQ) level, amounts to 5.8 kcal/mol classically, and diminishes to 5.1 kcal/mol after the inclusion of ZPE corrections. (The ZPE of the transition state (**TS**) is 14.5 kcal/mol, as predicted by B3LYP/aug-cc-pVTZ). The imaginary vibrational mode of **TS** (Fig. III.12) moves the terminal carbon atom towards one of cyano groups, thus distorting the structure in the direction of **1**. The vibrational mode of **10**, which promotes the **1**←**10** isomerization, is ν_9 (*cf.* Table III.18) with a corresponding harmonic vibrational quantum of *ca.* 1 kcal/mol. Consequently, it takes several such quanta to climb the barrier towards **1**. These qualitative considerations suggest dicyanovinylidene to be a well bound species.

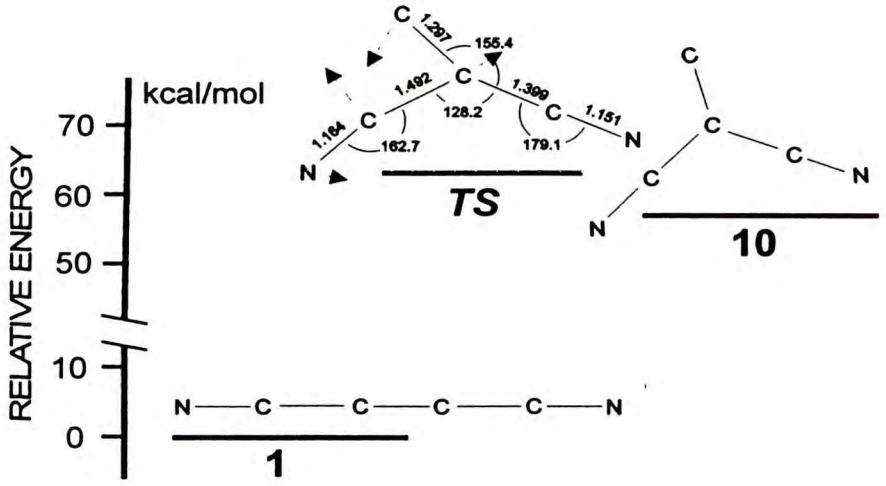

Figure III.12. Scheme of relative energies, as supplied by CCSD(T)// MP4(SDTQ), for the dicyanovinylidene ↔ dicyanoacetylene isomerization. Transition state geometry calculated with B3LYP/aug-cc-pVTZ. Bond lengths given in angstroms, arrows represent displacement vectors for the imaginary normal mode (Kołos 2002).

It is of interest at this point to recall the result of Hu & Schaefer (1993), who accomplished similar calculations on cyanovinylidene, CC(H)CN (see Section III.1*d*). Their study yielded 2.2 kcal/mol (with ZPE) as the barrier height for the reverse isomerization (towards cyanoacetylene), which meant roughly two quanta of the cyanovinylidene mode leading to the transition state.

Shortly after the publication on proposed "exotic" C_4N_2 molecules (Kołos 2002), the existence of species **4**, CCCNCN, was confirmed with the discovery made by Guennoun *et al.* (2003)[1], who photolysed dicyanoacetylene in argon matrices. Guennoun *et al.* noticed that the prolonged irradiation with a Hg-Xe lamp (λ>235 nm) developed cyanoisocyanoacetylene (NCCCNC, isomer **2**) bands (formerly observed by Smith *et al.* (1993), who used 235 nm from a frequency doubled dye laser). The Hg-Xe radiation range overlapped several vibronic bands of the dicyanoacetylene $^1\Delta_u$—$^1\Sigma_g^+$ electronic system (*cf.* Fig. III.10), and the $^1\Sigma_u^-$—$^1\Sigma_g^+$ system.

The same result was obtained during photolysis experiments with the monochromatic 268 nm beam, supplied by an optical parametric oscillator. However, additional spectral features appeared when the monochromatic 235 nm radiation was directed at the sample previously treated with 268 nm. Namely, apart from the bands, which Smith *et al.* assigned to isomers **2** and **9**, a group of three mutually correlated bands was detected at 1927, 2219 and 2275 cm^{-1}. Guennoun *et al.* assigned these to species **4**. The agreement with Kołos's calculations (*cf.* Tables III.18, III.20) was remarkable, also in terms of intensities.

The bands assigned to **4** were also generated in a one-step irradiation with a hydrogen discharge lamp (λ>120 nm). The actual mechanism of CCCNCN generation from NCCCCN in a rigid matrix is a bit mysterious. Apparently, it has to involve the translation of a cyano group to the opposite end of the CCCN moiety. This may happen in the course of the far-UV photolysis, when a huge amount of excess energy has to be dissipated, and locally disrupt ("melt") the matrix structure. The action of less energetic UV quanta, delivered in an intense laser beam, can probably be explained by a two-photon absorption, which also leaves the system with a lot of excess energy. The reasons behind the effectiveness of a particular sequence of irradiations (268, 235 nm) used by Guennoun *et al.* is not clear.

Table III.20 summarizes the experimental and theoretical work on currently known C_4N_2 isomers **1**, **2**, **4**, and **9**. The Y-shaped species **10**, dicyanovinylidene, remains as yet undiscovered. It can probably be isolated in cryogenic rare gas matrices, after the suitable decomposition and rearrangement of gaseous dicyanoacetylene.

The entire C_4N_2 hypersurface, with transition states linking numerous minima, deserves further exploration in order to adequately evaluate the stabilities of different isomers, including the highly energetic ones. Likewise, the availability of synthetic routes, which could possibly lead to the interstellar formation of polycarbon-dinitrogen molecules, is an open issue.

---

[1] In the research group of Jean-Pierre Aycard, Université de Provence, Marseille, France.

Table III. 20
Summary of experimental and theoretical results for selected C_4N_2 molecules

Species	Energy relative to species **1** in kcal/mol	μ_e (D)	Rotational constant (GHz)			Main IR vibrational transitions			
						Frequency (cm^{-1})		Intensity	
			Exp. B_0	Theory B_e	Exp.+ Theor. [h] B_e	Exp.[i]	Theory	Exp.[l]	Theory km/mol
NCCCCN (1)	0	0	1.33668 [d]	1.3300 [f]	1.3334 [f]	471 1154 2241	466 [j] 1134 2272	100 8 76	—
CNCCCN (2)	25.3 [a, m] 25.7 [b]	1.04 [c]	1.40998 [e]	1.40858 [g]	1.40892 [e]	2053 2210 2296	2061 2231 [c] 2321	100 54 54	186 78 [c] 57
CCCNCN (4)	66.1 [m]	1.58 [n]		1.46 [p]		2275 2219 1927	2278 2216 [p] 1918	100 50 14	1680 900 [p] 250
CNCCNC (9)	52.5 [a] 52.6 [m]	0				1288 2115	1213 2122 [k]	13 100	9 553 [k]

[a] CEPA-1 (Botschwina *et al.* 1993a)
[b] CCSD(T), zero-point energy included (Bartel *et al.* 1998)
[c] CCSD(T) (Horn *et al.* 1994)
[d] (Winther *et al.* 1992)
[e] (Bartel *et al.* 1998)
[f] (Oswald 1995)
[g] CCSD(T), geometry corrected for systematic errors (Bartel *et al.* 1998)
[h] $B_e = B_0(\text{exp.}) + \Delta B(\text{theor.})$, see text
[i] Gas phase data (Khanna *et al.* 1997, Bartel *et al.* 1998) for species **1** and **2**, Ar matrix data for **9** (Smith *et al.* 1993) and **4** (Guennoun *et al.* 2003)
[j] CEPA-1 (Oswald 1995); frequency 466 cm^{-1} derived with the harmonic approximation
[k] Unpublished *ab initio* results of Botschwina *et al.*, as cited by Smith *et al.* (1993)
[l] Gas phase data (Khanna *et al.* 1997) for species **1**, Ar matrix data for **2** & **9** (Smith *et al.* 1993), and for **4** (Guennoun *et al.* 2003), intensity of the strongest band arbitrarily taken as 100 for each isomer
[m] CCSD(T)/cc-pVTZ // MP4(SDTQ)/cc-pVTZ (Kołos 2002)
[n] MP4(SDQ)/cc-pVTZ (Kołos 2002)
[p] B3LYP/aug-cc-pVTZ (Kołos 2002); rotational constant scaled by 0.99

III.3 Isomers of dicyanodiacetylene, NC_6N

As mentioned above, the astrophysical rôle of the *di*cyano analogues $N{\equiv}C\text{-}(C{\equiv}C)_n\text{-}C{\equiv}N$ of well known *mono*cyanopolyacetylenes (and of corresponding isomers), is an appealing possibility. Quite extensive photochemical studies on the n = 1 compound, dicyanoacetylene, disclosed its possible conversions, and pinpointed new subjects of interest to the interstellar chemistry.

In contrast, photochemical experiments with the n = 2 member of the series, dicyanodiacetylene (NC_6N), were accomplished solely by Kołos (1999, 2000; **papers III and V**). This seems surprising, given the interesting structure of the compound (long, hydrogen-less rod; four conjugated triple bonds in the linear arrangement) and the fact that its vibrational (Miller & Lemmon 1967) and electronic (McSwiney & Merritt 1970, Connors *et al.* 1974) spectroscopy was known. Other research on this molecule included the excitation and ionisation with low energy electrons (Kloster-Jensen 1979), and the study of the radical cation (Agreiter *et al.* 1995, Fornay *at al.* 1995).

Table III.21. Fundamental vibrational frequencies of dicyanodiacetylene

mode	symmetry	Gas (IR, Raman) Miller & Lemmon (1967)		Ar matrix (IR) Kołos (1999)	
		Frequency / cm^{-1}	Intensity *)	Frequency / cm^{-1}	Intensity *)
ν_1	σ_u	2266	*s*	2269.5**)	*s*
ν_2	σ_g	2235		2232.0	*w*
ν_3	σ_g	2183			
ν_4	σ_u	2097	*m*	2101.3	*m*
ν_5	σ_g	1287.5			
ν_6	σ_u	717	*s*	719.3	*m*
ν_7	σ_g	571			
ν_8	π_g	501			
ν_9	π_u	490.5	*vs*	489.8	*s*
ν_{10}	π_g	455			
ν_{11}	π_u	276	*vvs*		
ν_{12}	π_g	170			
ν_{13}	π_u	61.5	*vs*		

*) *s* – strong, *m* – medium, *w* – weak, *v* –very

**) main site; other sites: 2266.7 and 2271.8 cm^{-1}

The vibrational frequencies of NC_6N, as measured both in the gas phase and in solid argon, are listed in Table III.21; a fragment of the corresponding absorption spectrum, essential for subsequent identifications of NC_6N decomposition products (Kołos 1999), is shown in Fig. III.14A. All infrared-active fundamentals of NC_6N (with the exception of two far-IR bands, which fall beyond our detection range) were observed in matrices. A weak feature at 2232.0 cm^{-1} can probably be assigned to the symmetric stretching vibration (Miller & Lemmon, 1967). An intense band at 2300.1 cm^{-1}, and a weak feature at 2162.9 cm^{-1} may result (again following Miller & Lemmon, who reported gas phase frequencies of 2295 cm^{-1} and 2150 cm^{-1}), to combination bands.[1]

As measured by McSwiney & Merritt (1970), the UV spectroscopy of NC_6N begins at ~ 330 nm with a system of weak structured bands (the upper state remains unassigned). The second electronic transition, ~10^3 times stronger (probably $^1\Sigma_g^+ — ^1\Sigma_g^+$), is presented in Figure III.13; the transition energies measured in a matrix are about 700 cm^{-1} lower than those in the gas phase (Kołos 1999). A fully allowed $^1\Sigma_u^+ — ^1\Sigma_g^+$ transition ($f \approx 0.66$), with well resolved vibrational bands separated by 2100 cm^{-1}, was observed by Connors *et al.* (1974) in the region 192 – 167 nm.

The relative scarcity of publications dealing with NC_6N can perhaps be explained by the difficult (and potentially dangerous) preparation of the compound. Moureu & Bongrand, the discoverers of cyano- and dicyanoacetylene, reported in 1920 on minute quantities of needle-shaped crystals, synthesized by the action of potassium ferricyanide on the cuprous salt of cyanoacetylene. They tentatively identified this substance as NC_6N, a supposition confirmed one generation later by Brockman (1955). A sizeable pressure of NC_6N vapour over crystals (*ca.* 15 Torr at room temperature) facilitates the handling of this substance in matrix-isolation experiments.

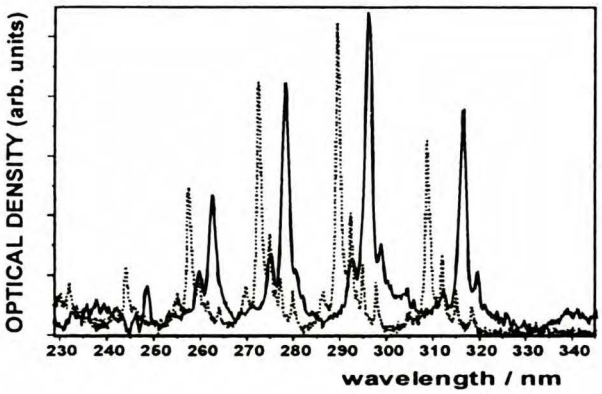

Figure III.13. Electronic spectra of dicyanodiacetylene (NC_6N) in the gas phase (*dotted line*), and in solid argon (*full line*), as measured by Kołos (1999).

[1] The origin of a weak band at 2242.8 cm^{-1} (Ar matrix), not observed previously, is unknown.

III.3a Formation of NC-(CC)$_2$-NC

Kołos (1999, **paper III**) used the 248 nm irradiation to photolyse dicyanodiacetylene in argon matrices. This wavelength (a KrF* excimer laser line) happens to coincide with a vibronic band of NC_6N (*cf.* Fig. III.13), but the corresponding quantum is not energetic enough to cleave any bond of the molecule. Thus, similarly as in previous experiments on NC_4N (Smith *et al.* 1993), the photolysis could only be accomplished via two-photon processes.

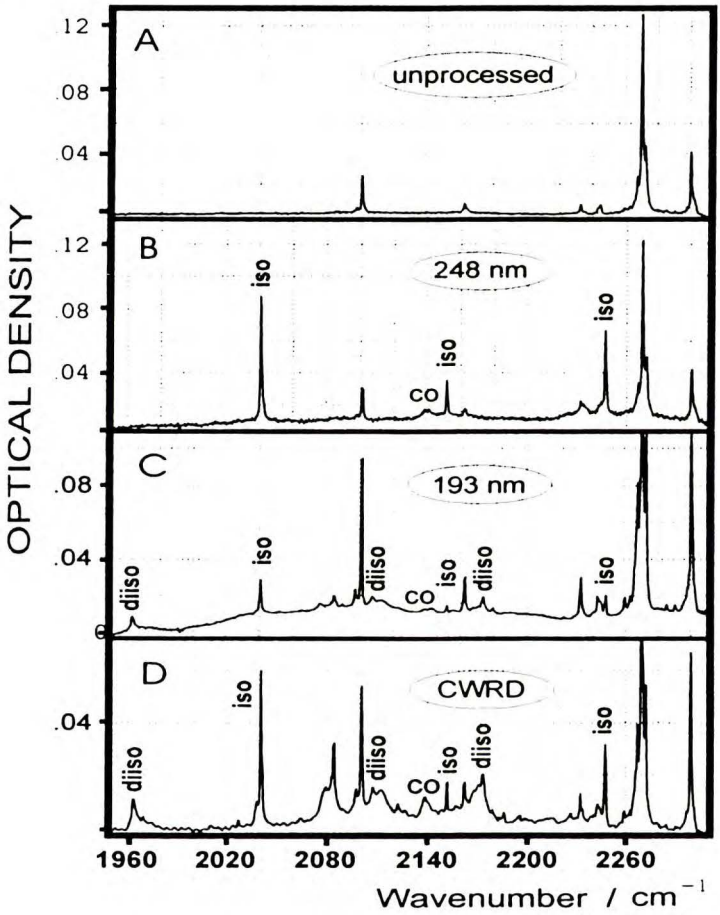

Figure III.14. Triple bond stretching region in IR absorption spectra of NC_6N/Ar matrices: unprocessed sample (A), after 248 nm photolysis (B), after 193 nm photolysis (C), and trapping of electrical discharge products (D). The relative efficiencies of three conversion methods can be estimated by comparing the intensities of product bands to those of the precursor compound. "Iso" and "diiso" denote the sets of spectral features assigned to NC_5NC, and CNC_4NC, respectively. (Kołos 1999, 2000)

Figure III.14B illustrates the IR results of irradiating the NC_6N/Ar matrix with a KrF laser. Three new, strong bands readily showed up: 2041.0, 2151.7 and 2247.6 cm^{-1}. Their intensity ratio (10:2:7), measured in different samples, remained constant indicating a common carrier.[1] The most likely photoreactions, given the operation of a cage effect, were isomerisation and ionisation of the parent molecule. The UV/Vis spectrum of the same sample revealed no electronic absorptions due to NC_6N^+ (discovered independently by Agreiter *et al.* (1995) and Fornay *et al.* (1995)). The lack of cation bands pointed to photoisomerisation, namely to the emergence of cyanoisocyanodiacetylene,

$$N{\equiv}C\text{-}(C{\equiv}C)_2\text{-}N{=}C:$$

(NC_5NC), resulting from the inversion of a single CN fragment, The reversal of both nitrile groups and creation of CNC_4NC should be less probable, as evidenced by the work on NC_4N isomerisations (Smith *et al.* 1993).

Kołos (1999) backed the discovery of NC_5NC with DFT and MP2 calculations of harmonic vibrations. The agreement between the theory and experiment was acceptable, especially in terms of frequencies; the MP2-predicted pattern of intensities, however, was markedly different from the experimental one.[2] The ensuing CCSD(T) study, carried out by Botschwina & Oswald (2000), led to the recognition of an unusual anharmonicity effect in NC_5NC (which made earlier IR intensity calculations unreliable), and to the unambiguous confirmation of proposed spectral assignments. (Table III.22).

Table III.22.
Stretching fundamental modes of NC_5NC. Experiment vs. theory.

mode / symmetry	CCSD(T) / cc-pVTZ Botschwina & Oswald (2000)		Ar matrix Kolos (1999)	
	anharmonic frequency (cm^{-1})	IR intensity (km/mol)	frequency (cm^{-1})	IR intensity [a]
ν_4 / σ	2041.0	223.5	2041	223.5
ν_3 / σ	2151.7	49.8	2152	45
ν_2 / σ	2247.6	155.6	2247	156
ν_1 / σ	2289.1	0.8		0

[a] Normalized to the CCSD(T) prediction for ν_4.

III.3b Formation of CN-(CC)$_2$-NC

NC_5NC was the only product observed by Kołos (1999) in the course of the two-photon 248 nm photolysis of NC_6N in solid argon. However, the chemistry was more complicated when the 193 nm radiation (ArF* laser line) or electrical discharges were applied (Kołos 2000, paper **V**).

---

[1] The first two of these features were previously observed by Smith *at al.* (1994b), and tentatively identified as due to C_5N_2 – which proved to be incorrect (*cf.* Section III.4).

[2] A DFT study on C_6N_2 isonitriles was also accomplished by Lee (1998).

The choice of 193 nm as the photolysis wavelength was partly suggested by former photochemical work on shorter analogues of NC_6N. Namely, the gas phase experiments (Halpern *et al.* 1988, 1990) pointed to 244 nm and 232 nm as thresholds for CN production from cyano- and dicyanoacetylene, respectively. It was reasonable to expect a similar threshold value for the cleavage of any single C—C bond in NC_6N.

The exact shape of the strong $^1\Sigma_u^+ \leftarrow {}^1\Sigma_g^+$ vacuum-UV absorption system in NC_6N/argon matrices is not known. Still, it is clear from the gas phase work by Connors *et al.* (1974) that the 193 nm radiation should be absorbed by the molecule, since it coincides with the long-wavelength slope of a very intense $^1\Sigma_u^+ \leftarrow {}^1\Sigma_g^+$ band.[1]

Apart from the photolysis, Kołos (2000) applied electrical discharges through the NC_6N/argon gas mixture on its way to the cold target (CWRD technique, see Section II.2*b*). Both methods, 193 nm irradiation and discharges, led to fairly rich spectra (Figure III.14C-D); Kołos listed 17 spectral features in the original paper. Bands due to the fundamental frequencies of NC_5NC were the strongest. Apart from these, it was possible to discern a set of 3 bands: 1963.8, 2108.1 and 2173.6 cm^{-1}, seemingly of the common origin.

Just like after the 248 nm photolysis, no electronic bands due to NC_6N^+ cations were detected. Thus, it seemed justified to assign the group of three bands to yet another obvious rearrangement product, CNC_4NC (diisocyanodiacetylene),

$$:C{=}N{-}(C{\equiv}C)_2{-}N{=}C:$$

Small quantities of the analogous centrosymmetrical compound, diisocyanoacetylene, CNC_2NC, photochemically generated from NC_4N, were found by Smith *et al.* (1993), as described in Section III.2*a*.

To test this hypothesis, MP2 and DFT computations were carried out (the latter employed BLYP and B3LYP functionals).[2] CNC_4NC, according to the calculations, is a linear compound (just like NC_5NC and the parent NC_6N), less stable than NC_6N by 65.7 kcal/mol (MP2) or 53.2 kcal/mol (BLYP). Theoretical predictions (Table III.23) give a characteristic pattern of its IR spectrum, with just two outstandingly strong features, either of 1:1 (MP2) or of 2.8:1 (BLYP) intensity ratio; other IR-active fundamental bands are predicted as much weaker (by at least one order of magnitude). These results point to CNC_4NC as responsible for the bands at 1963.7 and 2173.6 cm^{-1}; the calculated frequency values (unscaled) are

---

[1] In practice, the irradiations had to be performed "layer by layer", during the matrix deposition, to overcome the inner filter effect; the photolysis product(s) appeared to be efficient absorbers of incident photons.

[2] The performance of these methods was first tested with NC_6N; the popular hybrid functional B3LYP seemed less accurate than BLYP. This coincided with the finding of Botschwina & Oswald (2000), who noticed BLYP superiority over B3LYP in reproducing the electric dipole moment of NC_5NC. The band intensity patterns generated by BLYP and by MP2 were not very reliable. However, the predictive power of computations seemed enhanced when the results of both MP2 and BLYP were taken into account (*e.g.* bands, for which the two methods suggested high intensities, were indeed strong).

higher by not more than 5% (MP2) or 2% (BLYP). One of the explanations for the presence of the band at 2108 cm^{-1}, which apparently also belongs to the same group, is a combination mode of the overall π_u symmetry *i.e.* $\nu_3+\nu_{13}$.

The above-mentioned absorption of 193 nm radiation by photolysis products, possibly by NC_5NC, suggests a two-step diisonitrile formation:

$$NC_6N \rightarrow NC_5NC \rightarrow CNC_4NC.$$

Naturally, given the relative stabilities of involved species (*cf.* Table III.24) the back photoreaction of NC_5NC should be more effective than its transformation into CNC_4NC. This, however, can be compensated by the relative ease of CNC_4NC detection; the calculations predict its IR transition intensities to be *ca.* 2 times higher than for NC_5NC, and 1 - 2 orders of magnitude higher than for NC_6N.

Table III.23 Calculated (harmonic) vibrational frequencies and absolute IR intensities of CNC_4NC, compared to the measured values (Kołos 2000, Kołos & Grabowski 2000)

mode / symmetry	MP2 6-31G*		B3LYP 6-311+G*		BLYP [a]) 6-311+G*		Experimental (Ar matrix)	
	Freq. (cm^{-1})	Intensity (km/mol)	Freq. (cm^{-1})	Intensity (km/mol)	Freq. (cm^{-1})	Intensity (km/mol)	Freq. (cm^{-1})	Intensity [b]) (relative)
ν_1 / σ_g	2288	0	2334	0	2227	0		-
ν_2 / σ_u	**2280**	**141**	**2321**	**244**	**2223**	**127**	**2174**	**1**
ν_3 / σ_g	2101	0	2135	0	2023	0		-
ν_4 / σ_u	**2034**	**135**	**2080**	**464**	**1970**	**350**	**1964**	**1**
ν_5 / σ_g	1366	0	1387	0	1363	0		
ν_6 / σ_u	971	14	994	12	968	6.5		
ν_7 / π_g	567	0	520	0	473	0		
ν_8 / σ_g	484	0	493	0	483	1.8		
ν_9 / π_u	425	0	477	0.2	442	0.0		
ν_{10} / π_g	401	0	413	0	399	0		
ν_{11} / π_u	261	2	272	2.0	264	2.4		
ν_{12} / π_g	161	0	175	0	168	0		
ν_{13} / π_u	72	4	71	3.0	68	3.5		

[a]) BLYP/6-311G* calculations carried out by Lee (1998) gave practically identical results.

[b]) arbitrary units, accuracy *ca.* ±15%

An additional conclusion – drawn from an unexpectedly rich IR spectrum of 193 nm photolysis products – is that other compounds, apart from isonitriles, are generated. It can probably be rationalised in terms of a strong absorption of the 193 nm laser beam by the photolysed sample. This characteristic could lead to a transient thermal softening of the matrix surface upon pulse photolysis, thus allowing for some photoinduced reactions, normally inefficient within the rigid bulk of rare gas solids. Such an effect, amplified by the layer-by-layer irradiation

technique, could finally give rise to compounds other than NC_5NC or CNC_4NC.[1] The unassigned bands were particularly strong in CWRD experiments - indicating the preferential formation of their carriers in discharges. This issue will return in Section III.4, devoted to the molecule NC_5N.

III.3c
Bare carbon-dinitrogen chains as a possible new class of interstellar molecules

Given the well documented interstellar presence of cyanopolyacetylenes and other asymmetrical unsaturated carbon chains ($C_{2n}H$, $C_{2n+1}H$, C_3N) one has to consider the importance of similar unsaturated gas phase species, which escape radio astronomical detection due to zero (or low) electric dipole moments. As mentioned in Section I.5, several such compounds – C_3, C_5, $HC_{2n}H$ (n = 1, 2, 3) – have already been detected in an evolved stellar envelope – owing to their IR absorptions.

A lot of attention has already been paid to the family of linear bare carbon chains C_n or their ions. Several species of this class were proposed to explain the presence of diffuse interstellar bands (*cf.* Section I.3)

While the synthesis of bare carbon chains and centrosymmetric polyacetylenes is consistent with current models of interstellar reactions, nobody predicted, to the best of author's knowledge, the interstellar abundance of polyacetylenic *dicyano-* molecules $N{\equiv}C\text{-}(C{\equiv}C)_n\text{-}C{\equiv}N$. The solar system abundance ratio [C]/[N] (~3.3) should not be treated as an argument against the formation of two-nitrogen species. The [C]/[N] value is likely to vary, depending on local particularities of Galactic environments (history, elemental depletion mechanisms). Moreover, an interstellar molecule bearing two nitrogen atoms, namely cyanamide ($H_2N\text{-}C{\equiv}N$), has already been found in the molecular cloud Sgr B2 (Turner *et al.* 1975). It is approximately as abundant as acetonitrile ($H_3C\text{-}C{\equiv}N$). Interstellar nitrous oxide (N_2O) was also detected (Ziurys *et al.* 1994).

The assumption of substantial dicyanopolyyne abundance implies the probable coexistence of corresponding isocyano- species. The lack of microwave observations for the interstellar dicyanoacetylene isomer NC_3NC (see below), is consistent with the molecule low dipole moment, only 1.04 debye (Horn *et al.* 1994). Likewise, the calculated dipole moment of another relevant molecule, also undetected in space, CNCN, (which should mark the existence of the more stable but symmetric NCCN), is only 0.71 debye, as reported by Gerry *et al.* (1990).

Two examples above suggest that isomerisations do not generate substantial polarities in the homologous series of linear, conjugated dicyano molecules. Table III.17 of Section III.2*b* supplies more similar instances. Dipole moments of C_4N_2 isomers are generally low; the two exceptions correspond to thermodynamically improbable species.

Conversely, the isomerization of dicyanoacetylenes often leads to a

[1] For instance, an *in situ* synthesis of more complicated NC_6N isomers, reminiscent of the processes, which led to the formation of C_3NCN from NC_4N (Guennoun *et al.* 2003), should be taken into account.

substantial increase of IR transition probabilities (*cf.* Table III.17). This is fully illustrated by Table III.24, with predictions on various C_6N_2 isomers. An intuitively feasible isomer C_3NC_3N has been included in the theoretical study (Kołos & Grabowski 2000, **paper IV**). C_3NC_3N can formally be regarded as the product of a head-to-tail recombination of two C_3N radicals; it is also evocative of C_3NCN, an already discovered isomer of NC_4N (Kołos 2002, Guennoun *et al.* 2003).

Table III.24. Triple Bond Stretching Frequencies, IR Intensities and Selected Molecular Properties for C_6N_2 Isomers (Kołos & Grabowski 2000).

mode & symmetry	MP2/6-31G* [a]		CCSD(T)/cc-pVTZ (Botschwina & Oswald 1999)		Experiment (Ar matrix)	
	Harmonic frequency (cm^{-1})	Intensity (km/mol)	Anharmonic frequency (cm^{-1})	Intensity (km/mol)	Frequency (cm^{-1})	Relative intensity [b]
N≡C-C≡C-C≡C-C≡N [c,d]; E=0 [e], B_e=550 MHz						
ν_1, *u*	2229	3			2266	1.0
ν_2, *g*	2208	0			2235	0.01
ν_3, *g*	2124	0			2183	0
ν_4, *u*	2039	6			2097	0.1
:C=N-C≡C-C≡C-C≡N [c]; E=33 kcal/mol [e], μ_e=1.378 debye [f], B_e=580.2 MHz [f]						
ν_1 [h]	2231	2	2289	0.4		0
ν_2	2282	82	2280	157	2247	0.7
ν_3	2121	43	2154	51	2152	0.2
ν_4	2039	63	2040	224	2041	1.0
:C=N-C≡C-C≡C-N=C: [g]; E=66 kcal/mol [e], B_e=589 MHz						
ν_1, *g*	2288					
ν_2, *u*	2280	141			2174	1
ν_3, *g*	2101					
ν_4, *u*	2034	135			1964	1
:C=C=C=N-C≡C-C≡N [g]; E=74 kcal/mol [e], μ_e=0.7 debye [i] B_e=596 MHz [i]						
ν_1	2388	2187				
ν_2	2269	0				
ν_3	2130	29				
ν_4	1968	101				

a) accomplished with Gaussian 98 Rev. A3 program (Frish *et al.* 1998)
b) the intensity of a most intense band arbitrarily taken as 1 for each species
c) as reported by Kołos (1999)
d) ν_2 and ν_3 symmetrical stretch frequencies from Raman spectra (Miller & Lemmon 1966)
e) relative MP2 energy with respect to the most stable isomer; zero-point energy included
f) as calculated by Botschwina & Oswald (1999)
g) Kołos & Grabowski (2000)
h) numbering of modes as derived by Botschwina & Oswald
i) μ_e and B_e calculated with a larger basis set, 6-311G*

The MP2 calculations of IR absorptions may not reliably reproduce relative intensities of bands for a given compound, but should allow to describe general trends in IR absorption intensity changes from species to species, especially

between alike (*e.g.* isoelectronic) molecules. (Notably, it was checked that such predictions, irrespective whether accomplished with MP2 or DFT methods, were qualitatively similar.) For the lowest energy isomer, NC_6N, the expected intensities are very low (just several km/mol). The turn-around of a single CN group leads to an at least 10-fold increase of the IR intensity; for the diisonitrile this value is an additional factor of 2 higher. The product of the formal reversal of the whole C_3N moiety, *i.e.* C_3NC_3N, is characterised by an extremely high intensity of IR absorption, 2 - 3 orders of magnitudes higher than that of the main isomer NC_6N. At the same time, a very low value of the electric dipole moment of C_3NC_3N makes it a tough object for microwave studies.

This suggests that some members of the carbon-dinitrogen family, not necessarily those of the highest thermodynamical stability, may conveniently be detected in space due to their supreme IR absorption capacity. In fact, within the sub-families C_2N_2, C_4N_2, and C_6N_2, the probability of IR absorption was found to change in the *opposite* direction to the stability of isomers. This was first noticed by Smith *et al.* (1993), who discovered the substantial rise of IR bands when moving from NC_4N to NC_3NC.

C_nN_2 compounds clearly deserve more experimental and theoretical work. Particularly important is the *electronic* spectroscopy of isomers having one or both nitrogen atoms inside the chain. Kołos and Grabowski (2000) supposed that their carbenic character (two nonbonding electrons on a terminal carbon atom) may herald relatively low-lying excited electronic states, and the corresponding presence of visible transitions. This could offer a chance to explain the origin of some diffuse interstellar bands (see Section I.3).

Nitrogen-containing chain compounds may be produced via gas-phase chemistry, but may also arise within radiation-precessed "dirty snow" mantles of interstellar grains. This line of research will certainly be pursued with realistic analogues of interstellar ices (Section I.4).

III.4 Molecule NC_5N

In the spectroscopic quest for the elusive C_3N radical, Smith *et al.* (1994b) carried out electrical discharges through argon/NC_4N mixtures, and trapped the products in matrices. They hoped to isolate both radicals generated in the well known (*cf.* Section III.2) gas-phase reaction:

$$NC_4N + h\nu \rightarrow C_3N + CN$$

Corresponding spectra disclosed – in addition to the strong violet transition of CN – a previously unobserved electronic system, with origin at 440 nm (22 737 cm^{-1}). This system (detected in absorption and emission) showed the vibronic structure suggestive of a linear molecule with triple bonds. Consecutive experiments forced Smith *et al.* to reject C_3N as its possible carrier. Annealing of the matrix *increased* the intensity of the unknown spectrum (the opposite was expected for a free radical); the spectrum could not be produced *in situ* from a logical parent, HC_3N. On the other hand, it was generated from HC_3N subjected to discharges, but the yield was low. The *in situ* photolysis of NC_4N gave just the two isonitriles (Smith *et al.* 1993, 1994a), as described in Section III.2*a*.

Smith *et al.* succeeded in producing the mysterious spectrum from a mixture of discharged HCN and C_2H_2, which allowed them for most informative measurements, with isotopically enriched gases. Experiments with hydrogen cyanide containing both ^{14}N and ^{15}N atoms revealed the tripling of emission bands, which indicated a molecule with two equivalent nitrogen atoms. Experiments with HCN and acetylene both containing the two isotopes of carbon, ^{12}C and ^{13}C, resulted in the splitting consistent with more than three carbon atoms in the carrier compound. Finally, the measurement of splitting, which originated from the natural content of ^{13}C, suggested that the molecule is most likely centrosymmetric. All this evidence permitted Smith *et al.* to tentatively assign the 440 nm system to the linear species NC_5N (dicyanopropynylidene) – a previously unknown, hypothetical compound.

In parallel to the electronic spectroscopy, Smith *et al.* (1994b) observed also the IR absorption of discharged samples, and reported on IR features, namely 2152 and 2041 cm^{-1}, well correlated to unidentified visible transitions. As such, the two bands were also assigned to NC_5N.

Kołos (1999, paper III) studied the *in situ* photolysis of dicyanodiacetylene, NC_6N. His results cast some doubts on the validity of deductions published by Smith *et al.* (1994b). The two infrared bands previously explained by the presence of NC_5N turned out to be related to a third band, 2247 cm^{-1}, and all three were unambiguously assigned to an isonitrile, NC_5NC (*cf.* Section III.3*a*). In the course of the same study, Kołos performed electric discharges through gaseous NC_6N in argon, close to the cold trapping surface (CWRD technique), and detected the

440 nm absorption[1] in spectra of thus obtained matrices. This visible absorption was also generated during the 248 nm, and 193 nm photolysis experiments (the latter performed *in situ*, but during the matrix deposition (*cf.* Section III.3*a*).

Kołos was not able to check for the correlation between the 440 nm absorption and three IR bands assigned to NC_5NC. Consequently, he reported on NC_5N being *not* the carrier of these IR features, but could neither support nor falsify the tentative assignment of the 440 nm system to NC_5N, previously proposed by Smith *et al.* (1994b). However, the next paper by Kołos (2000) brought into view an alternative explanation for the 440 nm absorption, namely CNC_4NC, an isomer of NC_6N, which had all the characteristics deduced by Smith *et al.* (linear, centrosymmetric, more than three carbons, two equivalent nitrogens).

A theoretical study on NC_5N (Tittle *et al.* 1999) predicted the vibrational frequencies. The authors compared their results to vibrational spacings measured by Smith *et al.* in a resolved fluorescence spectrum (selectively excited at the origin of the 440 nm system). Tittle *et al.* gave support to the original assignment, but also added to the confusion by making use of symmetry-forbidden transitions, and by the neglect of some bands reported by Smith *et al.*

The puzzle was ultimately solved with an advanced experiment, recently performed in Garching (Smith-Gicklhorn *et al.* 2002a, **paper VIII**) – the mass selection of matrix-isolated species[2]. An electron impact source was used for the ionisation. NC_6N and NC_4N were tried as precursor compounds, however tetracyanoethene, $(CN)_2CC(CN)_2$, turned out to be the most practical choice. Figure III.15 shows the corresponding mass spectrum with a small peak due to 88 amu (C_5N_2). Neon was chosen as the matrix gas. During prolonged (12 – 20 h) depositions of mass-selected C_5N_2, the growing matrix was continuously sprayed with electrons, to neutralize the positive charge.

The selective narrow-band excitation of the resulting samples in the 440 nm region revealed the presence of two matrix sites – which perfectly matched the spectra, obtained by Smith *et al.* (1994b) in conventional neon matrices. A series of control experiments (see Figure III.16) verified the unambiguous relation of both spectral features to a species of 88 amu.

The study was further extended with predictions at the density functional theory level (UB3LYP), which employed a basis set larger than the one used by Tittle *et al.* (1999), and dealt with a higher number of isotopomeric species. Assisted by the results of these calculations Smith *et al.* could not only assign the main vibronic transitions to centrosymmetric fundamental modes of NC_5N, but could also explain the origin of minor bands, produced by overtones and combination modes.

It was verified that the NC_5N arrangement is lower in energy than two other linear centrosymmetric C_5N_2 isomers. The triplet multiplicity of its ground

---

[1] More specifically, two strongest vibronic bands, 22.7 and 24.7 $\times 10^3$ cm^{-1} (previously described by Smith *et al.* 1993), were found in these experiments, in addition to the strong absorption of CN radical at 25.9×10^3 cm^{-1}.

[2] See Section II.3 for the basics of this method and for technical details.

electronic state was predicted, the lowest singlet being 19 kcal/mol more energetic. Calculated harmonic vibrational frequencies of NC_5N are given inTable III.25. While these numbers may be of use for some future assignments, it should be noticed that expected IR intensities are quite low. This is consistent with the current lack of relevant experimental data; Smith-Gicklhorn *et al.* (2002a) accomplished a careful search for IR absorptions of NC_5N, which gave a negative result.[1]

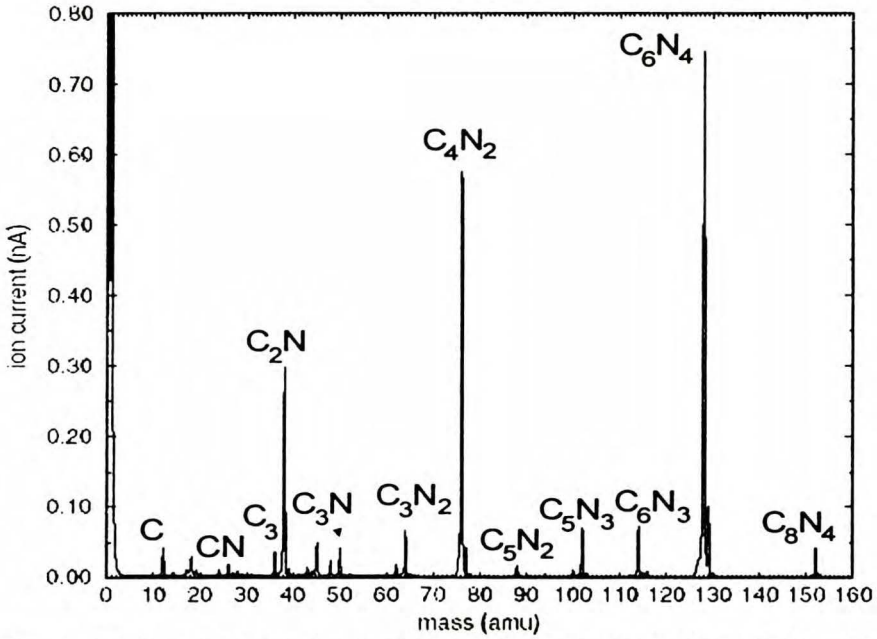

Figure III.15. Quadrupole mass spectrum produced from C_6N_4 with the electron-impact ion source. Smith-Gicklhorn *et al.* (2002a); reprinted with the permission from Elsevier Ltd.

In parallel to the study described above, the optical absorption of gaseous NC_5N has been measured by Linnartz *et al.* (2001) [2], who used the cavity ring down technique. NC_5N formed in a discharge through He/NC_2N (cyanogen) mixture. In this elegant experiment Linnartz *et al.* scanned the narrow region around 440 nm, pinpointed in the original study by Smith *et al.* (1994b). The resulting spectrum was sufficiently well resolved to allow for the measurement of the rotational structure. Three parameters, namely the ν_{00} frequency (22832 cm^{-1}), and B_0', B_0'' rotational

[1] In this context, it has to be remarked that even the electronic fluorescence signals of NC_5N (strong in conventional experiments) were very weak, which reflects the difficulties in making a neutral out of an ionic species. Evidently, the attachment of electrons is not very efficient, and/or some bond breaking or isomerization takes place when ~10 eV of energy is released following the recombination. Thus, the method is best suited for the spectroscopy of ions (see the next chapter).
[2] In the research group of John P. Maier at the University of Basel, Switzerland.

constants, were obtained from the fit to the spectrum. Based on the DFT study by Tittle *et al.* (1999), Linnartz *et al.* assumed the transition to be $A^3\Sigma_u^- — X^3\Sigma_g^-$, and compared the B_e'' constants, theoretically derived for three centrosymmetric linear isomers: NC_5N, CNC_3NC, C_2NCNC_2 with the experimental value of B_0''. This clearly pointed to NC_5N as the carrier of the spectrum. Linnartz *et al.* have also succeeded in the detection of a vibronic band at 24 791 cm^{-1}, consistently with previous Smith's *et al.* (1994b) matrix measurements. This feature was at least 2 times weaker than the one at 22 832 cm^{-1}.

Table III.25.
IR-active vibrational frequencies and intensities for NC_5N ($X^3\Sigma_g^-$), as predicted with B3LYP/6-311+G(3d,3pd); Smith-Gicklhorn *et al.* 2002a

symmetry	Frequency *) (cm^{-1})	Intensity (km/mol)
σ_u	2027	1.3
σ_u	1652	30
σ_u	1022	1.6
π_u	485	4.4
π_u	402	6.8
π_u	75	7.2

*) scaled with the factor 0.97

The shorter member of the $NC_{2n+1}N$ homologous series, linear dicyanocarbene NC_3N, was recently found to be a stable and detectable species (Hajgato 2002), with a triplet ground state.[1] The relative ease, with which NC_3N and NC_5N are created from numerous precursors, may suggest the likelihood of their occurrence in space. However, to date no interstellar bands at 22 832 cm^{-1} (4379.7 Å) and 24791 cm^{-1} (4033.7 Å) were reported.

A comment on a closely related homologous series of linear molecules $HC_{2n}N$, is appropriate here. The electronic structure of linear $HC_{2n}N$ resembles that of $NC_{2n+1}N$; the ground states in both series are of the triplet multiplicity. Obviously, the important difference lies in the polarity of $HC_{2n}N$. The microwave emission from n=1 species, cyanomethylene, was found in several astronomical sources, in particular around the carbon star IRC +10°216 (Guélin & Cernicharo 1991), after its rotational spectrum had been measured in the laboratory (Brown *et al.* 1984, Saito *et al.* 1990). Molecules HC_4N and HC_6N were also formed in laboratories (in discharges, from HC_3N parent), and characterised by the microwave spectroscopy (Tang *et al.* 1999, Gordon *et al.* 2000a). No interstellar traces of these two species were found though, in spite of their substantial dipole moments (almost 5 D for HC_6N). It remains to be verified, whether these negative results – together with the possible lack of interstellar absorptions at 4380 and 4034 Å – indicate the

[1] It was obtained by the dissociative ionization from several parents, including tetracyanoethene, and detected with mass spectrometry.

inefficiency of the interstellar synthesis of triplet chain molecules longer than cyanomethylene.

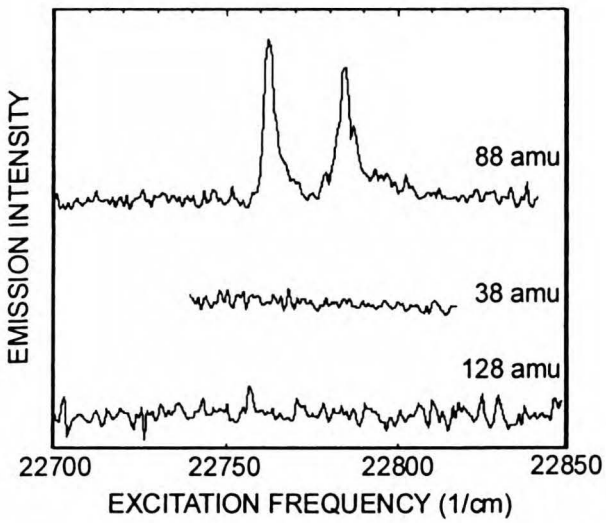

Figure III.16. Laser excitation scans of the region in the vicinity of two C_5N_2 matrix sites (in neon). Spectra corresponding to the mass selector set at 38 and 128 amu were measured for control purposes. Smith-Gicklhorn *et al.* (2002a); reprinted with the permission from Elsevier Ltd.

III.5 The ions

III.5a Molecular cations HC_3N^+, NC_4N^+ and NC_3N^+

Given the crucial rôle of ionic species at different stages of the interstellar chemical synthesis (*cf.* Section I.4), surprisingly little is known on their infrared spectroscopy[1]. This was particularly true, for a long time, for the cation of the compound, whose astrophysical significance was revoked in preceding chapters, namely of cyanoacetylene. Based on the photoelectron spectrum, Baker & Turner (1968) assigned 2180 ± 40 cm^{-1} to the C≡N stretching mode of HC_3N^+. Fulara *et al.* (1985) succeeded in generating this ion in a neon matrix, recorded its electronic system $B^2\Pi_{3/2}\leftarrow X^2\Pi_{3/2}$ in the visible (516 nm), but were not equipped to measure the corresponding IR absorption. The analysis of a photoelectron spectrum led Maier *et al.* (1979) to assign the frequencies 2290 ± 10, 2119 ± 10, and 570 ± 10 cm^{-1} to totally symmetric vibrational modes of NC_4N^+.

Later on, the electronic spectroscopy of $HC_{2n+1}N^+$ and $NC_{2n}N^+$ species was quite extensively studied — experimentally (Fornay *et al.* 1995, Agreiter *et al.* 1994, 1995), and theoretically (Lee & Adamowicz 2001) — in hope to explain the diffuse interstellar bands mystery.

The description of the HC_3N^+ vibrational spectroscopy had to wait until Smith-Gicklhorn *et al.* (2001, **paper VII**) carried out the matrix isolation of the mass-selected cation, and backed it with a density functional theory study. The deuterated analogue (DC_3N^+), and, even more importantly, the cation of dicyanoacetylene (NC_4N^+), were also included in this study.

Principles of the mass-selection technique developed in Garching were explained in Section II.3. HC_3N, DC_3N, and NC_4N were an obvious choice of precursor molecules. The experimental procedure was very similar to that used in experiments with NC_5N; the understandable difference consisted in much higher concentrations of isolated species – due to their ionic character. This allowed to obtain informative IR spectra, which were interpreted with the help of DFT calculations. Table III.27 lists the frequencies of stretching fundamentals. The vibrationally resolved *A-X* fluorescence (origin at 600 nm) was additionally measured for NC_4N^+, which gave the frequencies of infrared-inactive modes. These appear in the Table without intensity values.

As evidenced by Figure III.15, the electron impact source, fed with tetracyanoethene, produced not only NC_4N^+ (Smith-Glickhorn *et al.* 2001), or NC_5N^+ (Smith-Glickhorn *et al.* 2002a), but also the variety of other ions. Several of these were scrupulously studied in consecutive experiments (Smith-Glickhorn *et al.* 2002b), and the most interesting, from the astrophysical point of view, was perhaps the linear NC_3N^+ cation, for which a neon matrix band at 1920 cm^{-1} has been

[1] H_3^+ cation, discovered in space by Oka and coworkers via its IR absorption (see Section I.5), is the reamarkable exception.

identified, based on the agreement with a B3LYP/6-311+G(3d,3pd) calculation result. DFT predicted a very high IR intensity of this transition: 1.1×10^3 km/mol. Thus, all three ions: HC_3N^+, NC_4N^+ and NC_3N^+ are strong infrared absorbers.

Table III.27. Frequencies of stretching modes (cm^{-1}), and IR intensities (km/mol, in brackets) for cyanoacetylenic cations. Experiment (neon matrix) *vs.* B3LYP/ 6-311++G(3d, 3pd) calculations. (Smith-Gicklhorn *et al.* 2001)

HC_3N^+	Expt.[a]	3196.5 (160)	2175.8 (31)	1852.8 (372)		
	DFT[b]	3208 (212)	2169 (4)	1852 (372)	893 (7)	715 (26)
DC_3N^+	Expt.[a].	2499 (66)	2114.8 (55)	1795.6 (360)		
	DFT[b]	2494 (38)	2106 (21)	1784 (360)	876 (9)	570 (10)
NC_4N^+	Expt[c]	2220	1942	613	2015	1208
	DFT[b]	2194	1942	602	2026 (1141)	1179 (0.2)

[a] Intensities are normalised to the DFT prediction for the strongest band.

[b] Scaled with the factor 0.96. DFT calculations on HC_3N^+ and NC_4N^+ cations were also carried out by Lee (1996), at a slightly lower level of theory.

[c] Only one asymmetric stretching mode was observed in IR. Four remaining frequencies are taken from *A-X* electronic emission measurements (Agreiter *et al.* 1994).

III.5b Cyanoethynylium cation C_3N^+

In the course of experiments with mass-selected HC_3N^+ (51 amu), care was taken to eliminate the contamination of IR spectra with bands coming from any species of 50 amu (corresponding to the composition C_3N). This seemed important, since the peak due to C_3N^+ was well visible in mass spectra of HC_3N and DC_3N. Indeed, with the quadrupole filter set to mass 50, the bands assigned to HC_3N^+ did develop, though weaker.

As an ultimate check, the same deposition (mass 50) was carried out with the NC_4N^+ precursor. This time the three bands of HC_3N^+ were absent, confirming the original assignment. Interestingly, though, a band at 2202.4 cm^{-1} appeared. Smith-Gicklhorn *et al.* (2002, **paper VII**) tentatively related it to C_3N^+ and noticed that 2202.4 cm^{-1}, measured in solid neon, may correspond to 2194 cm^{-1} reported for argon by Kołos & Waluk (1997).[1] The latter band resulted from the *in situ* photolysis of HC_3N in matrices irradiated at 193 nm. Kołos & Waluk (again: tentatively) assigned the 2194 cm^{-1} feature to the cyanoethynyl radical C_3N, based on an isotopic substitution study (*cf.* Sections III.1*a-b*, Table III.2).[2] It is presently known from a CCSD(T)//B3LYP study by Ding *et al.* (1998) that the lowest energy

[1] The corresponding neon-to-argon spectral shift of 0.4% would be consistent with values typically found for ions (Jacox 1984). The 2194 cm^{-1} band was also observed in Bondybey's laboratory following the in situ irradiation of HC_3N/Ar matrices with Lyman-α radiation (private information; unpublished).

[2] Guennoun *et al.* (2003) interpreted the 2194 cm^{-1} (Ar) feature as due to the *anion* C_3N^-. The validity of this assignment is discussed in the next section.

isomer of C_3N^+ is a quasi linear triplet, but – to the author's knowledge – no reliable predictions on vibrational transitions exist for this computationally challenging cation.

III.5c Cyanoacetylide anion C_3N^-

Many authors pointed to the potential importance of negative ions in the interstellar synthesis. An anion may form in the radiative attachment reaction from a neutral molecule (M) characterised by a positive electron affinity (Duley & Williams 1984):

$$M + e \rightarrow M^- + h\nu$$

Conversely, the collision with a photon may release an extra electron:

$$M^- + h\nu \rightarrow M + e \qquad \text{(photodetachment).}$$

Anions can also lose their charge in the associative detachment [1], *i.e.*:

$$M^- + L \rightarrow ML + e$$

and, obviously, can be destroyed in the anion-cation mutual neutralisation:

$$M^- + L^+ \rightarrow M + L\,.$$

Given the high number density of electrons in interstellar clouds[2], the potential rôle of anions created via radiative attachment (see Section I.4) is important. Lepp & Dalgarno (1988) expect as much as 10-50% of polyatomic interstellar molecules to be in the form of anions (and less than 10% in form of cations). In connection to the subject of this monograph, the homologous series of closed shell species $C_{2n+1}N^-$ is of particular interest. Wang *et al.* (1995) obtained a series of $C_{2n+1}N^-$ ions by the laser ablation of potassium ferricyanide, $K_3Fe(CN)_6$, detected them by mass spectrometry, and discovered that their stability is much greater than for $C_{2n}N^-$ species. In a theoretical study, Zhan & Iwata (1996) found that most stable structures $C_{2n+1}N^-$ are linear and of singlet multiplicity (whereas the ground states of $C_{2n}N^-$ are triplet). Pascoli & Lavendy (1999), who carried out DFT and coupled clusters calculations, reported on $C_{2n}N^-$ (n=2-7) molecules being all linear ($^1\Sigma^+$ for odd n, and $^3\Sigma^-$ for even n). Both latter groups published the theoretical predictions for harmonic vibrational frequencies; unfortunately they provided no information on corresponding IR intensities. Prior to the recent report by Guennoun *et al.* (2003) no spectroscopic evidence for C_nN^- anions was given — to the author's knowledge — with one noteworthy exception. Zhou *et al.* (1996) used cyanoacetylide anions, C_3N^-, as ligands in complexes with Ni^{2+}, Pd^{2+}, and

---

[1] Notably, the fastest gas-phase route towards molecular hydrogen (Janev & Van Regemorter 1974) is:

$$H + e \rightarrow H^- + h\nu$$
$$H^- + H \rightarrow H_2 + e$$

At particular conditions (like elevated temperature) this may even compete with the H_2 synthesis on grains.

[2] It is probably ~4 orders of magnitude lower than the number density of hydrogen. Electrons come mostly from the photoionization of atomic carbon.

Pt^{2+}. Infrared frequencies were given, and related to vibrational modes in these bound C_3N^- species.

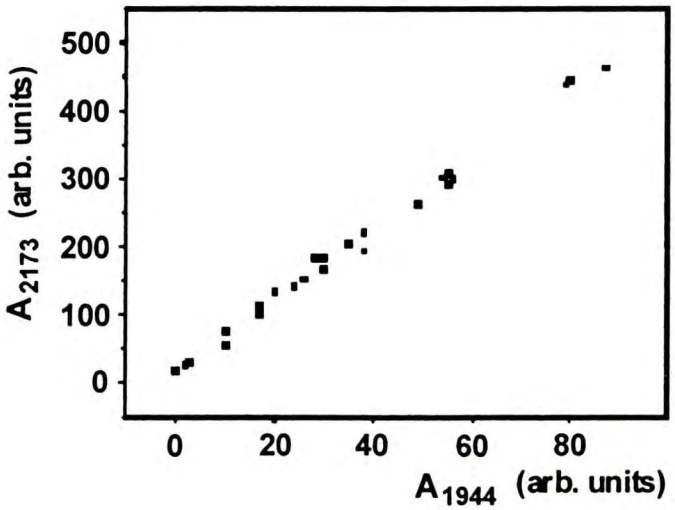

Figure III.17. Correlation of integrated optical densities (A) for IR absorption bands 2173 and 1944 cm^{-1}, tentatively assigned to C_3N^-. Bands generated with the CWRD source in a HCCCN/Ar matrix. Points correspond to the varying degree of CWRD processing.

Guennoun *et al.* (2003), used the far-UV radiation to photolyse HC_3N/Ar matrices. Based on deuterium-substitution experiments, and on B3LYP/6-31G** calculations, they assigned one of the unidentified product bands, 2194 cm^{-1}, to C_3N^-. Furthermore, they explained a pair of apparently correlated bands, 2090 and 1931 cm^{-1}, as due to the isocyanoacetylide anion, $CCNC^-$. The adequacy of both assignments is now in question.

Kołos (2003) analysed the IR spectra of species that were generated in electrical discharges through HC_3N/Ar mixture, and subsequently isolated in matrices (see Section II.2*b* for a résumé on CWRD technique). Three isotopomeric modifications of cyanoacetylene were used, namely $^1HC_3{}^{14}N$, $^1HC_3{}^{15}N$ and $^2HC_3{}^{14}N$. Based on the isotopic substitution study, and on theoretical (B3LYP) predictions, Kołos picked up two mutually correlated bands, 2173 and 1944 cm^{-1}, (see Figure III.17) as candidates for C_3N^- vibrational transitions.

For the theoretical predictions, a correlation-consistent polarized valence triple-zeta basis set (Dunning 1989) was employed in its "doubly augmented" version (d-aug-cc-pVTZ), to better account for the diffuse anionic wavefunctions. Table III.28 lists relevant frequencies and intensities. Both bands were insensitive to the $^1H \leftrightarrow {}^2H$ exchange in parent cyanoacetylene.

Table III.29. B3LYP/aug-cc-pVTZ-derived harmonic frequencies (scaled by 0.96) and absolute IR intensities for the isocyanoacetylide anion $CCNC^-$. Are the bands 2090 & 1931 cm^{-1} due to $CCNC^-$?

mode	Bands generated in solid Ar from $^1HC_3{}^{14}N$ precursor			B3LYP/aug-cc-pVTZ (Kołos 2003)		
	(Guennoun *et al.* 2003)		Kołos & Waluk 1997	$C_2{}^{14}NC^-$		$^{14}N \rightarrow {}^{15}N$ shift (cm^{-1})
	cm^{-1}	*Rel. intensity*	$^{14}N \rightarrow {}^{15}N$ shift (cm^{-1})	cm^{-1}	*km/mol*	
ν_1	2090	100 %	0.5 *)	2076	125	-31
ν_2	1931	13 %		1932	59	-10
ν_3				888	5	-5
ν_4				461	4	-9
ν_5				228	14	-1

*) at the instrumental resolution of *ca.* 0.2 cm^{-1}

between 2194 cm^{-1}, and the frequency ν_1 computed for C_3N^-. The perfect match of two frequencies proposed by Kołos with those theoretically predicted may well be accidental. In fact, the calculations refer to the gas phase, while for the anions one could anticipate substantial matrix shifts (Bondybey & Miller 1983).

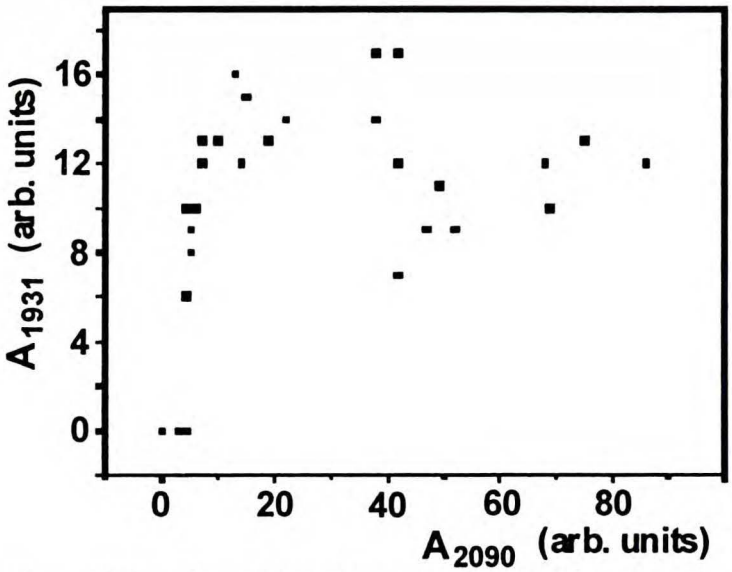

Figure III.18. Correlation of integrated optical densities (A) for IR absorption bands 2090 and 1931 cm^{-1}. Bands generated with the CWRD source in a HCCCN/Ar matrix. Points represent the varying extent of CWRD processing.

The situation is less ambiguous with spectral assignments, which Guennoun *et al.* proposed for $CCNC^-$ (Table III.29). The collected evidence suggests these to be incorrect. First, as reported by Kołos & Waluk (1997), the $^{14}N \rightarrow {}^{15}N$ isotope shift of the 2090 cm^{-1} band is less than 1 cm^{-1}, in disagreement with theoretical predictions for $CCNC^-$.[1] Secondly, the bands 2090 and 1931 cm^{-1} were found (Kołos 2003) to be uncorrelated, as illustrated by Figure III.18.

The C_3N, C_3N^+, and C_3N^- issues, described in this and preceding sections, illustrate well the difficulties in the identification of matrix-isolated species – but also the potential for future discoveries and assignments.

[1] This puzzling spectral feature was generated by Kołos & Waluk (1997) and Kołos (2003) in photolysis and CWRD experiments (*cf.* Table III.2, Section III.1*a*).

Table III.28. The tentative assignment of spectral features 2173 & 1944 cm^{-1} to vibrational transitions of $CCCN^-$ (Kołos 2003).

	Experimental, in Ni^{2+}, Pd^{2+}, Pt^{2+} complexes (mean values) Zhou *et al.* (1996)	B3LYP/d-aug-cc-pVTZ scaled by 0.96			Product of electric discharges through HCCCN, Ar matrix		
		$CCC^{14}N^-$		$^{14}N \rightarrow ^{15}N$ freq. shift & *percent int. change*	from a ^{14}N-precursor		$^{14}N \rightarrow ^{15}N$ freq. shift & *percent int. change*
		cm^{-1}	*km/mol*	cm^{-1} *(% int.)*	cm^{-1}	*Rel. int.*	cm^{-1} *(% int.)*
ν_1	2213	2170	591	-18 *(+1)*	2173	100%	-18 *(+76)*
ν_2	2045	1943	35	-9 *(-37)*	1944	17%	-8 *(-10)*
ν_3		867	6				
ν_4		544	11				
ν_5		215	14				

It follows from Table III.28 that the results of DFT calculations match the proposed experimental frequency values and corresponding $^{14}N \rightarrow ^{15}N$ isotope shifts. The relative IR intensity of two bands is reproduced reasonably well; one generally cannot expect any better performance from DFT methods. However, the reproduction of IR intensity variations relative to the $^{14}N \rightarrow ^{15}N$ exchange is more troublesome. Higher level calculations are necessary to conclude whether the observed large increase of ν_1 intensity upon the ^{15}N substitution could be ascribed to the anharmonicity of vibrations. The effect of anharmonicity on IR intensities can indeed be this large, as demonstrated by the advanced theoretical study on NC_5NC (Botschwina & Oswald 2000).

It is interesting to compare the tentatively proposed (and theoretically predicted) C_3N^- frequencies to those measured for C_3N^- ligands. Higher values of the latter are most probably the effect of electronic density being shifted from ligands towards the central metal ion.

At the current stage, experiments and calculations done by Kołos neither confirm nor prove false the assignment of 2194 cm^{-1} band to cyanoacetylide anion, recommended by Geunnoun *et al.* (2003). The band has already been detected by Kołos & Waluk (1997), who reported a $^{14}N \rightarrow ^{15}N$ shift of -24 cm^{-1}. Such a shift value may still be consistent with the one predicted for C_3N^- (*cf.* Table III.28), given the moderate level of theory applied. The same concerns the agreement

Summary and Outlook

The research in the "unsaturated carbon-nitrogen chain" subsection of laboratory astrophysics proceeds along several lines, three of which, coincident with the author's scientific interests, were described in detail.

i) On one hand, there are efforts to synthesize unusual chemical compounds of some known astrophysical significance, and to carry out extensive spectroscopic studies on these species. In particular, it is currently important to explore the vibrational and electronic spectroscopies of species originally identified via the microwave (pure rotational) emission. Bürger *et al.* (1992) managed to obtain isocyanoacetylene, HCCNC, and measured its gas-phase IR spectrum. An imine isomer, HNCCC, was synthesized in solid argon by Kołos & Waluk (1997, paper II) and Kołos & Sobolewski (2001, paper IX), who assigned the corresponding stretching vibrational bands, as described in Section III.1*c*. These data may prove useful for the IR spectroscopy of stellar (AGB) envelopes and proto-planetary nebulae.

ii) Another approach is to synthesize and characterize molecules that might reasonably be *expected* to exist in space. Of special importance, among such hypothetical species, are those, which possess no (or low) dipole moment, and hence no (or only weak) microwave rotational spectra. Studies on photochemical transformations of centrosymmetric dicyanoacetylenes led to the discovery and spectral measurements (IR and/or optical) of following linear species: NC_3NC, CNC_2NC (Smith *et al.* 1993, 1994a; see Section III.2*a*), NC_3NC, (Kołos 1999, paper III; Section III.2*a*), CNC_2NC (Kołos 2000, paper V; Section III.2*b*), NC_5N (Smith *et al.* 1994b, Smith-Gicklhorn *et al.* 2002a, paper VIII; Section III.4). Moreover, the electronic spectroscopy of cations $NC_{2n}N^+$ and $HC_{2n+1}N^+$ was studied (Fulara *et al.* 1995, Fornay *et al.* 1995, Agreiter *et al.* 1994, 1995). Infrared spectra of NC_4N^+ and HC_3N^+ were measured by Smith-Gicklhorn *et al.* (2001, paper VII; Section III.5*a*).

iii) The third way is a purely theoretical approach, and consists in *inventing* "interstellar-like" molecules from scratch. This tactic originates from the assumption (Green & Herbst 1979) that quite unstable isomers of known species may be abundant in the interstellar gas due to expected peculiarities of the

astrochemical synthesis (see Section I.4). This line of reasoning led Kołos (2002, paper IX, Section III.2*b*) to launch a series of quantum chemical calculations for as many as 13 species of the common composition C_4N_2. Apart from known isomers of dicyanoacetylene, the project yielded two additional, reasonably stable molecules: linear C_3NCN and Y-shaped $C_2(CN)CN$, and supplied reliable predictions on corresponding IR absorptions. Very recently, the existence of C_3NCN was IR-spectroscopically confirmed by Guennoun *et al.* (2003). Kołos & Dobrowolski (2003, paper X; Section III.1.*d*) calculated the geometry, dipole moment and vibrational frequencies of HCNCC, the probable linear isomer of cyanoacetylene, whose existence was first postulated by Osamura *et al.* (1999). Guennoun *et al.* (2003), who did a separate theoretical and experimental research, recently reported on the IR identification of HCNCC (Section III.1*d*). Another isomer of cyanoacetylene, that is cyanovinylidene, $C_2(H)CN$, first "invented" (Hu & Schaefer 1993), then mass-spectrometrically found (Goldberg & Schwarz 1994), remains a challenge for spectroscopists.

iv) Finally, the interstellar chemical synthesis schemes for the production of already detected molecules, as well as those postulated, are necessary. Cyanoacetylene is probably created from HC_2H and CN (Woon & Herbst 1997); the production of its chain isomers HC_2CN, HNC_3, and $HCNC_2$ was fully analysed by Osamura (1999). A newly proposed scheme for the interstellar synthesis of the fifth cyanoacetylene isomer, cyanovinylidene, (Kołos & Dobrowolski 2003b) was described in Section III.1*e*.

In general, the quest for the spectroscopic characterization of relatively simple (4-6 atoms) molecules of a broadly defined "cyanoacetylene family", is far from being completed. While the current collection of corresponding IR spectra (experimental and/or theoretical) is quite rich, less is known on the relevant electronic transitions of exotic molecules (with important exceptions of NC_3NC, NC_5N, and several $NC_{2n}N^+$, $HC_{2n+1}N^+$ ions). More experimental work, in particular involving the matrix isolation of mass-selected species (see Section II.3) is needed, especially in connection to the diffuse interstellar band issue. The methodology adopted in the group of J.P. Maier (Basel), that of first locating the frequency of the transition by a mass-selective matrix spectroscopy, and than scanning the neighbouring frequency range in gas-phase cavity ring-down measurements, is particularly promising.

Of course, the mass-selective matrix spectroscopy alone is not a remedy for all assignment problems encountered in this type of research, in particular when it comes to the separation of isomers. Its combination with isotopic substitution studies, and quantum chemical calculations, proved to be the supreme approach (as exemplified by the demanding case of C_5N_2).

For linear isomers of dicyanoacetylene and dicyanodiacetylene, an interesting (and potentially useful) rule was found: while most stable species, NC_4N and NC_6N, are relatively weak IR absorbers, other linear arrangements of the same

atoms, like cyanoisocyano-, diisocyano-, and also C_3NCN or C_3NC_3N, are characterised by very strong IR stretching transitions. Similar effect is predicted for the isomers of cyanoacetylene. This, along with the availability and efficiencies of interstellar synthesis mechanisms, should be taken into account when estimating the likelihood of finding diverse isomers in the outer space (Section III.3*c*).

Ultimately, one expects to use the wealth of accumulated laboratory data for the interpretation of astronomical spectra. While some hitherto unknown interstellar molecules may still be discovered in the Infrared Space Observatory (ISO) archive, the main expectations currently concentrate around the mission Herschel.

Herschel Space Observatory (HSO) will be launched in 2007 to commemorate the bicentennial of the discovery of IR radiation by Sir Frederick William Herschel. It will reside around the Lagrangian point L2 of the Sun-Earth system, at the distance of 1 500 000 km from Earth (which is 4 times more than the mean Earth-Moon distance). Such location, far from both Earth and Moon, will facilitate the detection of radiation corresponding to low black-body temperatures. HSO will carry three spectrometers dedicated to the far-IR region. The heterodyne instrument, acronymed HIFI[1], will cover the spectral ranges 16 – 41.7 and 47.0 – 63.7 cm^{-1} (which corresponds to 0.48 – 1.25 and 1.41 – 1.91 THz) with an unparalleled resolution ($\lambda/\Delta\lambda$ of the order of 10^7). Second spectrometer, devoted to the imaging, as well as middle and low resolution spectroscopy, (PACS[2]) will operate in the range 47.6 – 175 cm^{-1} (or 1.43 – 5.23 THz).

These capabilities may permit to detect the lowest frequency vibrational modes for some unsaturated chain molecules. The third instrument aboard will be dedicated mostly to the IR imaging. Table III.30 lists some bending transitions, which fall within the HIFI or PACS ranges.

In this context one can also mention Y-shaped molecules of cyanovinylidene CC(H)CN (~147 cm^{-1}, intens. 23 km/mol; Kołos 2003b), and dicyanovinylidene CC(CN)CN (127 and 130 cm^{-1}, intens. 10 and 5 km/mol; Kołos 2002).

It should be noted, that IR intensities of bending transitions are relatively low for unsaturated chain molecules, thus the spectral ranges offered by HSO are not perfectly well suited for the detection of these species. The spectral region of choice, on the other hand, is in the mid-IR, where strong, or even extremely strong, stretching transitions of conjugated triple or cumulenic double bonds were found (Section III.3*c*). Luckily, this region is largely coincident with one of atmospheric transmission windows (the *M* band, centred at 4.8 μm), so the successful ground-based observations seem quite possible, either with existing instruments, like UKIRT (see Section I.5), or those planned for the future.

[1] Heterodyne Instrument for Far Infrared.
[2] Photodetector Array Camera and Spectrometer.

Table III.30.
Examples of IR vibrational transitions of possible interest to the HSO mission.

Molecule	Frequency (cm^{-1})	gas-phase (*G*), RG matrix (*M*) Theory (*T*)	Theoretical intensity (km/mol)	Reference
NC_4N	107	*G*	11	Khanna *et al.* (1987) Kołos (2002)
NC_6N	62	*G*	6	Miller & Lemmon (1967) Kołos (1999)
NC_3NC	45, 158	*T*	31, 15	Smith *et al.* (1994a) Horn *et al.* (1994)
CNC_2NC	119	*T*	6.5	Kołos, unpublished (B3LYP/aug-cc-pVTZ)
C_3NCN	52, 161	*T*	9, 3	Kołos (2002)
NC_5NC	70	*T*	5	Kołos (1999)
NC_5N	75	*T*	7	Smith-Gicklhorn *et al.* (2002a)
HC_5N	108.5	*T*		Botschwina *et al.* 1997a
HC_4NC	114	*T*		Botschwina *et al.* 1998
HC_6NC	64, 163	*T*		*ibid*
HC_7N	62, 163	*T*	0.1, 5.3	Botschwina *et al.* 1997b
C_3O	120	*M*	5.2	Botschwina & Reisenauer 1991
C_7	70	*T*		Botschwina 2002
SiC_4	88	*T*		Gordon *et al.* 2000b
SiC_6	56	*T*		*ibid*
SiC_8	38	*T*		Botschwina *et al.* 2000
SiC_5Si	40.8	*T*		Botschwina 2003a
SiC_2S	115	*T*		Botschwina *et al.* 2002
SiC_3S	97	*T*		*ibid*
SiC_4S	63	*T*		*ibid*

*

* *

Moureu & Bongrand (1920) synthesized cyanoacetylene, Turrel *et al.* (1957) measured its IR spectrum, Turner (1971) detected the microwave emission from interstellar HC_3N, Okabe & Dibeler (1973) started the photochemical studies of the compound, Wilson (1978) and Green & Herbst (1979) were the first to speculate on theoretically possible isomers. These landmarks initiated basic threads of investigation on unsaturated carbon-nitrogen chain molecules, threads, which are presently entangled. As a rule, the researchers in this field steer clear of "science sans conscience" (Rabelais 1532); astrophysicists are often engaged in the laboratory work and/or quantum chemical calculations, while laboratory spectroscopists and theoretical chemists are perfectly conscious of the astronomical aspects of their findings.

APPENDICES

APPENDIX *A*

Reported Inter- & Circumstellar Molecules

2	3	4	5	6	7
H_2	C_2H	c-C_3H	**C_5**	C_5H	C_6H
AlF	C_2O	l-C_3H	C_4H	l-H_2C_4	CH_2CHCN
AlCl	C_2S	C_3N	C_4Si	C_2H_4	CH_3C_2H
C_2	CH_2	C_3O	l-C_3H_2	CH_3CN	HC_5N
CH	***HCN***	C_3S	c-C_3H_2	CH_3NC	$HCOCH_3$
CH+	HCO	CH_2D+?	CH_2CN	CH_3OH	NH_2CH_3
CN	HCO+	HCCN	CH_4	CH_3SH	c-C_2H_4O
CO	HCS+	HCNH+	**HC_3N**	HC_3NH+	CH_2CHOH
CO+	HOC+	HNCO	HC_2NC	HC_2CHO	
CP	**H_2O**	HNCS	HCOOH	NH_2CHO	
CSi	H_2S	HOCO+	H_2CHN	**HC_4H**	
HCl	HNC	H_2CO	H_2C_2O		
KCl	HNO	H_2CN	H_2NCN		
NH	MgCN	H_2CS	HNC_3		
NO+	MgNC	**H_3O+**	SiH_4		
NS	N_2H+	**NH_3**	H_2COH^+		
NaCl	N_2O	SiC_3			
OH	NaCN	**HC_2H**			
PN	OCS				
SO	SO_2				
SO+	c-SiC_2				
SiN	CO_2				
SiO	**NH_2**				
SiS	**SiCN**				
CS	**H_3+**				
HF	***C_3***				
SH	AlNC				
FeO					

8	9	10	11	12	13
CH_2C_3N	CH_3C_4H	CH_3C_5N?	HC_9N	**C_6H_6**	$HC_{11}N$
$HCOOCH_3$	CH_3CH_2CN	$(CH2)_2CO$			
CH_2COOH?	$(CH_2)_2O$	NH_2CH_2COOH?			
C_7H	CH_3CH_2OH				
CH_2OHCHO	HC_7N				
HC_6H	C_8H				

The list is based largely on the Wootten's (2002) compilation. Entries in *italics* correspond to the optical detection, those typed in **bold** were found at infrared wavelengths.

APPENDIX *B*

Glossary of abbreviations

AGB – asymptotic giant branch (highly evolved red giant stars)

amu – atomic mass unit

aug-cc-pVTZ – correlation-consistent polarised valence triple-zeta basis set augmented with diffuse functions

B3LYP, BLYP – hybrid functionals due to Becke, Lee, Young, and Parr

BP86 – a hybrid functional due to Becke and Perdew

CAS – Complete Active Space

CEPA – Coupled Electron Pair Approximation

CCSD(T) – single, double and perturbative triple excitations coupled-clusters

CWRD – Cold Window Radial Discharge

cc-pVTZ – correlation-consistent polarised valence triple-zeta basis set

DFT – Density Functional Theory

HF – Hartree-Fock method (Self Consistent Field)

ISM – interstellar medium

MP*n* – *n*-th order of the Møller-Plesset perturbation theory

NBO – Natural Bond Orbital

PAH – polycyclic aromatic hydrocarbons

RG – rare gas

SCF – Self Consistent Field method (Hartree-Fock)

TS – transition state

U... – (as the first letter in computational methods abbreviations) – marks the "unrestricted" treatment of electrons

ZPE – zero-point energy

APPENDIX *C*

Conversion factors for non-SI units

$Å^3$ (polarizability)	$1\ Å^3 = 1.1127 \times 10^{-40}\ C\ m^2\ V^{-1}$
Debye (electric dipole moment)	$1\ D = 3.3356 \times 10^{-30}\ C\ m$
kcal/mol (energy)	$1\ kcal/mol = 4.184\ kJ/mol = 6.9477 \times 10^{-21}\ J$
parsec (distance)	$1\ pc = 3.26$ light years $= 3.0856 \times 10^{16}\ m$
Torr (pressure)	$1\ Tr = 1.31579 \times 10^{-3}\ atm = 133.322\ Pa$

REFERENCES

References to papers by the author of this monograph, of the direct relevance to its subject, are discernible by Roman numerals, and arranged in order of appearance in the text. Other articles are listed alphabetically, according to the first author's name.

[I] R. Kołos; „A novel source of transient species for matrix isolation studies"; *Chem.Phys.Letters*, **247** (1995) 289

[II] R.Kołos & J.Waluk; „Matrix isolated products of cyanoacetylene dissociation"; *J. Mol. Structure* **408/409** (1997) 473

[III] R. Kołos; „Photolysis of dicyanodiacetylene in argon matrices"; *Chem. Phys. Letters* **299/2** (1999) 247-251

[IV] R. Kołos & Z.R. Grabowski; „The chemistry and prospects for interstellar detection of some dicyanoacetylenes and cyanoacetylene-related species"; *Astrophysics & Space Science* **271** (2000) 65

[V] R. Kołos, „Evidence for the formation of diisocyanodiacetylene in argon matrices"; *Polish J. Chem.* **74** (2000) 1723

[VI] R. Kołos & A.L. Sobolewski, „The infrared spectroscopy of HNCCC: matrix isolation and density functional theory study" *Chem. Phys. Letters* **344** (2001) 625

[VII] A.M. Smith-Gicklhorn, M. Lorenz, R. Kołos, V.E. Bondybey, „Vibrational spectra of matrix-isolated mass-selected cyanoacetylene cations", *J. Chem. Phys.* **115** (2001) 7534

[VIII] A.M. Smith-Gicklhorn, M. Lorenz, .M. Frankowski, R. Kołos, V.E. Bondybey, „C_5N_2 revisted: Mass-selective matrix isolation and DFT studies", *Chem. Phys. Letters* **351** (2002) 85

[IX] R. Kołos, "Exotic isomers of dicyanoacetylene: A density functional theory and *ab initio* study", *J. Chem. Phys.* **117** (2002) 2063

[X] R.Kołos, and J.Cz. Dobrowolski „HCNCC – the possible isomer of cyanoacetylene", *Chem. Phys. Letters* **369** (2003) 75

Agreiter, J., Smith, A.M., Hartle, M., Bondybey, V.E. 1994, *Chem. Phys. Letters*, **225**, 87

Agreiter, J., Smith, A.M., Bondybey, V.E. 1995, *Chem. Phys. Letters*, **241**, 317

Allin, E.J., Hare, W.F.J., MacDonald, R.E. 1955 *Phys. Rev.* **98**, 554

Allamandola, L. 1990, in Conference Proc. *Physics and Composition of Interstellar Matter*, J. Krełowski & J. Papaj Eds., page 9.

Allamadola, L.J., Tielens, A.G.G.M., Barker, J.R. 1985, *Astrophys. J.*, **290**, L25

Allamadola, L.J., Tielens, A.G.G.M., Barker, J.R. 1989, *Astrophys. J. Suppl. Ser.*, **71**, 733

Allamadola, L.J., Hudgins, D.M., Sandford, S.A. 1999, *Astrophys. J.* **511**, L115

Andrews, L., Moskovits, M. ed. 1989, *Chemistry and Physics of Matrix–Isolated Species*, North Holland, Amsterdam.

Avery, L.W. 1980, in: *Interstellar Molecules*, B.H.Andrew, ed; IAU; 47

Bajdor, K., Glice, M.M., Leś, A., Adamowicz, L., Kołos, R. 1999, *J. Mol. Struct.* **511-512,** 107

Baker, C., Turner, D.W. 1968, *Proc. Roy. Soc. London* **A308**, 19

Balucani, N., Asvany, O., Huang, L. C. L., Lee, Y. T., Kaiser, R. I., Osamura, Y., & Bettinger, H.F. 2000, *Astrophys. J.*, **545**, 892

Bartel, C., Botschwina, P., Bürger, H., Guarnieri, A., Heyl, Ä., Huckauf, A., Lentz, D., Merzliak, T., Mkadmi, E.B. 1998 *Angew. Chemie* **110**, 3036

Becke, A.D. 1993, *J. Chem. Phys.* **98**, 5648

Bell M.B., Matthews H.E. 1985, *Astrophys. J.* **291**, L63

Bell, M.B., Feldman, P.A., Travers, M.J., McCarthy, M.C., Gottlieb, C.A., Thaddeus, P. 1997, *Astrophys. J.* **483**, L61

Benson P.J., Myers P.C. 1983, *Astrophys.J.* **270**, 89

Bernath, P.F., Hinkle, K.H., Keady, J.J. 1989, *Science* **244**, 562

Bersohn, R. 1987, in *Molecular Photodissociation Dynamics*, M.N.R. Ashfold and J.E. Baggott, eds., Royal Society, London, p. 1

Bettens, R.P.A, Lee, H.H., Herbst, E. 1995, Astrophys. J. **443**, 664

Birks, J.P., ed. 1975, *Organic Molecular Photophysics*, vol.2

Bockelée-Morvan, D.,Lis, D.C., Wink, J.E., Despois, D., Crovisier, J., Bachiller, R., Benford, D.J., Biver N., Colom P., Davies, J.K., Gérard, E., Germain, B., Houde, M., Mehringer, D., Moreno, R., Paubert, G., Phillips, T.G., Rauer H. 2000, *Astron. & Astrophys.* **353**, 1101

Bondybey, V.E., Miller, T.A. 1983; in *Molecular Ions: Spectroscopy, Structure and Chemistry*, T.A. Miller and V.E. Bondybey, ed., North Holland, p. 125-173

Bondybey, V.E., Smith, A.M., Agreiter, J. 1996, *Chem. Rev.* **96**, 2113

Borget, F. 2000, *Ph.D. Thesis*, Université de Provence (Aix-Marseille I)

Botschwina P, Reisenauer H.P. 1991, *Chem. Phys. Letters* **183**, 217

Botschwina, P., Horn, M., Seeger, S., Flügge, J. 1992, *Chem. Phys. Letters* **195**, 427

Botschwina, P., Horn, M., Flügge, J., Seeger S. 1993a, *J. Chem. Soc. Farday Trans.* **89**, 2219

Botschwina, P., Horn, M., Seeger, S., Flügge, J. 1993b, *Molec. Phys.* **78**, 191

Botschwina *et al.* 1993c; unpublished results, as cited by Smith *et al.* (1993)

Botschwina, P., Heyl, Ä., Oswald, M., Hirano, T. 1997a, *Spectrochimica Acta A* **53**, 1079

Botschwina, P., Horn, M., Markey, K., Oswald, R. 1997b, *Mol. Phys.* **92**, 381

Botschwina, P, Heyl, Ä., Chen, W., McCarthy, M.C., Grabov, J.-U, Travers, M.J., Thaddeus, P. 1998, *J. Chem. Phys.* **109**, 3108

Botschwina, P., Oswald, M., 2000, *Chem. Phys. Letters* **319**, 587

Botschwina, P., Schulz, B., Oswald, R., Stoll, H. 2000, *Z. Physik. Chem.* **214**, 797

Botschwina, P., Sanz, M.E., McCarthy, M.C., Thaddeus, P. 2002, *J. Chem. Phys.* **116**, 10719

Botschwina, P. 2002, *Chem. Phys. Letters* **354**, 148

Botschwina, P. 2003a, *Z. Physik. Chem.* **217**, 177

Botschwina, P. 2003b, *Phys.Chem.Chem.Phys.*, in press

Bréchignac, P, Pino, T., Boudin, N. 2001, *Spectrochim. Acta* **A57**, 745

Brockman, F.J. 1955, *Can. J. Chem.* **33**, 507

Brown, F.X., Saito, S., Yamamoto, S. 1984, *J. Mol. Spectrosc.* **143**, 203

Brunck, T.K., Weinhold F. 1979, *J. Am. Chem. Soc.* **101**, 1700

Bürger, H., Sommer, S., Lentz, D., Preugschaft, D. 1992, *J. Mol. Spectrosc.* **156** 360

Carr, B.R., Chadwick, B.M., Edwards, C.S., Long, D.A., Wharton, S.C. 1980, *J. Mol. Struct.* **62**, 291

Cernicharo, J. Bachiller, R., Duvert, G. 1986, *Astron. & Astrophys.* **160**, 181

Cernicharo, J., Yamamura, I., González-Alfonso, E., de Jong, T., Heras, A., Escribano, R., Ortigoso, J. 1999, *Astrophys. J.* **526**, L41

Cernicharo, J., Heras, A.M., Tielens, A.G.G.M., Pardo, J.R., Herpin, F., Guélin, M., and Waters, L.B.F.M. 2001, *Astrophys. J.* **546**, L123

Cherchneff, I., Glassgold, A.E.: 1993, Astrophys. J. **419**, L41

Cherchneff, I., Glassgold, A.E., Mamon, G.A. 1993, Astrophys. J. **410**, 188

Cheung, A.C., Rank, D.M., Townes, C.H., Thornton, D.D., Welch, W.J. 1968, *Phys. Rev. Letters* **21**, 1701

Cheung, A.C., Rank, D.M., Townes, C.H., Thornton, D.D., Welch, W.J. 1969, *Nature* **221**, 626

Clarke, D.W., Ferris, J.P. 1995, *Icarus* **115**, 119

Clarke, D.W., Ferris, J.P. 1996, *J. Geophys. Res.* **101**, 7575

Clary, D.C., Haider, N., Husain, D., Kabir, M.: 1994, *Astrophys.J.* **422**, 416

Cole, G.H.A.,Woolfson, M.M., Cole, D. 2002, *Planetary Science: The Science of Planets Around Stars*, Institute of Physics Pub., 1st edition.

Connors, R.E., Roebber, J.L., Weiss, K. 1974, J. *Chem. Phys.* **60**, 5011

Conrad, M.P., Schaefer, H.F. 1978, *Nature* **274**, 456

Coustenis, A., Bezard, B., Gautier, D., Marten, A., Samuelson, R. 1991, *Icarus* **89** 152

Crawford, M.K., Tielens, A.G.G.M., Allamandola, L.J. 1985, *Astrophys. J.*, **293**, L45

Creswell, W.A., Winnewisser, G., Gerry, M.C.L. 1977, J. Mol. Spectrosc., 65, 421

DeLeon, R.L., Muenter, J.S. 1985, *J. Chem. Phys.* **82**, 1702

Dello Russo, N., Khanna, R.K. 1996, *Icarus* **123**, 366

Dewar, J. 1894, *Proc. Royal Soc.* **55**, 340

Ding, Y.H., Huang, X.R., Lu, Z.Y, Feng, J.N. 1998, *Chem. Phys. Letters* **284**, 325

Douglas, A.1977, *Nature* **269**, 130

Douglas, A.E., Herzberg, G. 1941, *Astrophys. J.*, **94**, 381

Duley, W.W., Williams, D.A. 1984, *Interstellar Chemistry*, p.115, Acad.Press, New York

Dunkin, I.R. 1998, *Matrix Isolation Techniques. A Practical Approach*, Oxford Univ. Press, Oxford

Dunning, T.H. 1989, J.Chem.Phys. 90, 1007

El Goresy, A., Donnay, G. 1968, *Science* **161** 363

Fitzpatrick, E.L. 1999, *Publ. Astron. Soc. Pacific* ,**111**, 63

Foing, B.H., Ehrenfreund, P. 1994, *Nature* **369**, 296

Fornay, D., Freivogel, P., Fulara, J., Maier, J.P. 1995, *J. Chem. Phys.*, **102**, 1510

Foster, J. P., Weinhold F. 1980, *J. Am. Chem. Soc.* **102**, 7211

Friberg, P. Hjalmarson, A. and Irvine, W.M. 1980, *Astrophys. J.* **241**, L99

Freeman, , C.G., Harland, P.W., McEvan, M.J. 1979, *Mon. Not. Roy. Astron. Soc.* **187**, 441

Frisch, M. J., Trucks, G. W., Schlegel, H. B., Scuseria, G. E., Robb, M. A.,

Cheeseman, J. R., Zakrzewski, V. G., Montgomery, Jr. J. A., Stratmann, R. E., Burant, J. C., Dapprich, S., Millam, J. M., Daniels, A. D., Kudin, K. N., Strain, M. C., Farkas, O., Tomasi, J., Barone, V., Cossi, M., Cammi, R., Mennucci, B., Pomelli, C., Adamo, C., Clifford, S., Ochterski, J., Petersson, G. A., Ayala, P. Y., Cui, Q., Morokuma, K., Malick, D. K., Rabuck, A. D., Raghavachari, K., Foresman, J. B., Ciosłowski, J., Ortiz, J. V., Stefanov, B. B., Liu, G., Liashenko, A., Piskorz, P., Komaromi, I., Gomperts, R., Martin R. L., Fox, D. J., Keith, T., Al-Laham, M. A., Peng, C. Y., Nanayakkara, A., Gonzalez, C., Challacombe, M., Gill, P. M. W., Johnson, B., Chen, W., Wong, M. W., Andres, J. L., Gonzalez, C., Head-Gordon, M., Replogle, E. S. and Pople J. A. 1998, *Gaussian 98, Revision A.7,* Gaussian, Inc., Pittsburgh PA

Fukuzawa, K., Osamura, Y. 1997, *Astrophys.J.* , 489, 113

Fulara, J., Leutwyler, S., Maier, J.P., Spittel, U. 1985, *J. Phys. Chem.* **89**, 3190

Fulara, J., Jakobi, M., Maier, J.P. 1993, *Chem. Phys. Letters* **211**, 227

Galazutdinov, G., Moutou, C. Musaev, F., Krełowski, J., 2000, *Publ. Astron. Soc. Pacific* ,**112**, 648

Galazutdinov, G.A., Musaev, F.A., Krełowski, J., Walker, G.A.H. 2002a, *Astron. & Astrophys.* **384**, 215

Galazutdinov, G.A., Pętlewski, A., Musaev, F.A., Moutou, C., Lo Curto, G., Krełowski, J. 2002b, *Astron. & Astrophys.* **395**, 223

Galazutdinov, G.A., Pętlewski, A., Musaev, F.A., Moutou, C., Lo Curto, G., Krełowski, J. 2002c, *Astron. & Astrophys.* **395**, 969

Galazutdinov, G., Galazutdinova, O.A. 2003, *Astron. & Astrophys.* to be published

Gałęcki, Z., Graczyk, M., Janaszak, E., Kołos, R., Krełowski, J., Strobel, A. 1984, *Astron. & Astrophys.* **122**, 207

Geballe, T.R., Oka, T. 1998, *Nature* **384**, 334

Gensheimer, P.D. 1997, Ap.J., 479, L75

Gerasimovič, B.P., Struve, O. 1929 , *Astrophys. J.* **69**, 7

Gerlich D., Horning S. 1992, *Chem. Rev.* **92**, 1509

Gerry, M.C.L., Stroh, F., Winewisser, M. 1990, *J. Mol. Spectrosc.* **140**, 147

Gillet, F.C., Forrest, W.J. 1973, *Astrophys. J.* **179**, 483

Gnaciński, P., Sikorski, J. 1999, *Acta Astron.* **49**, 577

Goldanskii, V.I. 1977, *Nature* **269**, 583.

Goldberg, N., Schwarz, H. 1994, *J. Phys. Chem.* **98**, 3080

Gordon, V.D., McCarthy, M.C., Apponi, A.J., Thaddeus, P. 2000a, *Astrophys. J.* **540**, 286

Gordon, V.D., Nathan, E.S., Apponi, A.J., McCarthy, M.C., , Thaddeus, P., Botschwina, P. 2000b, *J. Chem. Phys.* **113**, 5311

Graedel, T.E., Langer, W.D., Frerking, M.A. 1982, *Astrophys. J. Suppl. Ser.*, **48**, 321

Green, S., Herbst, E. 1979, *Astrophys. J.* **229**, 121

Greenberg, J.M. 1976, *Astrophys. Space Sci.* **39**, 9

Greenberg, J.M., Hong, S.S.: 1974, in *Planets, Stars and Nebulae Studied with Photopolarimetry*, T. Gehrels, ed., I.A.U. Coll. 23, Univ. of Arizona, p. 196

Greenberg, J.M. & Hagen, J.I.: 1990 *Astrophys. J.* **361**, 260

Greenberg, J.M., Li, A. 1996, *Astron. & Astrophys.* **309**, 258

Guélin, M, Cernicharo, J. 1991, *Astron. & Astrophys.* **244**, L21

Guélin, M., Thaddeus, P.:1977, *Astrophys. J.* **212**, L81

Guennoun, Z., Couturier-Tamburelli, I., Piétri, N., Aycard, J.P. 2003, *Chem. Phys. Letters* **368**, 574

Gush, H.P., Hare, W.F.J., Allin, E.J., Welsh, H.L. 1960, *Can. J. Phys.* **38**, 176

Güthe, F., Tulej, M., Pachkov, M.V, Maier, J.P. 2001, *Astrophys. J.* **555**, 466

Habing, H.J. 1996, *Astron. & Astrophys. Rev.* **7**, 97

Hajgato, B., Flammang, R., Veszpremi, T., Nguyen, M.T. 2002, *Mol. Phys.* **100**, 1693

Halls, M.D., Velkovski, J., Schlegel, H.B. 2001, *Theor. Chem. Acc.* **105**, 413

Halpern, J.B., Miller, G.E., Okabe, H., Nottingham, W. 1988, *J. Photochem. Photobiol. A: Chemistry*, **42**, 63

Halpern, J.B., Petway L., Lu, R., Jackson, W.M., McCrary, V.R. 1990, *J.Phys.Chem.*, **94,** 1869

Hartmann, J. 1904, *Astrophys. J.*, **19**, 268

Hasegawa T., Herbst E. 1993a, *Mon. Not. R. Astron. Soc.*, **261**, 83

Hasegawa T., Herbst E.: 1993b, *Mon. Not. R. Astron. Soc.*, **263**, 589

Heath, J.R., Cooksy, A.L., Gruebele, M.H.W., Schmuttenmauer, C.A., Saykally, R.J. 1989, *Science* **244**, 564

Heger, M.L. 1922, *Lick Obs. Bull.*, **337**, 141

Heithausen, A., Brüns, C., Kerp J., Weiss, A. 2001, Proc. Symposium *The Promise of the Herschel Space Observatory* 12-15 Dec. 2000, Toledo, Spain, ESA SP-460, eds. G.L. Pilbratt et al., p. 431

d'Hendecourt, L, Dartois, E. 2001, *Spectrochim. Acta* **A57**, 669

Herbst, E. 1978, *Astrophys. J.*, **222**, 508

Herbst, E., Leung, C.M. 1990, *Astrophys. J.*, **233**, 177

Hinkle, K.W., Keady, J.J., Bernath, P.F. 1988, *Science* **241**, 1319

Hirahara, Y., S. Ohshima, Y., Endo Y.1993, *Astrophys. J.* **403** L83

Hodges, J.A., McMahon, R.J., Sattelmeyer, K.W., Stanton, J.F. 2000, *Astrophys. J.* **544**, 838

Hohenberg, P., Kohn, W. 1964, *Phys. Rev.* **136** B864

Horn, M, Botschwina, P.,Flügge, J. 1994, *Theor. Chim. Acta* **88**, 1

Hu, C-H., Schaefer H.F. 1993, J. Phys. Chem., 97, 10681

Huang, L. C. L., Asvany, O., Chang, A. H. H., Balucani, N., Lin, S. H., Lee, Y. T., Kaiser, R. I., Osamura, Y. 2000, J. Chem. Phys. 113, 8656

Hudgins, D.M., Bauschlicher, Jr, C.W., Allamandola, L.J. 2001, *Spectrochim. Acta* **A57**, 907

Huffman, D. R. 1977, *Adv. Phys.* **26**, 129

Hulst, H.C. van de 1949, *Rech. Astr. Obs.* Utrecht, **11**

Irvine, W.M. Goldsmith, P.F., Hjalmarson, A. 1987, in *Interstellar Processes*; D.J. Hollenbach and H.A. Thronson jr., eds; Reidel, Dordrecht; p. 561

Jacox, M.E. 1984, *J. Phys. Chem. Ref. Data* **13**, 945

Jacox, M.E. 1985, *J. Molec. Spectr.* **113**, 286

Janev, R.K., Van Regemorter, H. 1974, *Astron. & Astrophys.* **37**, 1

Job, V.A., King, G.W. 1966a, *J. Molec. Spectrosc.* **19**, 155

Job, V.A., King, G.W. 1966b, *J. Molec. Spectrosc.* **19**, 178

Jodl, H. 1989, in *Chemistry and Physics of Matrix–Isolated Species*, L. Andrews and M. Moskovits, ed., North Holland, Amsterdam.

Jonas, V., Bohme, M, Frenking, G. 1992, *J. Phys. Chem.* **96**, 1640

Jortner, J., Bixon, M.: 1968, *J. Chem. Phys.* **48**, 715

Jortner, J. Chock, D.P., Rice, S.A. 1968, *J. Chem. Phys.* **48**, 715

Kaifu, N. 1990, in *Molecular Processes in Space*, Eds. T. Watanabe et al. Plenum Press, New York, p. 205

Kaiser, R.I., Lee, Y.T., Suits, A.G. 1996, *J. Phys. Chem.* **105**, 8705

Kaiser, R.I., Suits A.G. 1995, *Rev. Sci. Instr.* **66**, 5405

Kaiser, R.I. 2002, *Chem. Rev.* **102**, 1309

Kawaguchi, K., Ohishi, M., Ishikawa, S-I., Kaifu, N. 1992a, *Astrophys. J. Letters* **386** L51

Kawaguchi, K., Takano, S., Ohishi, M., Ishikawa, Miyazawa, K., Kaifu, N. Yamashita, K., Yamamoto, S., Saito, S. Ohshima, Y., Endo Y.1992b, *Astrophys. J. Letters* **396** L49

Kawaguchi, K., Kasai, Y., Ishikawa, S., Ohishi, M., Kaifu, N. 1994, *Astrophys. J. Letters* **420** L95

Khanna, R.K., Perera-Jarmer, M.A., Ospina, M.J. 1987, *Spectrochim. Acta* **43A**, 421

Khlifi, M., Raulin, F, Arie, E, Graner, G. 1990, *J. Mol. Spectry.* **143**, 209

Kirkwood, D.A., Linnartz, H., Grutter, M., Dopfer, O., Motylewski, T.D., Pachkov, M., Tulej, M., Wyss, M., Maier, J.P. 1998, *Faraday Discuss.* **109**, 109

Kiszkurno, E., Kołos, R., Krełowski, J., Strobel, A. 1984, *Astron. & Astrophys.* **135**, 337

Kloster-Jensen, E., Maier, J.P., Morthaler, O., Mohraz, M., 1979, *J. Chem. Phys.* **71** 3125

Koch, W., Holthausen, M.C. 2002, *A Chemist's Guide to Density Functional Theory*; Wiley, Weinheim

Kohn, W. Sham, L.J. 1965, *Phys. Rev. A* **140**, 1133

Kołos, R., Zieliński, Z., Grabowski, Z.R., Mizerski, T. 1991, *Chem.Phys.Letters*, **180**, 73

Kołos, R., Zieliński, Z., Grabowski, Z.R., Mizerski, T. 1992, *Radiat.Phys.Chem.* **39**,159

Kołos 1995, listed separately as "paper I"

Kołos, R., Salloum, A., Dubost, H. 1996, *Chem. Phys. Letters*, **254**, 47

Kołos & Waluk 1997, listed separately as "paper II"

Kołos 1999, listed separately as "paper III"

Kołos 2000, listed separately as "paper V"

Kołos & Grabowski 2000, listed separately as "paper IV"

Kołos & Sobolewski 2001, listed separately as "paper VI"

Kołos 2002, listed separately as "paper IX"

Kołos & Dobrowolski 2003a, listed separately as "paper X"

Kołos 2003, in preparation

Kołos & Dobrowolski 2003b, in preparation

Krełowski, J. 2002, *Adv. Sp. Res.* **30**, 1395

Kriegler, R.J., Welsh, H.L. 1968, *Can. J. Chem.* **46**, 1181

Kroto, H.W., Kirby, C., Walton, D.R.M., Avery, L. Broten, N.W. McLeod, J.M. and Oka, T. 1978, *Astrophys.J.* **219**, L133

Krüger M., Dreizler H., Preugschaft D., Lentz, D., *Angew. Chemie* 1991, **103** 1674

Kudryavtsev, Y.P, Evsyukov, S., Guseva, M., Babayev, V., Khvostov, V. 1997, *Chemistry and Physics of Carbon* **25**, 1

Lafferty, W.J., Lovas, F.J. 1978, *J. Phys. Chem. Ref. Data* **7**, 441

Lang, K.R. 1980, *Astrophysical Formulae*, pp. 335-372, Springer Verlag, Berlin

Le Bourlot, J., des Forets, G.P., Roueff, E., Schilke, P. 1993, *Astrophys. J.* **416**, L87

Lee, C., Yang, W., Parr, R.G. 1988, *Phys. Rev. B* **37**, 785

Lee, J.M., Adamowicz, L. 2001, *Spectrochim. Acta* **A57**, 897

Lee, S. 1996, *J. Phys. Chem* **100**, 13959

Lee, S. 1998, *J. Molec. Struct. (Teochem)* **427**, 267

Lewis, G.N., Kasha, M 1945, *J. Am. Chem. Soc.* **67**, 994

Léger, A., Puget, J.L 1984, *Astron. & Astrophys.* **137**, L5

Léger, A., d'Hondecourt, L., Défourneau, D. 1989, *Astron. & Astrophys.* **216**, L148

Léger, A., d'Hendecourt, L. 1985, *Astron. & Astrophys.* **146**, 81

Lepp. S., Dalgarno, A. 1998, *Astrophys. J.* **335**, 769

Linnartz, H., Vaizert, O., Cias, P., Gruter, L., Maier, J. P. 2001, Chem. Phys. Letters **345**, 89

Lorenz, M., Bondybey V.E. 2000, *Low Temp. Physics*, **26**, 778

Lyngå, G. 1982, *Astron. & Astrophys.* **109**, 213

Maier, J.P., Morthallar, O., Thommen, F. 1979, *Chem. Phys. Letters* **60**, 193

Maier, J.P. 1992, *Mass. Spectrom. Rev.*, **11**, 119

Maier, J.P., Lakin, N.M., Walker, G.A.H., Bohlender, D.A. 2001, *Astrophys. J.* **553**, 267

Mallinson, P.D., De Zafra, R.L. 1978, *Molec. Phys.* **36**, 473

Manassen, J., Wallach, J. 1965, *J. Am. Chem. Soc.* **87**, 2672

Mathis, J.S. 1990, *Ann. Rev. Astron. & Astrophys.* **28**, 37

Mathis, J.S. 1996, *Astrophys. J.* **472**, 643

McCall, B.J., Geballe, T.R., Hinkle, K.H., Oka, T. 1998, *Science*, **279**, 1910

McKellar, A. 1940, *Publ. Astron. Soc. Pacific* **52**, 187

McLennan, J.C., Shrum, G,M. 1924, *Proc. Roy. Soc. (London) Ser A.* **106**, 138

McSwiney, Jr, H.D. Merritt J.A. 1970, *J. Chem.Phys.* **52**, 5184

Merrill, P.W. 1934, *Publ. Astron. Soc. Pacific* ,**46**, 206

Merrill, K.M., Russell, R.W., Soifer, B.T. 1976, *Astrophys. J.*, **207**, 763

Meyer, B. 1971; *Low Temperature Spectroscopy*, Elsevier, New York

Meyer W. 1973 *J. Chem. Phys.*, **58**, 1017

Miller, F.A., Hannan Jr., R.B. 1953, *J. Chem. Phys.* **21**, 110

Miller, F.A., Hannan Jr., R.B. 1955, *J. Chem. Phys.* **23**, 2127

Miller, F.A., Hannan Jr., R.B. 1958, *Spectrochim. Acta* **12**, 321

Miller, F.A., Lemmon, D.H. 1967, *Spectrochim. Acta* **23A**, 1415

Milligan, D.E., Jacox, M.A. 1967, *J. Chem. Phys.*, **47**, 278

Motylewski, T., Linnartz, H., Vaizert, O., Maier, J.P., Galazutdinov, G.A., Musaev, F.A., Krełowski, J., Walker, G.A.H., Bohlender, D.A. 2000, *Astrophys. J.* **531**, 312

Møller, C., Plesset, M.S. 1934, *Phys. Rev.* **46**, 618

Morris, M., Turner, B.E., Palmer, P., Zuckerman, B. 1976, *Astrophys. J.* **205**, 82

Moureu, C., Bongrand, J.C. 1909, *Bull. Soc. Chim.* **V**, 846

Moureu, C., Bongrand, J.C. 1920a, *Ann. Chim. (Paris)* **14**, 5

Moureu, C., Bongrand, J.C. 1920b, *Ann. Chim. (Paris)* **14**, 47

Ohishi, M., Irvine, W.M., Kaifu, N. 1992, in *Astrochemistry of Cosmic Phenomena*, ed. P.D. Singh, Kluwer, Dordrecht, p. 171

Ohishi, M., Kaifu, N. 1998, Faraday Discuss., 109, 205

Oka, T. 1983; in *Molecular Ions: Spectroscopy, Structure and Chemistry*, T.A. Miller and V.E. Bondybey, ed., North Holland, p. 73-90

Oka, T., Thorburn, J.E., McCall, B.J., Friedman, S.D., Hobbis, L.M., Sonnentrucker, P., Welty, D.E., York, D.G. 2003, *Astrophys. J.* **582**, 823

Okabe, H., Dibeler, V.H. 1973, J. Chem. Phys. 59, 2430

Osamura, Y., Fukuzawa, K., Terzieva, R., Herbst, E. 1999, *Astrophys. J.*, 519, 697

Oswald, M. 1995, Ph.D. Thesis, Cuvillier, Göttingen

Palafox, M.A. 2000, *Int. J. Quant. Chem.* **77**, 661

Palmer, P., Zuckerman, B., Buhl, D., Snyder, L.E. 1969, *Astrophys. J.* **156**, L147

Pascoli, G., Lavendy, H. 1999, *Chem.Phys.Letters*, **312**, 333

Pau, C.F., Hehre, W.J. 1982, *J. Chem. Phys.* **86**, 321

Platts, J.A., Howard, S.T., Fallis, I.A. 1998, *Chem.Phys.Letters*, **285**, 198

Pople, J.A., Seeger, R., Krishnan, R. 1977, *Int. J. Quant. Chem. Symp.* **11**, 149

Pople, J.A., Head-Gordon, M., Raghavachari, K. 1987, J. Chem. Phys., 87, 5968

Powell, M.F., Peterson, M.R., & Csizmadia, I.G. 1983, *J. Molec. Struct.* **92**, 323

Prochaska, F.T., and Andrews, L. 1977, *J. Chem. Phys.* **67** 1091

Rabelais, François 1532; *Gargantua, roi des Dipsodes*, originally published under the pen name *Alcofribas Nasier, abstracteur de Quinte Essence*. The whole passage from the famous letter written by Gargantua, in which he encourages his son Pantagruel to spend the time wisely, reads:
Sagesse n'entre pas en âme malveillante et
Science sans conscience n'est que ruine de l'âme.
("Wisdom entereth not into a malicious mind,
And science without conscience is but ruin of the soul")

Radziszewski, J.G., Waluk, J., Michl, J. 1989, *Chem. Phys.* **136**, 165

Ragavachari, K., Trucks, G.W., Pople, J.A., Head-Gordon, M. 1989, *Chem. Phys. Letters* **157**, 479

Rappaport, Z., ed. 1970, *The Chemistry of the Cyano Group*, Interscience Publishers, London, page 517

Sabety-Dzvonik, M.J., Cody, R.J., Jackson, W.M. 1976, *Chem. Phys. Letters* **44**, 131

Sadlej, J., Roos, B. 1991, *Chem. Phys. Letters* **180**, 81

Sagan, C., Khare, B.N. 1979, *Nature* **277**, 102

Saito, .S, Endo, Y., Hirota, E. 1984, *J. Chem. Phys.* **80**, 1427

Samuelson, R.E., Mayo, L.A., Knuckles, M.A., Khanna, R.J. 1997 *Planet. Space Sci.* **45**, 941

Sanchez, R.A, Ferris, J.P., Orgel, L.E. 1966, *Science* **154**, 784

Sandford, S. A.; Allamandola, L. J.; Tielens, A. G. G. M.; Sellgren, K.; Tapia, M.; Pendelton, Y.: 1991, *Astrophys. J.* **371**, 607

Sarre, P.J., Miles, J.R., Kerr, T.H. 1995, *Mon. Not. Roy. Astron. Soc.* **277**, 41

Schutte, W., Greenberg, J.M. 1991, *Astron. & Astrophys.* **244**, 190

Scott, A.P., Radom, L. 1996, *J. Phys. Chem.* **100**, 16502

Scuseria, G.E. 1991, *J.Chem.Phys.* **94**, 442

Seki, K., He, M., Liu, R., Okabe, H. 1996, *J. Phys. Chem.* **100**, 5349

Sepioł, J., Starukhin, A., Kołos, R., Latychevskaia, T., Jasny, J., Renn A. ,Wild U.P. 1999 *Chem. Phys.Letters*, **311** 29

Shalabiea, O.M., Greenberg, J.M. 1994, *Astron. & Astrophys.* **290**, 266

Shepherd, D.S., Churchwell, E. 1996, *Ap.J.* **472**, 225

Shiba, Y, Hirano, T., Nagashima, U., Ishii, K. 1998, *J. Chem. Phys.* **108**, 698

Shpol'skii, E.V., Personov, R.I., 1960, *Opt. Spectrosc. (USSR, English transl.)* **8**, 172

Snow, T.P. 2001, *Spectrochim. Acta* **A57**, 615

Smith, D. 1992, *Chem. Rev.*, **92**, 1473

Smith, A.M., Schallmoser, G., Thoma, A., Bondybey, V.E. 1993, *J. Chem. Phys.* **98**, 1776

Smith, A.M., Bondybey, V.E., Horn, M., Botschwina, P. 1994a, *J. Chem. Phys.* **100**, 765

Smith, A. M., Engel, C., Thoma, A., Schallmoser, G., Wurfel, B.E., Bondybey, V.E. 1994b, *Chem. Physics* **184**, 233

Smith-Gicklhorn *et al.* 2001, listed separately as "paper VII"

Smith-Gicklhorn *et al.* 2002a, listed separately as "paper VIII"

Smith-Gicklhorn, A.M., Lorenz, M., Frankowski, M., Bondybey, V.E. 2002b, *Phys. Chem. Chem. Phys.* **4**, 1425

Solomon, P.M., Wickramasinghe, N.C. 1969, *Astrophys. J.* **158**, 449

Stecher, T.P. 1965, *Astrophys. J.* **142**, 1683

Stecher, T.P., Donn, B. 1965, *Ap. J.* **142**, 1681

Stevens, B.: 1957, *Canad. J. Chem.* **36**, 96

Strahler, S.W.: 1984, *Astrophys. J.* **281**, 209

Struve, F.G.W. 1847, *Etudes d'Astronomie Stellaire*

Struve, O. 1939, *Z. Astrophys.*. **17**, 316

Sülzle, D, Schwarz, H. 1989, *Chem. Phys. Letters* **156**, 397

Suzuki, H., Yamamoto, S., Ohishi, M., Kaifu, N., Ishikawa, S., Hirahara, Y., Takano, S. 1992, *Astrophys.J.* **392**, 551

Swings, P., Rosenfeld, L. 1937, *Astrophys. J.* **86**, 483

Szczepanski, J., Personette, W., Vala M. 1991a,

Szczepanski, J., Personette, W., Pellow, R., Chandrasekhar, T.M., Roser D., Cory, M., Zerner, M., Vala, M. 1991b, *J.Chem.Phys.*, **96**, 35

Szczepanski, J., Fuller, J., Ekern, S., Vala, M. 2001, *Spectrochim. Acta* **A57**, 775

Talbi, D., Ellinger, Y., Herbst, E. 1996, *Astron. & Astrophys.* **314**, 688

Tang, J., Sumiyoshi, Y., Endo, Y. 1999, *Chem. Phys. Letters* **315**, 69

Terzieva R., Herbst, E. 1998 *Astrophys. J.* **501**, 207

Thoma, A., Wurfel, B.E., Schlachta, R, Lask, G.M. 1992, *J. Phys. Chem.* **96** 7231

Tielens, A.G.G.M., Hagen, W., 1982, *Astron. & Astrophys.* **114**, 245

Titarchuk, T., Halpern, J.B. 2000, *Chem. Phys. Letters* **323**, 305

Tittle, J., Merkoziaj, D., Liu, R. 1999, *Chem. Phys. Letters* **305**, 451

Trumpler, R.J. 1930, *Lick Obs. Bull.* **14**, 154; *Publ. Astron. Soc. Pacific* **92**, 411

Turner, B.E. 1971, Ap.J., 163, L35

Turner, B.E., Kislyakov, A.G., Liszt, H.S., Kaifu, N. 1975, *Astrophys. J.* **201**, L149

Turrel, G.C, Johns, W., Maki, A. 1957, *J. Chem. Phys.* **26**, 1544

Uyemura, M., Maeda, S. 1974, *Bull. Chem. Soc. Japan* **47**, 2930

Uyemura, M., Deguchi, S., Nakada, Y., Onaka, T. 1982, *Bull. Chem. Soc. Japan* **55**, 384

Vegard, L. 1924, *Nature*, **114**, 357

Walmsley, C.M., Güsten, R., Angerhofen, P,. Churchwell, E., Mundy, L. 1986, *Astron. & Astrophys.* **155**, 129

Wang, C-R., Huang, R-B., Liu, Z-Y., Zheng, L-S. 1995, *Chem. Phys. Letters* **237**, 463

Watson, W.D., 1976, *Rev. Mod. Physics*. **48**, 513

Wegner, W. 1995, *Międzygwiazdowe struktury absorpcyjne w kierunku bliskich gwiazd OB*, WSP Bydgoszcz

Wegner, W. 2002, *Lokalna struktura Galaktyki*, Wyd. Akademii Bydgoskiej, Bydgoszcz

Weinreb, S., Barret, A.H., Meeks, M.L., Henry, J.C. 1963, *Nature* **200**, 829

Welsh, H.L., Crawford, M.F., Locke, J.L. 1949, *Phys. Rev.* **76**, 580

White, R.S. 1996, *Astrophys. & Space Sci.*, **240** 75

Whitford, J. 1958, *Astron. J.* **63**, 201

Whittle, E., Dows, D.A., Pimentel, G.C. 1954, *J. Chem. Phys.* **22**, 1943

Whittaker, A.G., Kintner, P.L. 1969, *Science* **165**, 589

Whittaker, A.G., Watts, E.J., Lewis, R.S., Anders, E. 1980, *Science* **209**, 1512

Williams, D.A. 1986, *Quart. J. Royal Astron. Soc.* **27**, 64

Wilson, S. 1978, *Astrophys.J.* **220**, 363

Winnewisser, G. 1981, *Topics Curr. Chem.* **99**, 39

Winnewisser, G. and Walsley C.M. 1979, *Astrophys. & Space Sci.* **65**, 83

Winther, F., Schoenhoff, M., Le Prince, F., Guarnieri, A., Bruget, D.N., McNaughton, D. 1992 *J. Mol. Spectrosc.* **152**, 205

Woon, D. E., & Herbst, E. 1997, *Astrophys. J.*, **477**, 204

Wootten, A. 2002, http://www.cv.nrao.edu/~awootten/allmols.html

Zhan, C-G., Iwata, S. 1996, *J. Chem. Phys.* **104**, 9058

Zhou, Y, Arif, A.M., Miller, J.S. 1996, *Chem. Comm.* 1881

Ziurys, L.M., Apponi, A.J., Hollis, J.M., Snyder, L.E. 1994, *Astrophys. J.*, **436**, L181

Zubko, V.G., Krełowski, J., Wegner, W. 1996, *Mon. Not. Roy. Astron. Soc.* **283**, 577

Zubko, V.G., Krełowski, J., Wegner, W. 1998, *Mon. Not. Roy. Astron. Soc.* **294**, 548